THE UNIVERSITY
of EDINBURGH

Theoretical Considerations in the Use of Scalar-Tensor Theories of Gravity in Inflationary Models

David C. Edwards

Doctor of Philosophy
The University of Edinburgh
April 2018

Abstract

The inflationary paradigm is one which was designed to answer questions that arose from classical Hot Big Bang cosmology. The period of rapid expansion in the early Universe provides a mechanism to solve the flatness, horizon and relic problems. More importantly, since the theory was first introduced it has been realised that it also provides a mechanism to generate the initial perturbations from which structure in the Universe can grow.

In the zoo of potential inflationary models there is a dominant class: slow-roll inflation. The idea that the energy density of the inflationary field is dominated by its potential highly simplifies the calculations required to predict observable quantities. This simplification relies on all the information required to know the subsequent dynamics of the field to be encoded in the space $\phi - \dot{\phi}$; it must be an effective phase space. I show that $\phi - \dot{\phi}$ can be considered to be such a space for the most general scalar-tensor theory which gives second-order equations of motion: Horndeski theory. There are theoretical issues associated with this reduction that are illuminated through specific examples in which they occur.

A theoretical issue with inflation is that there is an overabundance of models, with some capable of predicting any value of the possible observables. The second block of work in this thesis looks at a particular set of models that make the same observational prediction. These "attractor" models utilise a non-minimal coupling between the inflationary fields and gravity and are studied in depth, both in the case of one and several fields.

Firstly, I examine the Universal Attractors, a single field subset of these models. I show, in detail, the observational prediction such a model makes in the case of a strong non-minimal coupling and then examine the constraints it would be possible to put on such a coupling if a confirmed detection of primordial gravitational waves was made. Despite the discussion existing in the literature

there is a small deviation of the Universal Attractor models from the predictions of the Starobinsky model. Furthermore, the coupling, ξ is found to be constrained so that $|\xi| < 1$ in the case where there a level of detectable primordial tensor modes.

While the attractor models have an effective one-field description in reality there are several other fields that are assumed to be fixed during the inflationary phase. This claim requires careful examination as the field-space of the models generally is not flat. This curvature can cause a destabilising effect with certain parameters and so I investigate how susceptible the α-attractors and related models are to the destabilisation. A key result of this chapter is to highlight how important it is to not rely on the slow-roll approximation when assessing the effect of the instability, as the region where the effect begins to become large corresponds with the region where slow-roll begins to break down. Assuming the slow-roll approximation is valid leads to an over-estimation of the effect that the instability mechanism has. Despite this, some of the models considered are seen to experience the instability for certain ranges of model parameters. Making the assumption that any occurrence of the instability will, at the very least, move the observational prediction of the model outside the currently constrained range allows a constraint on the model parameter in question which directly translates to a theoretical lower bound on the tensor-scalar ratio, $r > 0.0005$.

Lay Summary

Cosmology, the study of the Universe, is full of mysteries; there are many things that are poorly understood. One of the most fundamental of these mysteries, which dates back almost 14 billion years, to the very limit of well understood physics: why does the Universe look the way it does?

This question can be broken down into two separate ones; the first of which is why is the Universe nearly the same in every direction? The everyday world looks different in every direction but looking at larger and larger distances the Universe starts appearing more and similar in every direction. This is problematic since different sides of the Universe are so far apart that it seems no information can possibly have been exchanged between them.

The second mystery is where the structures in the Universe come from. Galaxies, stars and planets are all created by gravity causing clumps of matter slightly more dense than their surroundings to collapse. There has to be a mechanism that creates these original clumps, the seeds of structure in the Universe.

The leading theory that solves these problems is a period of rapid expansion in the early Universe lasting less than a billionth of a billionth of a second: inflation. Before inflation, the parts of the Universe that become what we observe today were very close together, and so in balance. During inflation these regions get blown apart to distances so vast it appeared to early theorists that they could never have interacted, when in fact they did. This explains why the Universe looks the same in all directions. During inflation there are tiny, random fluctuations that get blown up to huge scales by the rapid expansion. These originally microscopic fluctuations then become large enough to begin forming galaxies and other larger structures solving the mystery of the origin of structure in the Universe.

The purpose of this thesis is to examine the theoretical assumptions that have

gone in to various models of what may have been responsible for inflation. In particular, the models considered here are all based on an extension of the standard model of gravity, General Relativity. These models all have specific qualities that make them attractive. The main positive feature is that they appear to line-up very well with observations. The predictions of the models require certain assumptions to hold true and these are tested in this thesis. In some cases, the assumptions are valid but there appears to be a potential problem in models which require there to be more than one source of energy driving inflation. The interactions between the two energy sources are able to force the evolution of the Universe away from what we see today. This restricts the possible range of predictions made by these models and, in the long-term, may allow such models to be ruled out.

Declaration

I declare that this thesis was composed by myself, that the work contained herein is my own except where explicitly stated otherwise in the text, and that this work has not been submitted for any other degree or professional qualification except as specified.

Parts of this work have been published in [32, 33].

(*David C. Edwards, April 2018*)

Acknowledgements

Getting to the point where this thesis is complete has been a long and difficult journey. There have been many people that have helped me get to this point and here I wish to thank them.

The biggest thanks must go to Sara Schmidt. She helped me rediscover the drive and focus needed to work hard through the latter stages and finally finish my thesis. Without her support I do not think that I would have made it this far but with it I come out the other end stronger and ready for the rest of my life. This because outside of work she has provided me with both purpose and enjoyment, making my life better. Sara, the love that we share puts everything else in perspective and, very simply, makes me happy.

My parents have always supported me and encouraged me to push myself. Without them being actively involved in my life I would never have been able to make it to University, let alone complete my PhD. Going home provided much needed respite from research work and the interest they showed reminded me of how fortunate I was to be able to do what I have done. Thank you so much, I owe you both for getting to this point.

When I started out more than four years ago I had no idea on how to undertake professional research. For helping me understand the process and opening my eyes to the current state of the literature I wish to thank my supervisor Professor Andrew Liddle. The guidance and encouragement he provided during the course of my PhD has been invaluable.

In the same vein, it is very important to have people read your work who were not involved in the process of producing the final results. The extra insight they can offer into how to clarify an explanation or re-word a conclusion helps transform the finished product. Therefore I would also like to thank Alex Hall and Andy Taylor for their feedback on various chapters of this Thesis.

An important part of any research effort is the discussion to be found around the department. The Institute for Astronomy hosts many people whose input and general knowledge have been immensely helpful to my work and understanding of the wider subject.

Finally, there are people who made my time at the Royal Observatory Edinburgh a pleasure. So, once again, I wish to thank Alex Hall, as well as Alex Amon, Ami Choi, Michael Wilson, Joey Faulkner, Johanna Vos and Owen Turner. They made it a pleasure to be in the office.

Contents

List of Figures

List of Tables

Chapter 1

Gravitation

1.1 The Physics of Gravity

The currently favoured theory of gravity is the General Theory of Relativity. This section will introduce the key physical ideas that go into the theory while the subsequent sections will develop the mathematical toolkit.

1.1.1 Special Relativity

A fundamental assumption in pre-relativistic mechanics is that time is universal, every observer can agree upon it [69]. This is closely tied to the idea of simultaneity whereby if two events appear to occur at the same time to one observer then they must for all others. It is this assumption that must be broken first when moving into the realm of Special Relativity. Instead, it is axiomatic that the speed of light is constant. The effect that this statement has on simultaneity can be see in the canonical example of a train moving past a station. This example follows the basic idea of Ref. [23]. Consider a train with a passenger exactly in the middle of the carriage and a platform with an observer on it. As the train moves past the platform the passenger sends out light rays forwards and backwards. To the passenger, it is an equal distance to the front and back of the carriage and so the light rays must reach both ends at the same time, i.e. they arrive simultaneously. However, the observer on the platform would disagree with this conclusion if the speed of light is constant. To them it appears that the ray that

goes towards the back of the train has a shorter distance to cover as the back of the train is moving towards the point where the light emitted from. This means that it arrives at an earlier time than the other light ray leaches the front of the carriage.

The logical consequence of the constancy of the speed of light is that time and distance are measured differently by different observers. The invariant quantity is instead the interval between two events defined as:

$$ds^2 = -c^2 d\tau^2, \tag{1.1}$$

where τ is a quantity known as the proper time between two events. The coordinate systems of two different inertial observers are linked by a Lorentz transformation which, when represented by a matrix, is a solution to the equation:

$$\Lambda^T \eta \Lambda = \eta, \tag{1.2}$$

where η is known as the Minkowski metric and is given by:

$$\eta = \begin{bmatrix} -1 & 0 & 0 & 0 \\ 0 & 1 & 0 & 0 \\ 0 & 0 & 1 & 0 \\ 0 & 0 & 0 & 1 \end{bmatrix}. \tag{1.3}$$

The solutions, Λ, form a group known as the Lorentz group, $O(1,3)$. However, in physical applications it is usually required that the direction of time is preserved so the restricted Lorentz group, $SO^+(1,3)$, is used. The Minkowski metric allows the interval to be written as:

$$ds^2 = d\boldsymbol{x}^T \eta d\boldsymbol{x}, \tag{1.4}$$

where $d\boldsymbol{x}$ is a four-vector, $d\boldsymbol{x} = (dt, d\vec{x})$.

1.1.2 Newtonian Gravity

Special Relativity deals with dynamics but does not say anything about gravity. Before General Relativity gravity was described by Newton's Universal Law of Gravitation, given by:

$$\mathbf{F} = -\frac{GMm}{|\mathbf{r}|^2}\hat{\mathbf{r}}. \tag{1.5}$$

This simple equation is incredibly accurate. In the Solar System it accounts for the motion of nearly all the planets and their moons. The sole exception [106] indicates that the theory must be developed even before trying to combine it with Special Relativity. The particular problem is the advance of the perihelion of Mercury. While the, much smaller, precession of the other planets can be explained with Newtonian gravity it had been observed that Mercury was precessing roughly 40 arcseconds per century faster than that theory would predict.

1.1.3 Equivalence Principles

The *weak* equivalence principle states that gravitational and inertial mass are always equivalent. This statement has important consequences for Newtonian gravity in the framework of classical mechanics as it allows the equations for Newtonian gravity to be invariant under uniform acceleration. It is precisely this invariance that leads to the idea that objects in free-fall appear to be weightless in the frame where the acceleration due to gravity is zero. The weak equivalence principle has been extensively tested (to one part in 10^{13}) and will be further constrained in the future by the MicroSCOPE [12, 101] and STEP satellite missions [82].

While the weak equivalence principle works well with classical mechanics, problems develop rapidly in trying to reconcile it with Special Relativity, electromagnetism and Newtonian gravity [106]. According to Special Relativity, the speed of light in a vacuum is constant. However this leads to inconsistencies when photons in a Newtonian gravitational field are considered. The first statement that must be accepted is that since photons carry energy they must be affected by gravity. This is shown by, for example, Bondi's thought experiment where he argues that if photons were not affected by gravity then it would be possible to build a perpetual motion machine. This effect of gravity on photons, the gravitational redshift, was measured by Pound and Rebka [87]. The measurement was made by placing an emitter (consisting of atoms in an excited state) at the top of tower. As the electrons in the emitter fell to the ground state they would emitted photons of a fixed wavelength. Then, as these photons travel down to the bottom of the tower General Relativity predicts that they will blueshifted by the presence of gravity. The exact amount that they are blueshifted can be measured by moving an absorbing sample of the same atoms

used for emission (where these atoms are in the ground state). The relative velocity required will give the magnitude of the blueshift by the usual doppler formula. Any measured blueshift confirms the idea that photons are affected by gravity.

The problem that this gravitational redshift causes is that there is no explanation for it in the combination of Newtonian gravity and Special Relativity. As the light travels through the gravitational field there is nothing in the theory that causes the frequency of the light to change. The only further way in which the redshift could be explained is if there is a change in the time difference between the arrival of wavefronts at the point high in the gravitational field compared to the time difference of the emitted wavefronts lower in the field. This is not allowed by Special Relativity since there is no relative motion between the emission and detection points. Thus, there is no explanation of for gravitational redshift in the combination of Newtonian gravity with Special Relativity and electromagnetism.

The above calls for a new equivalence principle. The *strong* equivalence principle states: there is no observable distinction between the local effects of gravity and acceleration. This idea is often alternatively described by saying that there is no experiment one could perform in a sealed room to determine if the room was accelerating or if it was at rest on the surface of, for example, a planet. In essence, Special Relativity is believed to be a good theory in the absence of gravity. Thus, the starting point for a theory incorporating gravity is to say that Special Relativity holds locally, in a sense that will be made more concrete later, in free-falling frames. The key question which general relatively solves is how these frames tie together.

1.1.4 General Covariance

In the above discussion, the principle of covariance has been implicitly interwoven throughout. In classical mechanics, the theories are invariant under Galilean transformations (physically corresponding to rotations and translations). In Special Relativity this invariance is extended to the Poincaré group which includes translations and the Lorentz group. However, in General Relativity the principle of general covariance is adopted. This principle says that the laws of physics should hold true for all coordinate transformations, which leads to the idea that it is best to express physical laws in equations which are generally covariant, i.e. do not change under coordinate transformations.

1.2 Differential Geometry

This section outlines some textbook Mathematics that is required to fully grasp the notions of a "curved" spacetime. The following is a combination of several references blended together to be as concise but fully descriptive as possible. Refs. [18, 19, 24, 96, 97] form the main basis for this section with other references highlighted when appropriate.

1.2.1 Manifolds

Intuitively, a manifold can be thought of as the extension to n-dimensions of the idea of a smooth but otherwise arbitrarily curved surface. To define it formally requires the use of open sets, charts and atlases.

On $\mathbb{R}^n$ define the distance between two points, x and y by a map $\widetilde{d} : \mathbb{R}^n \to \mathbb{R}$ where $\widetilde{d}$ is quadratic in $x_i - y_i$.[1] An open ball around y is then $\{x \in \mathbb{R}^n : \widetilde{d}(x, y) < r, y \in \mathbb{R}^n\}$. An open set on $\mathbb{R}^n$ is a set constructed from any number of open balls. More formally, $V \subset \mathbb{R}^n$ is an open set if $\forall y \in V$ there is an open ball centred on y and wholly contained in V.

A chart is a coordinate system that maps part of a set, M to an ordered tuple of real numbers. Consider $U \subset M$ and a map $\phi : U \to \mathbb{R}^n$. If the image $\phi(U)$ is an open set in $\mathbb{R}^n$ then U is an open subset of M and (U, ϕ) is a chart. In general, for two charts (U, ϕ_1) and (V, ϕ_2) where $U, V \subset M$ and $U \cap V \neq \emptyset$ it is not true that $\phi_1(U \cap V) = \phi_2(U \cap V)$. However, if the composition $\phi_2 \circ \phi_1^{-1} : \phi_1(U \cap V) \to \phi_2(U \cap V)$ exists and is differentiable then it provides a way to relate the two charts known as a coordinate transform.

A set of charts $\{(U_\alpha, \phi_\alpha)\}$ is called an atlas if $\bigcup U_\alpha = M$ and where the $U_\alpha \cap U_\beta \neq \emptyset$ the coordinate transform exists. A manifold is then a set M along with its maximal atlas, the one that contains all possible charts. For example, the surface of a sphere with every possible projection to $\mathbb{R}^2$.

[1] The precise form of $\widetilde{d}$ is unimportant. The name open ball suggests picturing, for example, a circle in two-dimensions where the edge is not included. However, an equally valid definition would be, for example, an ellipse. In fact, $\widetilde{d}$ need only follow the following rules: [61] *i*) The distance is between two points, x and y, is zero only when $x = y$, *ii*) The distance from x to y is the same as y to x, *iii*) The triangle inequality is satisfied.

1.2.2 Curves and Vector Spaces

The goal of this section is to introduce the notion of vector spaces which are associated with a single point on the manifold. The first step in doing this is to introduce the simpler concepts of curves and functions on a manifold.

In simple language a curve may be thought of as a parameterised line on the manifold, M. More precisely it is a mapping, $\gamma : \mathbb{R} \to M$. A key point is that different parameterisations of the line give different curves. A point, p, is said to lie on a curve if it is in the image of γ.

Again starting with an English language description, a function, f, on a manifold, M, assigns a real number to every point on M. That is, it is a map $f : M \to \mathbb{R}$. The function f is said to be differentiable if the composition $f \circ \phi_\alpha^{-1} : V_\alpha \to \mathbb{R}$ is differentiable in $\mathbb{R}^n$ where (V_α, ϕ_α) is a chart of M. The space of all functions on M is denoted as $\mathcal{F}$ and the space of functions at a particular point p is denoted as $\mathcal{F}_p$.

The above definitions allow a vector space to be defined by considering a derivative along a curve γ which passes through the point p. Since this curve consists of points on M then the function f is defined along it and the derivative with respect to the parameter of the curve λ as:

$$\frac{df}{d\lambda} = \frac{d}{d\lambda} f \circ \gamma = \frac{d}{d\lambda}\left[(f \circ \phi^{-1}) \circ (\phi \circ \gamma)\right]. \tag{1.6}$$

Expanding the right-most expression using the chain rule (noting the domain and codomain of the functions[2]) gives:

$$\frac{df}{d\lambda} = \frac{\partial(f \circ \phi^{-1})}{\partial x^\mu} \frac{d(\phi \circ \gamma)^\mu}{d\lambda}. \tag{1.7}$$

This can then be written a little more informally to give a clear idea of the interpretation:

$$\frac{df}{d\lambda} = \frac{dx^\mu}{d\lambda} \frac{\partial f}{\partial x^\mu}. \tag{1.8}$$

Since the function f is arbitrary then the above equality holds for all possible functions and so:

$$\frac{d}{d\lambda} = \frac{dx^\mu}{d\lambda} \frac{\partial}{\partial x^\mu}. \tag{1.9}$$

That is, the partial derivatives $\frac{\partial}{\partial x^\mu}$ form a basis (necessarily of dimension n) of

[2]The compositions map: $\phi \circ \gamma : \mathbb{R} \to \mathbb{R}^n$ and $f \circ \phi^{-1} : \mathbb{R}^n \to \mathbb{R}$

the space T_pM.

1.2.3 Covariant Derivatives

The important point to note from the previous section is that tensors are defined at specific points on a manifold. This means that to compare tensors at different points (for example in calculating derivatives of a vector field) some way of comparing vectors at different points must be constructed. This is usually not an issue in when gravity is not an important effect in the problem at hand, since when considering Euclidean and Minkowski spaces in Cartesian coordinates the direction of, for example, a vector is well-defined across the space.

A problem can be seen to arrive if the standard Cartesian coordinates of Euclidean space are replaced with the spherical polar coordinate system. Now, each unit vector depends on the location of the point at which the vector is defined and so the coordinate description of the vector changes as it is moved around the plane. The situation becomes more troublesome when considering an arbitrary manifold, which doesn't necessarily permit a global Cartesian coordinate system. The point of this section is to establish a definition of a derivative which ignores such coordinate changes and measures the change in the underlying geometric object itself, in other words the derivative operation outlined below will be tensorial in nature.

The fact that vectors at different points cannot be naively compared is tied to the lack of a global idea of parallelism. A short thought experiment can demonstrate the concept, see Figure 1.1. Starting at the North Pole, imagine holding an arrow directly in front of you and walking in the direction that the arrow points until you reach the South Pole at which point you lay the arrow on the ground and return to the North Pole. Now, start out with an arrow pointing in the same direction as the first but instead of it being held in front of you, it is held to the side, pointing away from you at right angles. This time, when you walk to the North Pole (travelling straight ahead) the arrow in your hand will be anti-parallel to the one which is lying on the ground. So, even on a relatively simple manifold the question as to whether two vectors at different points are parallel is dependent on the path taken between the two points.

In the above example it is intuitive as to what is meant by the idea of parallel transport but this may not be the case for a general manifold. Suppose that there

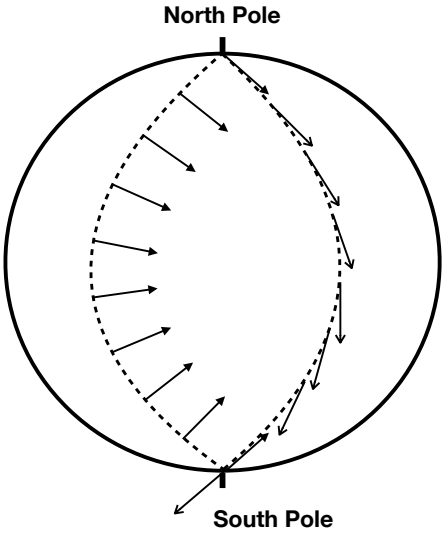

Figure 1.1 *A cartoon to illustrate the path dependence of the difference of two vectors on a curved surface. Here the initial vector is the same at the North Pole but depending on how the South Pole is reached the final directions of the vector can be anti-parallel.*

is a manifold, M, and a curve γ which has a tangent vector, $\bar{U}$. The definition of a vector, $\bar{V}$, which is parallel transported along γ is:

$$\nabla_{\bar{U}}\bar{V} = 0, \tag{1.10}$$

where ∇ is the covariant derivative operator.

Now a definition of the covariant derivative operator must be made. To begin, take a vector field, $\bar{W}$, which is defined along γ. This field takes different values along the curve at different points. In particular, at point P it takes the value $\bar{W}_P$ and at point Q it takes the value $\bar{W}_Q$. Notice that since $\gamma : \mathbb{R} \to M$ there is a parameter λ that encapsulates the difference between the two points. The parameter will be given the value λ_P at point P and λ_Q at point Q. It is possible to define a second vector field, $\bar{W}^*_Q$, by parallel transporting the vector $\bar{W}_Q$ along γ. Since P is a point on γ there is a vector in the field $\bar{W}^*_Q$ that is defined in the same tangent space as $\bar{W}_P$ and hence normal arithmetical operations can be performed on the two vectors. Denoting the vector in $\bar{W}^*_Q$ at P as $\bar{W}^*_Q|_P$, the

definition of the covariant derivative is:

$$\left(\nabla_{\bar{U}}\bar{W}\right)_P = \lim_{\epsilon\to 0}\frac{\bar{W}^*_Q|_P - \bar{W}_P}{\epsilon}, \tag{1.11}$$

where $\epsilon = \lambda_Q - \lambda_P$. Since this quantity is the difference of two vectors it is itself a vector. Hence, it is a geometric object which is independent of coordinate transformations. The interpretation of the covariant derivative is that it says how much a vector changes when it is moved in the direction of a second vector.

Despite the coordinate independent description being physically motivated by the principle of general covariance, in the real world tensorial quantities must be measured and this implies a particular choice of coordinates so studying the coordinate description of the covariant derivative is necessary. In particular, it is possible to ask how a basis vector $\bar{e}_i$ changes when it is moved in the direction $\bar{e}_j$. This allows the definition of the connection coefficients, Γ^k_{ij}, as:

$$\nabla_{\bar{e}_j}\bar{e}_i = \Gamma^k_{ij}\bar{e}_k.^{\,3} \tag{1.12}$$

Since tensors are by definition linear and ∇ follows the usual product rule for derivatives it is possible to construct:

$$\begin{aligned}
\nabla_{\bar{U}}\bar{V} &= U^i\nabla_{\bar{e}_i}(V^j\bar{e}_j) && (1.13)\\
&= U^i\left[\bar{e}_j\nabla_{\bar{e}_i}(V^j) + V^j\nabla_{\bar{e}_i}(\bar{e}_j)\right] && (1.14)\\
&= \left[U^i\frac{\partial V^j}{\partial x^i} + U^iV^k\Gamma^j_{ik}\right]\bar{e}_j. && (1.15)
\end{aligned}$$

This is the general expression for the vector $\nabla_{\bar{U}}\bar{V}$, with the components given inside the square brackets. it is common to be concerned with the covariant derivative in a particular coordinate direction, $\nabla_{\bar{e}_\beta}\bar{V} \equiv \nabla_\beta\bar{V}$. This is found by the use of the above expression with $\bar{U} = \bar{e}_\beta$ so that:

$$\nabla_\beta\bar{V} = \left[\frac{\partial V^\alpha}{\partial x^\beta} + V^\sigma\Gamma^\alpha_{\beta\sigma}\right]\bar{e}_\alpha, \tag{1.16}$$

where, once again, the components are inside the square brackets.

[3]The discussion above which leads to the definition of the covariant derivative introduces one of a more general collection of ways to connect vectors at different points in the manifold known as connections. In the literature, the phrases covariant derivative and connection are occasionally used interchangeable since the connection defines the covariant derivative and vice versa.

1.2.4 Riemannian Geometry

To keep the preceding discussion general, much of the previous sections has remained abstracted in mathematical notion and terminology. The purpose of this section is to introduce (pseudo-) Riemannian geometry which will connect the mathematics of differential geometry to the physics of General Relativity.

The new feature that is introduced in Riemannian geometry is the metric, $g(\bar{\cdot}, \bar{\cdot})$. This is a two-form (a tensor that maps two vectors to $\mathbb{R}$) and can be thought of intuitively as a way to define distance on a manifold. The infinitesimal squared displacement, ds^2, is given as:

$$ds^2 = g(d\bar{x}, d\bar{x}) = g_{\mu\nu} dx^\mu dx^\nu, \tag{1.17}$$

where the second equality is simply writing the infinitesimal line element in a coordinate form. The quantities $g_{\mu\nu}$ are known as the set of metric coefficients and are required to follow certain rules for use describing spacetime. Firstly, they must be smooth functions of the coordinates. They must also be symmetric so $g_{\mu\nu} = g_{\nu\mu}$. Thirdly, the signature of the metric must be the same at every point on the manifold [106]. The signature of the metric is a tuple of the number of positive and negative eigenvalues the matrix representing the metric has. Throughout this thesis the metric signature will be $(3, 1)$. Physically, this corresponds to the number of space-like and time-like directions respectively. This particular signature means that it is really pseudo$-$ (or sometimes semi$-$) Riemannian geometry which gives the mathematics behind General Relativity.

It is common to represent the metric as an $n \times n$ matrix as was done for the specific case of the Minkowski metric in equation (1.3). It can be shown that any metric which follows the rules laid out above can, at a point be written as the Minkowski metric. More precisely, it is possible to make a coordinate transformation such that:

$$g_{\mu\nu} = \eta_{\mu\nu} + O(\bar{x}^2), \tag{1.18}$$

where the expression $O(\bar{x}^2)$ encapsulates the fact that the approximation is accurate up to second-order in the components of $\bar{x}$ which is a vector describing the displacement from the point at which the coordinate transformation is defined.

Until now the precise form of the connection coefficients has been left unconstrained, in other words the reasoning above has left some freedom in precisely

how the connection connects vectors at different point. Specifying that the connection must be both metric compatible and torsion-free removes the freedom and provides an expression for the individual components of the connection. To be metric compatible and torsion-free, a connection must satisfy:

$$\nabla_\beta g_{\mu\nu} = 0 \text{ and } \Gamma^\rho_{\sigma\lambda} = \Gamma^\rho_{\lambda\sigma}. \tag{1.19}$$

These constraints allow for a unique connection to be defined, the Levi-Civita connection. The coordinate expression for the Levi-Civita connection is:

$$\Gamma^\rho_{\sigma\lambda} = \frac{1}{2} g^{\rho\delta} \left(\partial_\sigma g_{\lambda\delta} + \partial_\lambda g_{\delta\sigma} - \partial_\delta g_{\sigma\lambda} \right). \tag{1.20}$$

It can be seen from this expression that in the case of the Minkowski metric, and other constant metrics, the covariant derivative is precisely the usual partial derivative since $\Gamma^\rho_{\sigma\lambda} = 0$.

Unlike derivatives in $\mathbb{R}^3$ it is not generally true that covariant derivatives on a pseudo-Riemannian manifold commute. This is linked once again to the idea of path dependance. It matters which direction the vector is moved first, and allows the definition of a new tensor: the Riemann tensor. Expressed in terms of basis vectors $\bar{e}_\alpha, \bar{e}_\beta$ and a vector $\bar{Z}$, the Riemann tensor is given by:

$$R(\bar{e}_\alpha, \bar{e}_\beta)\bar{Z} = \nabla_\alpha \nabla_\beta Z - \nabla_\beta \nabla_\alpha Z. \tag{1.21}$$

The corresponding coordinate expression for the Riemann tensor is:

$$R^\rho{}_{\sigma\alpha\beta} = \partial_\alpha \Gamma^\rho_{\beta\sigma} - \partial_\beta \Gamma^\rho_{\alpha\sigma} + \Gamma^\rho_{\alpha\lambda}\Gamma^\lambda_{\beta\sigma} - \Gamma^\rho_{\beta\lambda}\Gamma^\lambda_{\alpha\sigma}. \tag{1.22}$$

Further useful quantities can be found by taking the trace of the Riemann tensor to obtain the Ricci tensor:

$$\mathrm{Ric}(X, Z) = \mathrm{trace}\left[Y \mapsto R(X, Y)Z \right] \tag{1.23}$$

and in coordinate form:

$$R_{\alpha\beta} = R^\lambda{}_{\alpha\lambda\beta}. \tag{1.24}$$

The geometric interpretation of the Ricci tensor is that it provides a measure of how much the volume of an object is distorted as it moves around the manifold. This can be seen by, for example, the appearance of the Ricci tensor in Raychaudhuri's equation which describes the evolution of the change in volume

of a congruence of geodesics [18]. The final quantity that will be of interest in this thesis is the Ricci scalar which is simply the contraction of the Ricci tensor, so:

$$R = g^{\alpha\beta} R_{\alpha\beta}. \tag{1.25}$$

The last two quantities play an important role in General Relativity. The Ricci scalar is the unique scalar quantity that it is possible to construct that consists of no more than the second derivative of the metric [24, 106]. This proves important when connecting it to a physical description of spacetime.

1.3 General Relativity

With the necessary mathematics now in place it is possible to outline the theory of General Relativity. The first question that should be answered is: what happens to the laws of physics in curved spacetime? Given the principle of general covariance and the strong equivalence principle outlined above the answer to this question is relatively simple. The minimal-coupling principle [18] is a recipe that says to generalise a law of physics that is known to be true in flat spacetime to a curved spacetime one must first write it in a tensorial form and then assert that the law in tensorial form is true in curved spacetime.

The second question which should now be asked is: how does the energy content of the Universe cause spacetime to curve? There are several alternative routes to answer this question but the most useful for this thesis is by use of the least action principle. In order to construct an action which is invariant under coordinate transformations (this is desirable since the physics should not depend on the chosen coordinate system) the action must be constructed in a specific way. Firstly, the integral measure should be invariant under coordinate transformations. This requires a departure from the usual d^4x measure adopted in flat spacetime as this will clearly change if the coordinate system does. Instead, the invariant $\sqrt{-g}\, d^4x$ is used. The second step in constructing the action is to pick a Lagrangian density which is invariant under coordinate transformations, in the language of manifolds this is a scalar. Another subtlety to note is that it is always possible to choose a set of coordinates on a manifold where derivatives of the metric vanish (this is related to the existence of local inertial coordinates). This statement means that the Lagrangian density should include second derivatives of the metric. As noted in the previous section the Ricci Scalar

is the unique scalar quantity consisting of no more than the second derivative of the metric and so this becomes a natural choice to use as a Lagrangian density in the action. This gives the gravitational action, known as the Hilbert action, as:

$$S_G = \kappa^{-1} \int \sqrt{-g}\, R\, d^4x, \tag{1.26}$$

where κ is a non-zero, but otherwise arbitrary, constant which will measure the relative strength of gravity. This action can then be combined with a matter action, S_M (e.g. that for a scalar field or the standard model action), to have a system that contains both matter and gravity. Varying such an action with respect to the metric will lead to the equations of motion for the metric while varying with respect to the matter content will provide the equations of motion for the matter. The metric's equations of motion are known as the Einstein equations and have the form:

$$R_{\mu\nu} - \frac{1}{2} g_{\mu\nu} R = \kappa T_{\mu\nu}, \tag{1.27}$$

where $T_{\mu\nu}$ is the energy-momentum tensor of the matter. Ths equation allows κ to be fixed by forcing the theory to match with Newtonian gravity in the corresponding limit. In units where $c = 1$, $\kappa = 8\pi G$ but for the remainder of this thesis $M_p^2 = \frac{1}{8\pi G}$ is used where M_p is known as the reduced Planck mass. There are some important points to note in the derivation of equation (1.27). Firstly, since the Lagrangian density used contains second derivatives of the metric, the standard Euler-Lagrange equations cannot be used[4] and the equation is derived by direct variation of the metric. Secondly, the energy-momentum tensor is given by:

$$T_{\mu\nu} = -2 \frac{1}{\sqrt{-g}} \frac{\delta S_M}{\delta g^{\mu\nu}}. \tag{1.28}$$

While this expression for the energy-momentum tensor may not be obviously connected with how the same quantity is defined in other contexts, it can be shown to correspond exactly in the case of, for example, a scalar field.

Finally, it is possible to add a constant scalar, Λ, to the Lagrangian density in the Hilbert action. This leads to the modified Einstein equation:

$$R_{\mu\nu} - \frac{1}{2} g_{\mu\nu} R + \Lambda g_{\mu\nu} = \kappa T_{\mu\nu}. \tag{1.29}$$

[4]This situation can be changed by the use of appropriate boundary terms. While this is not usually considered in the standard treatment of cosmology it can have important consequences, see chapter 3

This could be viewed as the simplest deviation from General Relativity and more complex deviations will be discuss in the next section.

1.4 Modifications to General Relativity

The work in this thesis will only deal with a particular subset of modified gravity theories known as scalar-tensor theories of gravity. These theories introduce a new scalar degree-of-freedom through the inclusion of a scalar field which is coupled to the metric in a "non-minimal" fashion. A minimal coupling to gravity is one where the only coupling between gravity and the energy content is from the $\sqrt{-g}$ in the invariant measure, so the action is written as:

$$S = S_G + \int \sqrt{-g}\,\mathcal{L}_M\, d^4x, \tag{1.30}$$

as is the case in General Relativity. A non-minimal coupling is then one where there are extra interaction terms between the matter content and the metric. In the case of a scalar-tensor theory the simplest interaction of this type is of the form $f(\phi)R$, though other more complicated interactions are possible as will be outlined in the succeeding sections.

There are many motivations for introducing a scalar field and a non-minimal coupling. The inclusion of the field can simply be motivated by the existence of an apparently fundamental scalar field: the Higgs field. Moreover, a scalar field is the simplest field that can be added to a theory and so is a logical place to start trying to answer questions such as, for example, is the gravitational constant time varying? The coupling terms can have a variety of effects such as making the theory conformally invariant, see below, or by introducing screening mechanisms which can be useful in late-time scenarios. When constructing a theory from an effective field theory perspective all terms that follow certain symmetries are included and this can include complicated coupling terms. Finally, when dealing with high energy beyond the Standard Model theories, extra fields and diverse couplings often appear in the limits which correspond to the physical Universe.

It is worth briefly noting that there are other approaches to modifying General Relativity which could be adopted. A conceptually simple approach is to say that instead of the Hilbert action, equation (1.26), a Lagrangian density which is a function of the Ricci scalar can be used instead so that the action takes the form:

$$S = \kappa \int \sqrt{-g}\, f(R)\, d^4x. \tag{1.31}$$

Theories of this type are known as $f(R)$ theories of gravity. It has been shown that it is possible, at least at the classical level, to re-write theories of this type as scalar-tensor theories [105]. However, it has been argued that once terms such as R^2 are included in the action there is no reason to not include other monomial contractions of the Riemann tensor such as $R^\mu_\nu R^\nu_\mu$ [15]. These theories are of a different type and seem to have some useful features such as being renormalisable to all orders.

A second potential modification to General Relativity is the introduction of a second metric to create a bi-metric theory. From a field theory point-of-view gravity is the theory of a massless spin-2 field [37] and so a natural extension to the standard model is the inclusion of further, potentially massive, spin-2 fields. These fields can be set-up so that they only directly couple to gravity with their effect on the matter sector only being due to the indirect link through such a coupling. This has the benefit of leaving the matter sector physics essentially unaffected by the new fields [95].

An early attempt to construct a theory which unifies gravity and electromagnetism is the Kaluza-Klein theory. The basic premise of this theory is to try and encode in geometry not only gravity but electromagnetism as well. This is done by introducing a fifth dimension and dealing with a new metric $\gamma_{\mu\nu}$ which now has 15 degrees of freedom corresponding to the 10 of gravity, 4 of electromagnetism and 1 residual scalar degree of freedom. To make the theory seem to be four-dimensional (like the world around us) the fifth dimension is compactified. It can be thought of, essentially, as being folded into a circle. This is reflected in the $U(1)$ symmetry of electromagnetism. The technique of compactification has been extended to, amongst others, Yang-Mills theory.

1.4.1 Scalar-Tensor Theories: Conformal Couplings

The Universal Attractor and N-dimensional attractor work is based on the idea of conformally coupled scalar field. Here I will motivate and introduce the conformal coupling as well as the idea of Einstein and Jordan frames.

The work covered in this thesis is all based on the idea of scalar-tensor theory of gravity but more specifically the work in chapters 4 and 5 is based largely

on a particular subset of scalar-tensor theories: those that have a scalar term multiplying the Ricci scalar in the gravitational action. This coupling can be considered a route to conformal invariance and as such is referred to a conformal coupling.

The General Theory of Relativity is not conformally invariant. That is, the equations of motion change under a conformal transformation[5] of the form:

$$g_{\mu\nu} \to \Omega^{-1}\tilde{g}_{\mu\nu}. \tag{1.32}$$

Intuitively, a conformal transformation is one which locally changes the lengths of lines but leaves angles intact. A sketch for two-dimensions is shown in Figure 1.2. The change in the equations of motion can be seen by considering the way in which the Ricci scalar subsequently transforms under such a transformation:

$$R \to \Omega\tilde{R} + 6\tilde{g}^{\alpha\beta}\Omega^{1/2}\tilde{\nabla}_\alpha\tilde{\nabla}_\beta\Omega^{1/2} - 12\tilde{g}^{\alpha\beta}\tilde{\nabla}_\alpha\Omega^{1/2}\tilde{\nabla}_\beta\Omega^{1/2}. \tag{1.33}$$

The only time that such a transform will be used in the work presented in this thesis will be inside an action. This means that the terms will be multiplied by $\sqrt{-g}$ and so there are some total derivative terms generated by the transformation (of the form $\sqrt{-g}\nabla_\alpha V^\beta$) which can be ignored in the action.

Since this transformed Ricci scalar is different (and not simply by a total derivative term) after the transformation, the resulting equations of motion will also be different. Physically, the theory of General Relativity is defined in relation to some fixed scale, κ in equation (1.26), and so local length changes do affect predictions. Another way of explaining the lack of invariance is saying that, if you try to construct a theory based solely on the use of light rays to measure lengths and times, this is possible only locally [40]. Therefore, some overall scale has to be imposed to compare measurements at different places.

The introduction of a scalar field and "conformal coupling" term can render the theory conformally invariant however. This is done in such a way that the extra terms generated under the transformation from the coupling precisely cancel with those that come from the the Ricci scalar. The conformally invariant action takes the form:

$$S_C = \int \sqrt{-g}\left[\frac{1}{2}(1 - \frac{1}{6}\phi^2)R - \frac{1}{2}\partial_\mu\phi\partial^\mu\phi + V(\phi)\right] d^4x. \tag{1.34}$$

[5]Alternatively known as a Weyl transformation.

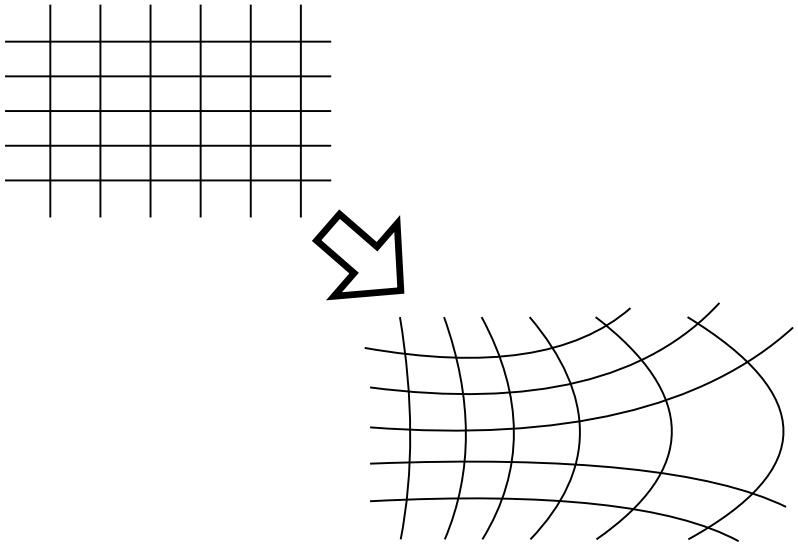

Figure 1.2 *A cartoon to illustrate the idea of a conformal transform. Here a regular cartesian grid has been warped so that the previously straight gridlines are now curved but they still meet at right-angles to one-another.*

Now when the transformation in equation (1.32) is made (with $\Omega = 1 - \frac{1}{6}\phi^2$) along with a field redefinition $\phi \to \Omega\phi$, the same equations of motion are recovered and so the theory is said to be conformally invariant.

The idea of this conformal coupling can be extended by altering the form of the coupling term from $\frac{1}{6}\phi^2$ to the more general $\xi f(\phi)$. This can be useful when considering how such parameters are linked to a high-energy theory where they may often be unconstrained by purely theoretical considerations. Once a particular $f(\phi)$ has been chosen it is possible to put constraints on the coupling parameter ξ in different scenarios, see chapter 4.

1.4.2 Scalar-Tensor Theories: Horndeski Theory

The conformal coupling and its generalisation is only one subset of the ways in which a scalar field can be non-minimally coupled to gravity. The purpose of this section is to introduce the most general possible scalar-tensor theory of gravity in four-dimensional spacetime with second order equations of motion: Horndeski

theory. The requirement of second order field equations ensures that there are no Ostrogradsky instabilities [81] in the theory. This theory was originally derived in specifically four-dimensions by Horndeski [48] but was more recently re-derived from the standpoint of generalising Galileon models in Ref. [25].

Wherever used in this thesis, the DGSZ [25] formulation of Horndeski theory will be used. The action is written as:

$$\begin{aligned} S_H = \int d^4x\sqrt{-g}\,\big(P(\phi,X) - G_3(\phi,X)\Box\phi + G_4(\phi,X)R + \\ [(\Box\phi)^2 - \phi^{;\alpha\beta}\phi_{;\alpha\beta}]G_{4X}(\phi,X) + G_5(\phi,X)G_{\alpha\beta}\phi^{;\alpha\beta} \\ -\frac{1}{6}\left[(\Box\phi)^3 - 3(\Box\phi)\phi_{;\alpha\beta}\phi^{;\alpha\beta} + 2\phi_{;\alpha\beta}\phi^{;\alpha\lambda}\phi^{;\beta}{}_{;\lambda}\right]G_{5X}(\phi,X)\Big) \quad . \end{aligned} \tag{1.35}$$

The functions $P(\phi, X)$ and $G_i(\phi, X)$ are arbitrary, analytic functions of the scalar field, ϕ, and $X = g^{\mu\nu}\partial_\mu\phi\partial_\nu\phi$. These arguments will not be written in the following to increase readability. Also, a subscript ϕ or X denotes a partial derivate with respect to that quantity, semi-colons denote covariant derivatives, $\Box$ is the covariant D'Alembertian operator and greek indices run over all four spacetime dimensions.

A recent development is the discovery of so-called "Beyond-Horndeski" models. These are models where the equations of motion contain third derivatives when the theory is considered in curved spacetime but these higher derivatives do not induce an Ostrogradsky instability. The phenomenology of these models is extended beyond that of the Horndeski models by phenomena such as the ability of the scalar sector to affect the sound speed of a minimally-coupled matter sector [43]. The extra terms appearing in beyond-Horndeski theories are precisely those which counter-terms were introduced to remove in Ref. [25]. Therefore, in some sense, the beyond-Horndeski theories could be considered more simple than the original Horndeski theory.

Chapter 2

Cosmology

This chapter introduces the current concordance model of cosmology, highlights some problems with such a model and then discusses a solution to these problems: inflation. It also introduces the most powerful feature of the inflationary paradigm, the spectrum of perturbations created it the early Universe which provide the initial seeds of structure.

2.1 Background Cosmology

2.1.1 Our Expanding Universe

It has long been known that when the velocity of galaxies are calculated it shows that they are moving away from us. In 1929 Hubble [49] showed that this relation is directly proportional to distance, and is independent of the direction to the galaxy. This relationship is known as Hubble's Law and can be written as:

$$v = Hd. \tag{2.1}$$

Despite the simple form of this equation it has profound consequences. The most commonly encountered explanation is that space is expanding isotropically. This is a powerful idea and is particularly useful to provide a global picture of the Universe. However, such a view can cause problems when considering the local expansion of the Universe such as those described in Ref. [85]. The resolution

presented in Ref. [85] is to consider the expanding space idea only to provide initial conditions in the local Universe and then apply standard Newtonian thinking. Fortunately, in the context of inflation such confusion does not arise so the expanding space interpretation is assumed throughout this thesis.

2.1.2 Homogeneity and Isotropy

The Cosmological Principle [62, 84] states that the Universe is both homogeneous and isotropic in space; it looks the same in every direction at every point in space on large scales. It is worth highlighting at this point that "perfect" homogeneity and isotropy, in both time and space, are not part of the Cosmological Principle. Another way to consider the Cosmological Principle is to say that every point in space exhibits both translational symmetry and rotational symmetry about it. From this starting point it is possible to construct a metric that encapsulates this information and, as such, represents the large-scale evolution of the Universe.

As mentioned in section 1.1.1 it must be possible to pick a local inertial frame about some point such that the metric reduces to the Minkowski metric, (equation 1.3). This does not provide much information *per se* other than the metric of the Universe must have the Lorentzian signature, though this is already clear since the tenants of Special Relativity (at least) are taken to hold.

The abandonment of time homogeneity and isotropy means that a universe that is described by such a theory will, in general, have some time evolution but the spatial part, following the Cosmological Principle, will be separate from it. This means that the four-dimensional spacetime manifold can be decomposed into temporal and spatial parts. In more formal language, the universe with which we are dealing is described by a manifold, M, that can be decomposed as $M = \mathbb{R} \times \Sigma$ where Σ is a spatial sub-manifold. This leads to a line element of the form:

$$ds^2 = -dt^2 + g_{ij}dx^i dx^j = -dt^2 + a^2(t)\gamma_{ij}dx^i dx^j. \tag{2.2}$$

In the second equality the time-dependent factor $a(t)$ has been separated as the only way in principle the spatial components of the spacetime metric can depend on time is through an overall multiplicative factor, with any other dependence breaking the cosmological principle by giving some preferred direction. From this point, $a(t)$ will be called the scale factor and represents the growth or contraction of the spatial sub-manifold. The spatial sub-manifold has its own metric whose

components, γ_{ij}, are dependent only on spatial coordinates.

It is convenient to consider the spatial coordinates to be polar coordinates so that $x^i = \{r, \theta, \phi\}$. The only constraint on the spatial sub-manifold is that is must be spherically symmetric and so can have no dependence on the angular coordinates. In the case of a Universe which exhibits Euclidean geometry then the spatial metric reads:

$$\gamma_{ij}dx^i dx^j = dr^2 + r^2(d\theta^2 + \sin^2\theta d\phi^2). \tag{2.3}$$

The situation for a non-Euclidean geometry becomes more complex. Imagining the three-dimensional space to be embedded in a four-dimensional space makes it easy to arrive at a form for the spatial metric. In the case, for example, that the Universe is closed (so that the angles in a triangle add up to more than π radians) it is possible to consider the Universe existing on the surface of a 4-sphere so that, with coordinates $\{w, x, y, z\}$, there is a condition:

$$w^2 + x^2 + y^2 + z^2 = R^2. \tag{2.4}$$

It is possible to eliminate the extra coordinate, w, from the infinitesimal line element which is:

$$\gamma_{ij}dx^i dx^j = dx^2 + dy^2 + dz^2 + \frac{(xdx + ydy + zdz)^2}{R^2 - x^2 - y^2 - z^2}. \tag{2.5}$$

This can then be rewritten as:

$$\gamma_{ij}dx^i dx^j = \frac{dr^2}{1 - R^2r^2} + r^2(d\theta^2 + \sin^2\theta d\phi^2). \tag{2.6}$$

A similar process could be repeated for an open Universe with the replacement of $R^2 \to -R^2$ in equation (2.4) [91]. For a general three-dimensional space a curvature parameter can be defined as:

$$k = KR^2, \tag{2.7}$$

and so the final expression for the infinitesimal line element is:

$$ds^2 = -dt^2 + a^2(t)\left[\frac{dr^2}{1 - kr^2} + r^2(d\theta^2 + \sin^2\theta d\phi^2)\right]. \tag{2.8}$$

It can sometimes be useful to use the conformal time η through the change of

coordinates $dt = ad\eta$. This gives the expression for the infinitesimal line element as:

$$ds^2 = a^2(\eta)\left(-d\eta^2 + \left[\frac{dr^2}{1-kr^2} + r^2(d\theta^2 + \sin^2\theta d\phi^2)\right]\right). \tag{2.9}$$

2.1.3 The Friedmann Equations

The metric, equation (2.8), allows the Einstein equations, equations (1.27) to be solved once an appropriate energy-momentum tensor has been defined. Here, the energy-momentum tensor of a perfect fluid is assumed. That is, when represented as matrix in the unit system of equation (2.8) it has the form:

$$T_{\mu\nu} = \begin{pmatrix} \rho & 0 & 0 & 0 \\ 0 & & & \\ 0 & & pg_{ij} & \\ 0 & & & \end{pmatrix}, \tag{2.10}$$

where ρ is the energy density of the fluid and p is the pressure of the fluid. Taking the trace of this energy-momentum tensor gives:

$$T = g^{\mu\nu}T_{\mu\nu} = -\rho + 3p. \tag{2.11}$$

The Ricci tensor, equation (1.24), for the FRW metric is diagonal with coefficients:

$$\begin{aligned} R_{tt} &= -3\frac{\ddot{a}}{a} && (2.12)\\ R_{rr} &= \frac{a\ddot{a}^2 + 2\dot{a}^2 + 2k}{1-kr^2} && (2.13)\\ R_{\theta\theta} &= r^2\left(a\ddot{a} + 2\dot{a}^2 + 2k\right) && (2.14)\\ R_{\phi\phi} &= r^2\sin^2\theta\left(a\ddot{a} + 2\dot{a}^2 + 2k\right). && (2.15) \end{aligned}$$

Note that the space-space components can be written as $R_{ij} = g_{ij}\left(a\ddot{a} + 2\dot{a}^2 + 2k\right)$. Since the Ricci tensor, metric tensor and energy-momentum tensor are all diagonal the Einstein equation can be split into separate time-time and space-space equations. The space-space equations read:

$$R_{ij} = g_{ij}\left(a\ddot{a} + 2\dot{a}^2 + 2k\right) = 8\pi G\left(pg_{ij} - \frac{1}{2}g_{ij}T\right). \tag{2.16}$$

There is a common multiplicative factor of g_{ij} in each term so it can be cancelled out and thus the space-space equations yield only one equation. This is what should be expected from the imposition of the Cosmological Principle as there is complete freedom to rotate and shift the spatial coordinates. The time-time and single space-space equations read:

$$\frac{\ddot{a}}{a} = -\frac{4\pi G}{3}(\rho + 3p), \tag{2.17}$$

$$\frac{\ddot{a}}{a} = 4\pi G(\rho - p) - 2\left(\frac{\dot{a}}{a}\right)^2 - 2\frac{k}{a^2}. \tag{2.18}$$

The first of these is referred to as the acceleration equation, as it provides information on the rate at which the expansion of the Universe is changing. Substituting the acceleration equation into the second equation above gives:

$$H^2 = \left(\frac{\dot{a}}{a}\right)^2 = \frac{8\pi G}{3}\rho - \frac{k}{a^2}. \tag{2.19}$$

This last equation is known as the Friedmann equation, though collectively the Friedmann equation and acceleration equation together can be referred to as the Friedmann equations. These equations hold, with minor differences, if there is more than one perfect fluid in the matter sector. In this case they are:

$$\frac{\ddot{a}}{a} = -\frac{4\pi G}{3}\sum_i (\rho_i + 3p_i), \tag{2.20}$$

$$H^2 = \left(\frac{\dot{a}}{a}\right)^2 = \frac{8\pi G}{3}\sum_i \rho_i - \frac{k}{a^2}. \tag{2.21}$$

There is one further equation that can be of interest when studying the background cosmology of our Universe and that is the continuity, or fluid, equation. This is simply a relativistic statement of energy conservation. The divergence of the energy-momentum tensor must vanish, so:

$$0 = \nabla_\mu T^\mu{}_\nu = T^\mu{}_{\nu,\mu} + \Gamma^\mu_{\mu\lambda} T^\lambda{}_\nu - \Gamma^\lambda_{\mu\nu} T^\mu{}_\lambda. \tag{2.22}$$

The first of these four equations gives the generalisation of conservation of energy, and so the fluid equation, as:

$$\dot{\rho} + 3\frac{\dot{a}}{a}(\rho + p) = 0. \tag{2.23}$$

If, as is assumed here, there is no conversion between different types of matter or energy in the Universe then the fluid equation must hold for each species

separately. To allow the equations to be solved it is usual to suppose an equation of state for each different fluid species. These equations of state take the form:

$$p_i = w_i \rho_i. \tag{2.24}$$

If w_i is taken to be a constant and the equation of state is inserted into the fluid equation a solution can be arrived at for $\rho(a)$. The solution takes the form:

$$\rho_i = k a^{-3(1+w_i)}, \tag{2.25}$$

where k is an unknown constant to be set by initial conditions.

In trying to relate observations to the underlying cosmology it is usual to deal with density parameters. These are defined for each component of the energy content of the Universe as:

$$\Omega_i = \frac{\rho_i}{\rho_c}, \tag{2.26}$$

where ρ_c is the critical density. This is the density required for the Universe to be flat given a value for H^2 and is defined as:

$$\rho_c = \frac{3H^2}{8\pi G}. \tag{2.27}$$

The definition of the density parameters allows the Friedmann equation to be written as:

$$\Omega - 1 = \frac{k}{a^2 H^2}, \tag{2.28}$$

where $\Omega = \sum_i \Omega_i$. From here a density parameter for curvature is sometimes constructed as:

$$\Omega_k = \frac{-k}{a^2 H^2}, \tag{2.29}$$

so that:

$$\Omega + \Omega_k = 1. \tag{2.30}$$

From this it can be seen that the density parameters can be considered a measure of how much influence each component has on the evolution of the Universe.

2.2 Perturbing Away from the Background

It is clear that the Universe that we live in is not precisely homogeneous and isotropic, if it were this thesis would not exist. However, the central tenet of cosmological perturbation theory is that any difference from the background value of a quantity is small compared to that background value on cosmologically relevant scales. This idea and its applications have proven successful in answering a variety of cosmological questions and are an important part of the standard model of cosmology.

2.2.1 Perturbation Theory in General Relativity

The starting point in any perturbative approach is to take a background quantity and ask what happens when a small shift is applied. In cosmological contexts there are two quantities which may be perturbed: the metric tensor and the energy-momentum tensor.

The background metric of interest is the spatially flat Robertson-Walker metric, equation (2.8), and, based on transformation properties, perturbations to this background can be decomposed as:

$$ds^2 = -(1+2\psi)dt^2 - 2a(t)B_i dx^i dt + a^2(t)\left[(1-2\phi)\delta_{ij} + 2E_{ij}\right]dx^i dx^j, \quad (2.31)$$

where a choice of Cartesian spatial coordinates has been made. Under changes in the spatial coordinates ψ and ϕ transform as scalars, B_i as components of a vector and E_{ij} as components of a traceless and symmetric tensor. The scalar perturbation ψ is also known as the lapse function and relates coordinate time to proper time. There is a further decomposition possible. Firstly, b_i can be decomposed into a divergence free part and a curl free part, so:

$$B_i = \partial_i B - B^{\mathrm{V}}{}_i. \quad (2.32)$$

In an extension of this idea, the tensor perturbation can be broken down into:

$$E_{ij} = \partial_{\langle i}\partial_{j\rangle} E + \partial_{(i} E^{\mathrm{V}}_{j)} + E^T_{ij} \quad (2.33)$$

where the vector E^{V}_j is divergence-free. Together with $B^{\mathrm{v}}{}_i$, E^{V}_j is known as the vector perturbation and the tensor E^T_{ij} is known as the tensor perturbation [8].

2.2.2 Gauges in Cosmological Perturbation Theory

Depending on the slicing and threading that is used, the perturbations will take different values. For example it is possible to choose a slicing where the matter has the same density across a slice, so that the scalar perturbations are now entirely contained in the metric. This is the essence of gauges in cosmological perturbation theory: a particular choice of slicing and threading that can simplify the problem at hand. Of course, the physical quantities which are measured should be independent of the choice of slicing and threading (which is after all only a choice of coordinate system) so it follows that physical quantities are gauge invariant.

The most important gauge invariant quantity in terms of the inflationary paradigm is the primordial curvature perturbation, ζ. This is defined, in the uniform energy density gauge, as:

$$g_{ij} = a(t)e^{\zeta(\mathbf{x},t)}\gamma_{ij}, \tag{2.34}$$

where:

$$\gamma_{ij} = (Ie^{2h})_{ij} \tag{2.35}$$

with I being the identity matrix and h is a traceless matrix. A similar expression for the spatial metric can be written on a generic slice, replacing ζ with the quantity ψ. Then, the number of Hubble times between two generic slices is given by:

$$\delta N_{12} = \psi(\mathbf{x}, t_2) - \psi(\mathbf{x}, t_1). \tag{2.36}$$

Now, it is possible to arrive at an expression for ζ that is valid on all slices by starting on the uniform density slicing and moving to a a generic slicing with the time coordinate $\tilde{t} = t + \delta t$. The number of Hubble times between the two slices is:

$$-H\delta t = \psi - \zeta. \tag{2.37}$$

Then, δt can be replaced by an expression for the density perturbation (or as will be used later, the perturbation in a scalar field) to give:

$$\zeta = \psi - H\frac{\delta\rho}{\dot{\rho}}. \tag{2.38}$$

In particular, on a flat slicing where $\psi = 0$, the primordial curvature perturbation

is given by:

$$\zeta = -H\frac{\delta\rho}{\dot{\rho}}. \tag{2.39}$$

2.3 Our Observable Universe

Recent observations by the *Planck* satellite [5] have given the best indication so far of the constituent parts of the Universe. It is dominated by Dark Energy, a poorly understood constituent of the Universe that drives acceleration of the expansion of the Universe. Such acceleration was first measured by observations of the distances to supernova type 1A and has since been confirmed by a variety of sources. Since it drives the expansion of the Universe it can be seen from equations (2.20) and (2.24) that for dark energy, $w < -\frac{1}{3}$. Measurements from the *Planck* satellite have constrained this to be very close to -1 in the present day and the time evolution of w to be very small. Dark energy makes up approximately 70% of the energy content of the Universe.

The next most dominant constituent of the Universe is dark matter. Dark matter is a cover-all term for an as yet unknown energy content of the Universe which interacts with other matter through gravity and, potentially, very weakly through other forces. It was originally devised to solve the problem of rotational velocity curves of galaxies which flatten at large radii as opposed to dropping off. While other ideas have been suggested to account for this phenomenon they have not been as successful in a variety of situations [22, 92]. The standard paradigm concerned cold dark matter which has not only negligible interactions with both itself and the Standard Model particles (expect through gravity), but also a negligible random velocity. Dark matter constitutes approximately 25% of the energy content of the Universe.

Dark matter is in contrast to the baryonic matter, both visible and non-visible, that makes up all of the "everyday" matter that interacts in the Standard Model. This means it is the only matter that it is possible to directly image though a huge amount of it still does not give off light. Despite constituting a small portion of the content of the Universe baryons can have an effect on the large scale structure of the Universe, see e.g. Refs. [21, 28].

The components are outlined above constitute the ΛCDM model of cosmology. This model needs just 6 parameters to describe it and it fits a large number

of observations, some constrained to within 1% accuracy. More recently, early measurements from the the Dark Energy Survey (DES) [1] show broad agreement with the *Planck* results [2].

2.4 Problems with the Classical Picture

Despite the successes of the ΛCDM model, there are some problems that can be considered a cause for concern. These problems are essentially problems of initial conditions. As highlighted in Ref. [9] it is possible to argue that predicting initial conditions is separate from defining the laws which govern a theory's evolution. Indeed, it is notable that some of the problems outlined below were not considered problems at all until a solution was proposed [16, 20]. However, it is a cause for concern if highly fine-tuned initial conditions are required for the model to predict a universe even remotely similar to the one that is observed. The problems are now considered to be real shortcomings of the standard Big Bang scenario and discussions of them can be found in major cosmology textbooks such as Refs. [73, 77, 104].

2.4.1 The Flatness Problem

In the standard big bang scenario $\dot{a}$ is always decreasing, the expansion is decelerating. Combining this fact with measurements that place the Universe very close to flat leads to a fine-tuning problem [27] as can be seen from equation (2.28). If $\dot{a}$ is getting smaller and smaller then the density parameter will get further away from 1 and curvature will become more and more important. This means that to have the low curvature measured today it would have had to have been very close to, but not exactly, 0 in the past. For example, taking Ω to be of order 1 today requires that, without inflation, at the Planck epoch $|\Omega - 1| < \mathcal{O}(10^{-64})$ [102].

2.4.2 The Horizon Problem

This problem concerns the exquisite isotropy measured in the Cosmic Microwave Background (CMB) [78]. The relative magnitude of the anisotropies are $\sim 10^{-5}$ and so, given the CMB is a blackbody, this means that the temperature of

different sides of the Universe at the time of last scattering was the same to one part in $\sim 10^{-5}$. This becomes a problem when comparing the relative size of the co-moving particle horizon (distance that light can have travelled since the start of the Universe) at last scattering to its size now. The co-moving distance from the big-bang until a time, t, is given by:

$$d_H(t) = \int_0^t \frac{dt'}{a(t')} \tag{2.40}$$

Now, based on the assumption that the matter-dominated era of cosmological expansion is the dominant contributor to the integral at both the time of last scattering ($t = t_{ls}$) and now ($t = t_0$), then the ratio of co-moving particle horizons is:

$$\frac{d_H(t_{ls})}{d_H(t_0)} \simeq \left(\frac{t_{ls}}{t_0}\right)^{1/3}, \tag{2.41}$$

and so the ratio of co-moving volumes defined by the particle horizons is:

$$\frac{V_H(t_{ls})}{d_H(t_0)} \simeq \frac{{d_H}^3(t_{ls})}{{d_H}^3(t_0)} \simeq \left(\frac{1.4 \times 10^{10}}{3.8 \times 10^5}\right) \simeq 10^5. \tag{2.42}$$

This implies that there must have been 10^5 causally disconnected regions at last scattering inside the observable Universe. The horizon problem is then the question: how did apparently unconnected regions of the Universe equilibrate?

2.4.3 The Relic Problem

This problem is not one concerned with Big Bang cosmology as such but rather its interaction with physics beyond the Standard Model of particle physics. As many such theories predict the existence of particles or topological defects and these are referred to as relics. Some of these can be considered unwanted as their presence would conflict with observations. For such relics with mass their energy density will scale like matter, so proportional to a^{-3}, which means that under the radiation dominated epoch of the ΛCDM model they will gain in relative importance. Since they are not observed today then this would imply some tension between models which predict such relics and the observational situation. As noted in Ref. [20] this problem is more model specific than the previous two but did serve as a major motivation for Guth in Ref. [45].

2.5 Inflation

2.5.1 Defining the Paradigm and its Successes

The definition of inflation is simply a period of accelerated expansion in the early Universe. This corresponds to:

$$0 < \frac{d^2a}{dt^2} = \frac{d\dot{a}}{dt} = \frac{d}{dt}(aH). \tag{2.43}$$

Since the definition of the comoving Hubble length is $(aH)^{-1}$, an accelerating Universe corresponds to one where the comoving Hubble length is decreasing. This is the important feature of inflation that solves the problems with the ΛCDM scenario.

It is clear from equation (2.28) how a period of inflation can solve the flatness problem. If the comoving Hubble length is decreasing then $|\Omega - 1|$ is getting closer to 0 rather than further away as it does during matter or radiation dominated epochs. Therefore, if inflation is sustained for long enough then $|\Omega_k|$ will get driven to 0.

The solution to the horizon problem is less immediately clear. However, consider a patch of the Universe which has had time to reach equilibrium before the onset of inflation. This patch has a fixed comoving scale and so as the comoving Hubble length shrinks the edges of the patch move outside the horizon and then re-enter at a later time. This has the apparent effect of giving more time to scales which are currently entering the horizon to interact than the standard ΛCDM scenario would suggest.

Finally, the relic problem is solved as a period of rapid expansion dilutes the relic particle density (which again scales as a^{-3}). There are some potential complications however. Firstly, there is the case where relic particle might be produced after inflation. This can still cause problems when comparing with observations. Secondly, some inflation scenarios [10, 11] can cause unwanted relics to be produced during inflation.

2.5.2 Background Evolution

The most easily understood starting point for the inflationary paradigm is to introduce a homogeneous scalar field with an arbitrary potential into an otherwise empty universe. This toy example demonstrates all the necessary phenomenology at the background level to solve the problems outlined above[1]. This toy model is represented by the action:

$$S = \int d^4x\sqrt{-g}\left[\frac{1}{2}R - \frac{1}{2}g^{\mu\nu}\partial_\mu\phi\partial_\nu\phi - V(\phi)\right]. \tag{2.44}$$

In this action, and for the remainder of the thesis, a choice of unit system has been made so that $M_p = 1$. From the action, and the knowledge that the toy universe has a Robertson-Walker metric, the energy-momentum tensor of the scalar field is found as:

$$T_{\mu\nu} = \begin{pmatrix} \frac{1}{2}\dot{\phi}^2 + V(\phi) & 0 & 0 & 0 \\ 0 & & & \\ 0 & & \left[\frac{1}{2}\dot{\phi}^2 - V(\phi)\right] g_{ij} & \\ 0 & & & \end{pmatrix}. \tag{2.45}$$

It can be seen to have the form of a perfect fluid and so by identifying:

$$\rho = \frac{1}{2}\dot{\phi}^2 + V(\phi), \tag{2.46}$$

$$p = \frac{1}{2}\dot{\phi}^2 - V(\phi), \tag{2.47}$$

the Friedmann equations become :

$$3H^2 = \frac{1}{2}\dot{\phi}^2 + V(\phi) - \frac{k}{a^2}, \tag{2.48}$$

$$\frac{\ddot{a}}{a} = -\left(\dot{\phi}^2 - V(\phi)\right), \tag{2.49}$$

and the equation of motion for the scalar field is:

$$\ddot{\phi} + 3H\dot{\phi} + \frac{dV(\phi)}{d\phi} = 0. \tag{2.50}$$

During inflation the scalar field is considered to be the dominant contributor to the energy-density of the Universe so the curvature term in the above equations can be ignored. Then, it can be seen from the second of these equations that for

[1] Actually, it does not seem to be necessarily true that the horizon problem is solved but instead it is deferred to an alternate location. This will be discussed further in chapter 6

accelerated expansion of the Universe, that is $\ddot{a} > 0$, the potential energy of the field must dominate its kinetic energy, $V(\phi) > \dot{\phi}^2$. An alternative condition for inflation can be defined via the acceleration equation. Re-writing the acceleration equation using equation (2.48) to replace the potential, $V(\phi)$, gives :

$$\frac{\ddot{a}}{a} = H^2 \left(1 - \frac{1}{2}\frac{\dot{\phi}^2}{H^2}\right). \tag{2.51}$$

Thus this model universe undergoes a period of inflation when

$$\epsilon_H \equiv \frac{1}{2}\frac{\dot{\phi}^2}{H^2} < 1, \tag{2.52}$$

where ϵ_H is known as the Hubble slow-roll parameter and equation (2.52) is the slow-roll condition. Alternatively, differentiating equation (2.48) gives :

$$2\dot{H} = -\dot{\phi}^2, \tag{2.53}$$

and so the slow-roll parameter is:

$$\epsilon_H = -\frac{\dot{H}}{H^2}. \tag{2.54}$$

In fact, during inflation it is almost always true the Universe is in a pseudo-de-Sitter state where the Hubble parameter is very close to constant:

$$\frac{|\dot{H}|}{H^2} \ll 1, \tag{2.55}$$

which means $\epsilon_H \ll 1$. Inserting this condition into the first definition of ϵ_H in equation (2.52) shows that this phase of expansion means that:

$$3H^2 \simeq V(\phi), \tag{2.56}$$

and so near-exponential expansion implies the strong inequality: $V(\phi) \gg \dot{\phi}^2$. In order to solve the classic problems of the Big Bang model and simultaneously generate the observed power spectrum of the primordial density fluctuations, inflation must be sustained for some period of time as will be shown later. This means that the time derivative of equation (2.56) should also be a valid approximation. This gives the approximate equality:

$$3H\dot{\phi} \simeq -\frac{dV(\phi)}{d\phi}. \tag{2.57}$$

Comparing this with the equation of motion for the scalar field, equation (2.50), implies that this approximation requires $\ddot{\phi}$ to be negligible compared to the other quantities so

$$|\ddot{\phi}| \ll 3H|\dot{\phi}| \quad , \quad \left|\frac{dV(\phi)}{d\phi}\right|. \tag{2.58}$$

This gives a second condition:

$$\eta_H \equiv -\frac{\ddot{\phi}}{H\dot{\phi}} \ll 1. \tag{2.59}$$

The two slow-roll parameters introduced so far are known as the Hubble Slow-Roll (HSR) parameters [64] however the slow-roll approximation can also be summarised by the Potential Slow-Roll (PSR) parameters. These place constraints on the form of the potential but in principle leave $\dot{\phi}$ as a free parameter. The first of these PSR parameters, ϵ_V, comes from combining equation (2.53), the Friedmann equation and the condition in equation (2.55) to give:

$$\epsilon = \frac{1}{2}\left(\frac{V'(\phi)}{V(\phi)}\right)^2 \ll 1, \tag{2.60}$$

where $V'(\phi) = \frac{dV(\phi)}{d\phi}$. When the kinetic term in the Friedmann equation is subdominant then this parameter is small. The second PSR parameter, η_V, is:

$$\eta_V = \frac{V''(\phi)}{V(\phi)}. \tag{2.61}$$

However, while the PSR parameters being small is a necessary condition for inflation it is not sufficient as $\dot{\phi}$ is a free parameter; a way to constrain it must be provided. It must be assumed that equation (2.57) holds during inflation. This is a condition which can be shown to hold for a wide range of initial conditions.

The Hamilton-Jacobi Formulation and Inflationary Attractor Behaviour

If ϕ varies monotonically with time then it can be thought of as the time variable and the slow-roll condition can be written in terms of the Hubble parameter and its derivatives as a function of ϕ. This can be done by dividing both sides of equation (2.53) by $\dot{\phi}$ to give:

$$\dot{\phi} = -2\frac{dH(\phi)}{d\phi}, \tag{2.62}$$

which can then be used to replace $\dot{\phi}$ in the Friedmann equation to obtain:

$$\left[\frac{dH(\phi)}{d\phi}\right]^2 - \frac{3}{2}H^2(\phi) = -\frac{1}{2}V(\phi). \tag{2.63}$$

This is known as the Hamilton-Jacobi equation. Perturbing an inflationary solution, $H_0(\phi)$, and linearising the resulting perturbed Hamilton-Jacobi equation gives an equation governing the evolution of the perturbation:

$$H_0'\delta H' \simeq \frac{3}{2}H_0\delta H. \tag{2.64}$$

The solution to this differential equation is:

$$\delta H = \delta H_i e^{-3N}, \tag{2.65}$$

where H_i is the value of the Hubble parameter at some initial condition. Provided that there is sufficient inflation then the inflationary attractor is approached exponentially quickly. Sufficient inflation means a high number of e-foldings and to solve the classic problems with the Big Bang model at least 50 e-foldings of inflation is required [63]. This is far enough before the end of inflation that it is consistent to use the slow-roll approximation for calculations.

The idea of ϕ becoming the time variable allows the HSR parameters to be re-written in a slightly different way. Returning to equation (2.62) immediately gives the first HSR parameter as:

$$\epsilon_H = 2\left[\frac{H'(\phi)}{H(\phi)}\right]^2, \tag{2.66}$$

and then taking the derivative of equation (2.62) gives the second HSR parameter as:

$$\eta_H = 2\frac{H''(\phi)}{H(\phi)}. \tag{2.67}$$

Re-expressing the HSR parameters in this way illuminates the parallels with the PSR parameters.

2.6 The Generation of Perturbations During Single-Field Inflation

During the inflationary epoch, fluctuations that are quantum in origin become important on cosmological scales. This section gives an outline of the mathematical derivation of the spectrum of such perturbations.

Starting from the definition of the curvature perturbation as given in equation (2.38) and fixing the gauge to the spatially-flat gauge where the curvature perturbation of the spatial hyper-surfaces is 0 implies that the scalar perturbations of the Universe are entirely contained within the scalar field so:

$$\zeta = -H\frac{\delta\phi}{\dot{\phi}}. \tag{2.68}$$

This relationship means that to calculate the spectrum of curvature perturbation, all that is required is the spectrum of the scalar field perturbations. The equation of motion for the scalar field in a general spacetime:

$$\Box\phi + \frac{dV(\phi)}{d\phi} = 0. \tag{2.69}$$

The d'Almbertian operator in this equation is the covariant one, the covariant derivative of a covariant derivative[2]. Introducing perturbations and restricting the equations to first-order in the perturbed quantities gives:

$$\ddot{\delta\phi} + 3H\dot{\delta\phi} - \frac{\nabla^2\delta\phi}{a^2} + \delta\phi\frac{d^2V(\phi)}{d\phi^2} = (\delta\Box)\phi, \tag{2.70}$$

where $(\delta\Box)\phi$ in the flat gauge is given by:

$$(\delta\Box)\phi = \left(\frac{1}{\sqrt{-g}}\,\partial_\mu\sqrt{-g}\,\delta g^{\mu\nu}\partial_\nu\right)\phi = \frac{1}{a^3}\frac{d}{dt}\left(\frac{a^3\dot{\phi}^2}{H}\right)\delta\phi. \tag{2.71}$$

For inflation light scalar fields are of interested rather than heavy ones and in a cosmological context this translates to the realisation that the term containing the second-derivative of the potential (the 'mass' term) must be subdominant to the term containing the Hubble parameter. Furthermore, on Fourier transforming

[2]Despite the fact that calculations take place in the so-called "flat" gauge", this gauge choice corresponds to spatial flatness (so $R^{(3)} = 0$) but does not imply the metric has no perturbations at all. In particular $\delta g_{tt} \neq 0$ in general

the above equation, $\nabla^2 \to k^2$ and k^2/a^2 will not be substantially less than the Hubble parameter until after horizon exit, thus the mass term is also subdominant to this term. The above means that the Fourier transformed equation reads:

$$\delta\ddot{\phi}_{\mathbf{k}} + 3H\delta\dot{\phi}_{\mathbf{k}} - \frac{1}{a^3}\frac{d}{dt}\left(\frac{a^3\dot{\phi}^2}{H}\right)\delta\phi_{\mathbf{k}} = 0, \tag{2.72}$$

where it is worth noting that the term in brackets is evaluated in terms of background quantities. This equation is usually used in an alternate form by making a change of variables $\varphi_{\mathbf{k}} \equiv a\delta\phi_{\mathbf{k}}$ and $z \equiv a\phi/H$. Upon this variable change, and taking derivatives with respect to conformal time, the Mukhanov-Sasaki equation, (2.73), is arrived at:

$$\frac{\partial^2\varphi_{\mathbf{k}}}{\partial\eta^2} + \left[k^2 - \frac{1}{z}\frac{d^2z}{d\eta^2}\right]\varphi_{\mathbf{k}} = 0. \tag{2.73}$$

The second term in square brackets has an exact expansion in terms of the HSR parameters:

$$\frac{1}{z}\frac{d^2z}{d\eta^2} = 2a^2H^2\left(1 + \epsilon_H - \frac{3}{2}\eta_H + \frac{1}{2}\eta_H^2 - \frac{1}{2}\epsilon_H\eta_H + \frac{1}{2H}\left[\frac{d\epsilon_H}{dt} - \frac{d\eta_H}{dt}\right]\right). \tag{2.74}$$

During slow-roll inflation the HSR parameters are much less than one and so equation (2.73) becomes:

$$\frac{\partial^2\varphi_{\mathbf{k}}}{\partial\eta^2} + \left[k^2 - \frac{2}{\eta^2}\right]\varphi_{\mathbf{k}} = 0, \tag{2.75}$$

where the smallness of the HSR parameters also means that the Universe is almost de-Sitter and so it is possible to define conformal time as $\eta = -1/aH$. This is precisely the expression that would be arrived at if scalar perturbations to the metric are ignored, that is if the quantity in equation (2.71) is 0. In other words, during single field slow-roll inflation the effect of back-reaction of the density perturbations on the metric is negligible.

The next stage is to quantise this theory of the Early Universe. To proceed on this front "ladder" operators are introduced alongside the mode function, φ_k, with:

$$(2\pi)^3\varphi_{\mathbf{k}} = \varphi_k\hat{a}(\mathbf{k}) + \varphi_k^*\hat{a}^\dagger(-\mathbf{k}). \tag{2.76}$$

This process mirrors the approach taken when dealing with quantum harmonic oscillators which is unsurprising given that equation (2.73) is the equation for

a harmonic oscillator with a time dependent frequency. In keeping with this equivalence $\hat{a}^\dagger(-\mathbf{k})$ is an operator that creates perturbations with momentum $\mathbf{k}$. Thinking in this way leads to the commutation relations[3]:

$$(2\pi)^{-3}[\hat{a}(\mathbf{k}), \hat{a}^\dagger(\mathbf{k}')] = \delta^3(\mathbf{k} - \mathbf{k}') \tag{2.77}$$

$$[\hat{a}(\mathbf{k}), \hat{a}(\mathbf{k}')] = 0 \tag{2.78}$$

At this point the vacuum state of the theory needs to be defined. In Minkowski space-time the quantum oscillator has a well defined vacuum state as the frequencies are not time dependent. The vacuum in such theories is then the state that minimises the expectation value of the Hamiltonian of the theory. However, when dealing with a time-dependent situation as in equation (2.73) more physical input is required to define a suitable background. The idea is as follows. There will be a time when all the modes of interest are contained within a small space-time volume where the expansion of the Universe is negligible; when the frequency of the oscillations, proportional to k, is much greater than the rate of expansion, $(aH)^{-1}$. This means that the Universe appears Minkowskian and the vacuum solution must follow the plane-wave solution that would be found in the standard quantum harmonic oscillator, namely:

$$\varphi_k \to \frac{1}{\sqrt{2k}} e^{-ik\eta} \quad \text{as} \quad \frac{aH}{k} \to 0. \tag{2.79}$$

This initial condition fixes the normalisation of the general solutions to equation (2.75), giving the solution as:

$$\varphi_k = \frac{e^{-ik\eta}}{\sqrt{2k}} \frac{k\eta - i}{k\eta}. \tag{2.80}$$

Several Hubble times after a mode has crossed outside of the horizon, $k \ll aH$ so $k\eta \ll 1$ therefore:

$$\varphi_k \to \frac{-i}{\sqrt{2k}} \frac{1}{k\eta} \quad \text{as} \quad k\eta \to 0. \tag{2.81}$$

The spectrum of the quantity φ is defined by:

$$\langle \varphi_{\mathbf{k}} \varphi_{\mathbf{k}'} \rangle = \frac{2\pi^2}{k^3} \mathcal{P}_\varphi \delta^3(\mathbf{k} + \mathbf{k}'). \tag{2.82}$$

[3]It is possible to start with the action for the theory and follow the canonical procedure for quantisation, defining the canonical commutators between position and momentum operators, and arrive at the same end point. The approach taken here leaves out a large amount of technical detail that is not of interest when discussing the work presented in this thesis.

Some rearranging using equations (2.77) and (2.76) leads to the expression:

$$\mathcal{P}_{\delta\phi}(k,\eta) = \frac{k^3}{2\pi^2}|\varphi_k(\eta)|^2. \tag{2.83}$$

Using equation (2.81) to evaluate the spectrum a long time after a mode has exited the horizon gives:

$$\mathcal{P}_{\delta\phi}(k) = \left(\frac{H_k}{2\pi}\right)^2. \tag{2.84}$$

Now, it is possible to reach an expression for the power spectrum of the gauge invariant quantity ζ. In the case of a scalar-field ζ is given by:

$$\zeta = -H\frac{\delta\phi}{\dot{\phi}}, \tag{2.85}$$

so the the power spectrum is given by:

$$\mathcal{P}_\zeta(k) = \frac{1}{4\pi^2}\left(\frac{H^2}{\dot{\phi}}\right)^2\Bigg|_k. \tag{2.86}$$

It is useful to write $\mathcal{P}_\zeta$ in terms of the HSR parameter ϵ_H. This gives:

$$\mathcal{P}_\zeta(k) = \frac{1}{8\pi^2}\frac{H^2}{\epsilon_H}\Bigg|_k. \tag{2.87}$$

At this point it is assumed that the power spectrum follows a power law, i.e. $\mathcal{P}_\zeta(k) \propto k^{n_s-1}$. This allows the calculation of the value of n_s as:

$$n_s - 1 = \frac{d\ln\mathcal{P}_\zeta}{d\ln k}. \tag{2.88}$$

Since this is evaluated when $k = aH$, it is possible to rewrite the derivative as $\frac{d}{d\ln k} = \frac{1}{H}\frac{d}{dt}$. Thus:

$$n_s - 1 = 2\frac{\dot{H}}{H^2} - \frac{\dot{\epsilon}_H}{H\epsilon_H}. \tag{2.89}$$

The second HSR parameter has a differential relationship to the first, $\eta_H = \epsilon_H - \frac{1}{2}\frac{\dot{\epsilon}_H}{H\epsilon_H}$. Thus, the final expression for the spectral index of the scalar spectrum is:

$$n_s - 1 = 2\eta_H - 4\epsilon_H. \tag{2.90}$$

A similar calculation using the slow-roll approximation gives

$$n_s - 1 = 2\eta_V - 6\epsilon_V. \tag{2.91}$$

Finally, a power spectrum for the tensor perturbations can be derived in a similar way to equation (2.86) and is:

$$\mathcal{P}_h(k) = 8\left(\frac{H_k}{2\pi}\right)^2, \tag{2.92}$$

which gives the tensor spectral index as:

$$n_T = -2\epsilon_H. \tag{2.93}$$

The ratio between the amplitude of the of the tensor modes to scalar modes, r, is

$$r = \frac{\mathcal{P}_h(k)}{\mathcal{P}_\zeta(k)} = 16\epsilon_H. \tag{2.94}$$

The derivation presented here is for a kinetically canonical theory in Einstein gravity. More elaborate theories, including all the way up to Horndeski Theory permit similar results and the corresponding equations can be found in Ref. [103].

2.6.1 The Lyth Bound

Combing the expression for r with the definition of the first HSR parameter allows a relationship between r and the distance that the field moves for the last N e-foldings of inflation, this is known as the Lyth Bound [71]. From equation (2.94):

$$r = 8\frac{\dot{\phi}^2}{H^2}. \tag{2.95}$$

Then, the number of e-foldings is given as:

$$N = \int \frac{1}{\sqrt{2\epsilon_H}} d\phi, \tag{2.96}$$

so that:

$$\frac{dN}{d\phi} = \frac{1}{\sqrt{2\epsilon_H}}. \tag{2.97}$$

That leads to the expression for $\Delta\phi$, the field distance traversed for the N e-foldings before the end of inflation. In integral form:

$$\Delta\phi = \int_0^{N_{\rm end}} \sqrt{\frac{r}{8}} dN. \tag{2.98}$$

Assuming that the scalar-field is slow-rolling during inflation, so that r is essentially independent of N gives the Lyth bound:

$$\Delta\phi \sim \left(\frac{r}{0.01}\right)^{1/2}. \tag{2.99}$$

Thus if r is significantly non-zero then the field must have travelled at least a Planck Mass during inflation[4]. This causes some concern with regards to the stability of corrections to the potential [72].

2.7 Motivating Inflation from High-Energy Physics

The general idea with many inflationary models is that they are some low-energy effective theory of a high-energy theory. The high-energy theory is an extension of the Standard Model of particle physics and it is usually taken to be supersymmetric [70]. While a detailed examination of such theories is outside the scope of this thesis some of the basic ideas give a physical content to the particular inflationary models being considered here.

In some cases the models can be directly related to string theory models. Here the fields undergoing inflation are often 'moduli' fields of a theory with extra dimensions. There is a specific sub-set of string theory inspired models that focus on the axion monodromy structure [76, 98]. An axion-like field is one which has a discrete shift symmetry, $\phi \to \phi + 2\pi$. This discrete symmetry is not necessarily fundamental but could instead be a continuous symmetry that has been broken by some non-perturbative effect. In the scenario where there is just one field, which is axion-like, a complete rotation of 2π leads to the same configuration as was started with. However, when there is a multi-field system it is said to undergo monodromy if on a full rotation of the axion field the system is in a different configuration. A canonical illustrative analogy is the idea of going down a spiral staircase. A particularly exciting aspect of monodromy models is that can generate a large tensor-scalar ratio without having to traverse a trans-Planckian field distance.

Another strand of inflationary model building is based on supergravity. The basic idea behind supergravity is that the local Poincare symmetry of General Relativity is supplemented by local supersymmetry. At arms-length supersymmetry can

[4]A slightly modified bound was found in Ref. [34] but the overall picture is the same.

be considered simply as a symmetry that mixes together fermions and bosons. Such a group of related particles is known as a supermultiplet and every particle in a supermultiplet is predicted to have the same mass if supersymmetry is not broken. Since there are no observations of super-partners to any of the Standard Model particles then the symmetry must be broken (if it exists at all).

Finally, it is worth noting that supergravity models are themselves often invoked as low energy limits of string theory models[5]. Specifically, this means that they don't claim to be fundamental but are instead based on some symmetry principles that are thought to be desirable. This is the case in the thinking that leads to the Universal Attractor models [58] that appear in chapter 4 and the α-attractor, and related, models [54, 56] discussed in chapter 5. Not only are these models based on supergravity but they also include a further conformal symmetry which is broken at some point before inflation takes place.

2.8 Observing the Early Universe: The Cosmic Microwave Background

Today, one of the key ways in which the spectrum of perturbations in the Early Universe is constrained is through the Cosmic Microwave Background (CMB). This is made up of photons which have been travelling unhindered since the decoupling epoch after originating on the surface of last scattering. The perturbations in the Early Universe correspond to photons of slightly different temperatures being emitted (or equivalently, photons of the same temperature being emitted at slightly different times). Thus, it is important to know how the primordial spectrum from inflation evolves until the point of decoupling. Since the CMB photons travel through the perturbed Universe it is also vital to know how they will be affected by the developing matter inhomogeneities up until the present day. Both of these pieces of information are contained in the transfer function $T_\ell(k)$.

The observational quantity of interest is the anisotropy of the CMB, the brightness function :

$$\Theta(\eta, \mathbf{x}, \mathbf{n}) = \frac{\delta T(\eta, \mathbf{x}, \mathbf{n})}{T(\eta)}, \tag{2.100}$$

where $\mathbf{n}$ is the direction of travel of the photon. Analogous to a Fourier

[5]Thus the above mentioned string theory models are also generally supersymmetric.

decomposition, the brightness function can be decomposed into multipoles:

$$\Theta(\eta, \mathbf{x}, \mathbf{n}) = \sum_{\ell m} (-1)^{\ell} \Theta_{\ell m}(\eta, \mathbf{x}) Y_{\ell m}(\mathbf{n}), \tag{2.101}$$

where $Y_{\ell m}(\mathbf{n})$ are spherical harmonics. The observed multipoles with $\ell \geq 2$ are the intrinsic anisotropies of the CMB, denoted $a_{\ell m} \equiv \Theta_{\ell m}(\eta_0, \mathbf{x}_0)$. Considering a small patch of the overall sky allows the use of the Flat-sky approximation. This allows the definition of anisotropies that are only dependent on $\vec{\ell}$. These $a(\vec{\ell})$ are given by:

$$a(\vec{\ell}) = \left(\frac{1}{2\pi\ell}\right)^{1/2} \sum_{m} a_{\ell m} i^{-m} e^{im\phi_{\vec{\ell}}} \tag{2.102}$$

The quantity that CMB experiments compared against predictions is the spectrum of $a(\vec{\ell})$:

$$\langle a^*(\vec{\ell}) a(\vec{\ell}') \rangle = C(\ell) \delta^2(\vec{\ell}' - \vec{\ell}). \tag{2.103}$$

The C_ℓ quantities are connected to the transfer function and primordial curvature spectrum by:

$$C_\ell = 4\pi \int_0^\infty T_\ell^2(k) \mathcal{P}_\zeta(k) \frac{dk}{k}. \tag{2.104}$$

To make predictions on the observed measurements in the sky the transfer function must be calculated. The precise calculation is outside the scope of this thesis but a flavour of how it progresses is useful. Firstly, a system of closed equations has to be assembled. This consists of the continuity and Euler equations for the components of the Universe (baryons, Cold Dark Matter, photons, and neutrinos). Further to this, the Boltzmann hierarchy for the neutrinos and photon temperature and polarisation perturbations is required. A Boltzmann hierarchy is an expansion of the derivatives of multipoles in terms of the multipoles. Finally, equations linking physical quantities, for example the density contrast, to the metric perturbations are required. This system of equations can then be solved, given suitable initial conditions, to give the full time evolution of the contents of the Universe and thus the required transfer functions.

Chapter 3

The Effective Phase-Space of Cosmological Scalar Fields

3.1 Introduction and Motivation

When introducing textbook inflationary scenario of a single, kinetically canonical scalar field that is minimally coupled to gravity it is common (as was done in chapter 2) to discuss the attractor nature of the slow-roll regime. This is demonstrated with plots in the $\phi - \dot{\phi}$ plane that show the inflationary trajectories converging towards a single one: the slow-roll solution. This convergence is useful as it allows one to say that the slow-roll behaviour is generic allowing calculations relating to inflation to become much simpler.

It is clear that $\phi - \dot{\phi}$ is not the canonical phase space of an FLRW universe for two reason. Firstly, such a universe is defined by two general coordinates: the value of the scalar field, ϕ, and the scale factor, a. This means that the phase space should be four dimensional. An alternative framing of the same idea is that since there are two second-order equations of motion, it might be naively expected that there are four initial conditions that need defined. Secondly, the velocity of the field, $\dot{\phi}$, is not the canonical momentum of ϕ in the same way that $\dot{x}$ is not the canonical momentum in classical mechanics. The question then arises: if $\phi - \dot{\phi}$ is not a phase space are the predictions of attractor as generic as they seem?

This issue and it's resolution in the case of a single, kinetically canonical scalar field that is minimally coupled to gravity was discussed and solved in Ref. [88].

The authors of Ref. [88] showed that it is possible to considered $\phi - \dot{\phi}$ as a phase space in the sense that trajectories in the space never cross. This means that defining a point in $\phi - \dot{\phi}$ is enough to completely describe the dynamics of such a universe. It also means that trajectories can never cross which ensures that Louiville's theorem will hold in the space. This theorem states that volume in phase-space must be conserved along the evolution dictated by the equations of motion. Since the attractor behaviour means that trajectories become closer as they evolve there must be a non-standard measure on $\phi - \dot{\phi}$.

The work in this chapter begins the process of extending the work in Ref. [88] to any FLRW universe that has second-order equations of motion. It is shown that $\phi - \dot{\phi}$ can be thought of as an effective phase space. This is a stepping stone on the way to be able deal with classical evolution of the measure of the initial conditions of inflation. Full understanding of this process would mean that it is possible to say how likely certain outcomes will be given a distribution of initial conditions. This seems to be an important step in answering the types of questions asked in, for example, Ref. [50]. A more thorough discussion of this is left to chapter 6.

3.2 Hamiltonian Cosmology

This chapter relies on concepts that are part of the canonical formalism. These ideas are most commonly encountered for the first time in the realm of classical mechanics and remain the same in essence when considering the Universe, with some changes. The process of finding generalised coordinates and their conjugate momenta is unchanged and the Hamiltonian is still given by the Legendre transform of the Lagrangian. So, starting with a theory defined with the Lagrangian $\mathcal{L}(q, \dot{q})$ the momenta conjugate the generalised coordinates, q, are given by:

$$p_i = \frac{\partial \mathcal{L}}{\partial \dot{q}_i}. \tag{3.1}$$

The Hamiltonian of the system is defined as:

$$\mathcal{H} = \sum_i \dot{q}_i p_i - L. \tag{3.2}$$

The first conceptual issue that needs to be tackled can be seen when considering

the action for the simplest possible Universe with some type of matter content, a scalar field. The action is:

$$S = \int \sqrt{-g} d^4x \left[\frac{R}{2} + \mathcal{L}\left(\phi(x)\right) \right]. \tag{3.3}$$

The problem is that since the field-value is dependent on its spacetime coordinate and the coordinates are continuous then there are an infinite number of degrees of freedom in the theory. The space that describes all possible configurations of all possible Universes is known as superspace. Symmetries can reduce the dimensionality of superspace and a subspace with finite degrees of freedom is known as minisuperspace. To this end, systems with exact homogeneity and isotropy are considered, the Friedmann-Lemaitre-Robertson-Walker universes with no perturbations. In this case the generalised coordinates are the scale factor of the Universe and the scalar field value. While a simple example this is adequate to describe the background dynamics during slow-roll single-field inflation.

In Friedmann-Lemaitre-Robertson-Walker universes there is a preferred direction of time (the one which makes the Universe appear homogeneous and isotropic) but there is no preference for the scale of time, the model is time diffeomorphism invariant. This invariance is encapsulated in the lapse function, $N_{\text{lapse}}(t)$, which appears in the metric and, as such, the infinitesimal line element, equation (3.4).

$$ds^2 = -N_{\text{lapse}}^2(t)dt^2 + a(t)^2 \left[dx^2 + dy^2 + dz^2 \right]. \tag{3.4}$$

The Hamiltonian constraint is a direct consequence of the time invariance of the model. Since the model is invariant under time diffeomorphisms, the lapse function should not appear in the equations of motion other than as an overall multiplicative factor which can be removed. Mathematically this translates to the requirement that:

$$\{N_{\text{lapse}}(t), H(t)\} = 0. \tag{3.5}$$

There is an unfortunate conceptual consequence of this restriction. Using the action above and the Lagrangian:

$$\mathcal{L} = -\partial^{\mu\nu}\phi\, \partial_{\mu\nu}\phi - V(\phi), \tag{3.6}$$

for the scalar field leads to the conclusion that the Hamiltonian is identically 0. Given that the Hamiltonian encapsulates time evolution through the Hamilton's

equations, equations (3.7) and (3.8), this is known as the problem of time,

$$\dot{q} = \{q, H\}, \tag{3.7}$$
$$\dot{p} = \{p, H\}. \tag{3.8}$$

For this work the problem of time is relegated to a conceptual issue to allow calculations to be made. This is done by fixing the gauge of the theory, i.e. by setting $N(t)$ to be an arbitrary constant which allows calculations to be made.

To increase readability the lapse function, scale factor and Hubble constant will be written without their argument for the remainder of the chapter.

3.3 Boundary terms for the Horndeski Action

For the purposes of the work contained in this chapter it is important that the action is well-posed since the ultimate aim is to define a phase-space upon which Louiville's theorem holds [29]. This is achieved by the use of the appropriate boundary terms that remove unwanted variations of derivatives of the generalised coordinates. This process is usually unnecessary as it is assumed that the boundary will be far from the area of interest. In this case the local equations of motion will be unaffected. When the Universe is being considered as a whole the boundary becomes relevant. In the case of General Relativity the boundary term is the Gibbons-Hawking-York term [41, 107]:

$$B = \int d^3x \sqrt{h} K, \tag{3.9}$$

where, in this case, h is the determinant of the induced metric on the boundary surface and K is the extrinsic curvature of the boundary surface.

The boundary terms for the general Horndeski theory have been previously calculated by Padilla and Sivanesan [83], equations (3.10) to (3.12) and the new terms in these equations will be introduced as they are used in Section 3.5,

$$B_3 = \int_{\partial N} F_3, \tag{3.10}$$

$$B_4 = \int_{\partial N} 2(G_4 K - [\partial_Y F_4]\, \bar{\Box}\phi), \tag{3.11}$$

$$B_5 = \int_{\partial N} -\frac{1}{2} s G_5 (K^2 - K^j{}_i K^i{}_j)\phi_n$$
$$- G_5 K \bar{\Box}\phi + G_5 \phi^{;ij}{}_{;i} K^i{}_j + \frac{1}{2}\bar{R} F_5 + \frac{1}{2}\left[\partial_Y F_5\right]\left((\bar{\Box}\phi)^2 - \phi^{;ij}{}_{;i}\phi^{;i}{}_{;j}\right). \quad (3.12)$$

3.4 Vector Field Invariant Maps and Effective Phase Spaces

The idea of a vector field invariant map is conceptually simple. It is a map from one space to another (potentially of lower dimension) that maps the vector field unambiguously, so that there is a unique vector defined at each point. To state this in more formal terms some notation must be introduced. The space of all smooth valued functions on a manifold, M, is $\mathcal{F}(M)$. A pullback of a function, $f \in \mathcal{F}(N)$, by a mapping $\psi : M \to N$ is $\psi^* : \mathcal{F}(N) \to \mathcal{F}(M)$. Finally, a definition of a vector field invariant map can be made. A map, $\psi : M \to N$, is a vector field invariant map with respect to a vector field, X, if, for any function, $f \in \mathcal{F}(N)$, and for all $q \in N$, $X_p(\psi^* f) = X_{p'}(\psi^* f)$ for all $p, p' \in \psi^{-1}(q)$.

With the concept of a vector field invariant map, the question of whether a space constitutes an effective phase space is now answerable. A space, N, can be thought of as an effective phase space if it possible to construct a map, ψ, from some region of the full phase space, M, so that the Hamiltonian vector field is invariant under ψ. The key point is that the Hamiltonian vector field is tangent to the curves of motion and so if it is mapped unambiguously from M to N then it is uniquely defined at all points in N. This means that the curves of motion do not cross and so specifying a point in N is enough to specify the dynamics of the system.

3.5 A Vector Field Invariant Map of the Horndeski Action

3.5.1 The Hamiltonian Constraint Surface

In this section the Hamiltonian constraint is explicitly constructed and the surface generated by it is shown to be independent of the scale factor of the model

universe when considered in the special coordinate system of $\phi - \dot{\phi}$. As with the work carried out in Ref. [88] this chapter is interested in the background dynamics of a spatially flat universe. This is the minisuperspace approximation laid out above with a further restriction to only flat universes. The next step involves putting the minisuperspace metric into the Horndeski action, equation (1.35), and ensuring that this action is well-posed. The general boundary terms given in Section 3.3 simplify in the case of the minisuperspace approximation.

The boundary manifold of interest for the minisuperspace approximation is one whose normal vector is a unit vector in the time direction, $n^\nu = (-1/N_{\text{lapse}}(t), 0, 0, 0)$, and this fact combines with the high symmetry of the system to simplify the B_αs considerably. The boundary is parameterised by the spatial coordinates of the four dimensional bulk and has an induced metric, $\mathbf{h}$,[1] given by:

$$h_{ij} = g_{ij}, \tag{3.13}$$

where latin indices denote summing over the boundary coordinates (equivalently in this case, the spacial coordinates of the bulk). Firstly, the normal derivative to the scalar field on the boundary, ϕ_n is given by:

$$\phi_n = n^\nu \partial_\nu \phi|_{\partial N} = \frac{\dot{\phi}}{N_{\text{lapse}}}. \tag{3.14}$$

Examining the covariant derivative on the boundary (rather than the bulk), homogeneity gives $\phi_{;i} = 0$. From this it follows that second covariant derivatives of ϕ are also 0 and $Y = 0$, where Y is the boundary analogue of X. The Ricci curvature of the boundary, $\bar{R}$, is 0 since only flat universes are of interest. Finally, s depends on whether the boundary is spacelike or timelike. Here the boundary is spacelike, $s = -1$. The extrinsic curvature tensor and scalar [18, 60] are given by:

$$K_{ij} = \frac{1}{2N_{\text{lapse}}} \frac{\partial h_{ij}}{\partial t}, \tag{3.15}$$

$$K = h^{ij} K_{ij} = \frac{3H}{2N_{\text{lapse}}}. \tag{3.16}$$

The final term to consider is the function F_3. This is defined in Ref. [83] and in

[1] Symbols in bold should be understood to represent the full tensorial quantity.

the case being dealt with here has the form:

$$F_3 = \int_0^{\phi_n} dx\; G_3\left(\phi, \frac{x^2}{2}\right). \tag{3.17}$$

The main point of note is that given this definition $\frac{\partial F_3}{\partial \phi_n} = G_3$. Using all of this information gives the boundary terms as:

$$B_3 = \int d^3x \left[a^3 F_3\right], \tag{3.18}$$

$$B_4 = \int d^3x \left[\frac{3G_4 a^3 H}{N_{\rm lapse}}\right], \tag{3.19}$$

$$B_5 = \int d^3x \left[\frac{3G_5 a^3 H^2 \dot{\phi}}{N_{\rm lapse}^3}\right]. \tag{3.20}$$

The full, well-posed, action is then:

$$\begin{aligned} S = S_H - \sum_{m=3}^{5} B_m = \int dt \frac{a^3}{N_{\rm lapse}^5} \Big[& P N_{\rm lapse}^6 - F_{3\phi}\dot{\phi} N_{\rm lapse}^5 - (3H\dot{\phi} + 6G_{4\phi}\dot{\phi}) N_{\rm lapse}^4 \\ & -3H^2\left(2G_4 N_{\rm lapse}^2 + G_{5\phi}\dot{\phi}^2 - 2G_{4X}\dot{\phi}^2\right) N_{\rm lapse}^2 + 3H^3 G_{5X}\dot{\phi}^3 \Big]. \end{aligned} \tag{3.21}$$

Now, the conjugate momenta can be calculated in the standard way from the Lagrangian as:

$$\begin{aligned} p_a &= \frac{\partial L}{\partial \dot{a}} = 3a^2 \left[\frac{-2G_{4\phi}\dot{\phi} + 1}{N_{\rm lapse}} - \frac{2H^2\left(2G_4 N_{\rm lapse}^2 + G_{5\phi}\dot{\phi}^2 - 2G_{4X}\dot{\phi}^2\right)}{N_{\rm lapse}^3} \right. \\ &\qquad \left. + \frac{H^2 G_{5X}\dot{\phi}^3}{N_{\rm lapse}^5} \right], \end{aligned} \tag{3.22}$$

$$\begin{aligned} p_\phi &= \frac{\partial L}{\partial \dot{\phi}} = a^3 \left[\frac{P_X\dot{\phi} - 6HG_{4\phi}}{N_{\rm lapse}} + \frac{\dot{\phi}^2 F_{3\phi X}}{N_{\rm lapse}^2} + \frac{6H\dot{\phi}}{N_{\rm lapse}^3}\left(HG_{4X} - HG_{5\phi} - G_{4\phi X}\dot{\phi}\right) \right. \\ &\qquad \left. - \frac{F_{3\phi}}{N_{\rm lapse}^5} + \frac{3H^2\dot{\phi}^2}{N_{\rm lapse}^5}\left(HG_{5X} + 2G_{4XX}\dot{\phi} - G_{5\phi X}\dot{\phi}\right) + \frac{H^3 G_{5XX}\dot{\phi}^4}{N_{\rm lapse}^7} \right]. \end{aligned} \tag{3.23}$$

Note that the momentum associated with $N_{\rm lapse}(t)$ is zero. This means that it is not dynamical and can be set to an arbitrary constant, here $N_{\rm lapse}(t) = 1$ is chosen. Since the key feature in what follows is the a dependency of flow vector

components it is useful to write the momenta as:

$$p_a = a^2\pi_a, \tag{3.24}$$

$$p_\phi = a^3\pi_\phi, \tag{3.25}$$

where the π_is contain all the functional dependency of the momenta on ϕ, $\dot{\phi}$ and H. The Hamiltonian is then constructed in the usual way, equation 3.2. Since the expressions for the momenta are kept general there is no way to invert the expressions to obtain the velocities. Therefore, the Hamiltonian is written as a function of ϕ, $\dot{\phi}$, a and H instead of as function of ϕ, p_ϕ, a and p_a and this also suits the purpose of this chapter.

The Hamiltonian constraint comes from varying the action with respect to the lapse function (before it is set to be constant), see e.g. [60], and gives the Friedmann equation:

$$\begin{aligned} H^3\dot{\phi}^3\left(G_{5XX}\dot{\phi}^2 + 5G_{5X}\right) - 3H^2\left[\dot{\phi}^2\left(\dot{\phi}^2(G_{5\phi X} - 2G_{4XX}) - 4G_{4X} + 3G_{5\phi}\right) + 2G_4\right] \\ - 6H\dot{\phi}\left(G_{4\phi X}\dot{\phi}^2 + G_{4\phi}\right) + \dot{\phi}^2 P_X - P = 0. \end{aligned} \tag{3.26}$$

The two-dimensional Hamiltonian constraint surface in the space of $(\phi, \dot{\phi}, H)$, $C_{a_\star}$, is the same for *all* possible values of $a_\star$ so that, as in the case of Remmen and Carroll [88], it is found that the full constraint surface, C, factorises as a product: $C = C_{a_\star} \times \mathbb{R}_+$.

3.5.2 The Hamiltonian Vector Field Components

The Hamiltonian vector field is defined by:

$$X_{\mathcal{H}} = \frac{\partial \mathcal{H}}{\partial p_i}\frac{\partial}{\partial q^i} - \frac{\partial \mathcal{H}}{\partial q^i}\frac{\partial}{\partial p_i}. \tag{3.27}$$

This definition lends itself to consider components in the ϕ, p_ϕ, a, p_a directions, but the space can be described in any choice of components such as $(\phi, \dot{\phi}, a, H)$. In this second coordinate system the $\dot{\phi}$ and H components of the flow vector are

given by:

$$X_{\mathcal{H}}^{(\dot{\phi})} = X_{\mathcal{H}}^{(p_\phi)} \frac{\partial \dot{\phi}}{\partial p_\phi} + X_{\mathcal{H}}^{(p_a)} \frac{\partial \dot{\phi}}{\partial p_a}, \tag{3.28}$$

$$X_{\mathcal{H}}^{(H)} = X_{\mathcal{H}}^{(p_\phi)} \frac{\partial H}{\partial p_\phi} + X_{\mathcal{H}}^{(p_a)} \frac{\partial H}{\partial p_a}. \tag{3.29}$$

In the case of the Horndeski action, the momenta are given in equations (3.22) and (3.23) and contain the unknown functions $G_i(\phi, X)$. It is impossible to invert these expressions without specifying $G_i(\phi, X)$ and so, to keep the approach in this chapter as general as possible, an alternative route must be found. Directly from Hamilton's equations the components $X_{\mathcal{H}}^{(p_\phi)}$ and $X_{\mathcal{H}}^{(p_a)}$ are given as:

$$X_{\mathcal{H}}^{(p_\phi)} = -\tfrac{\partial \mathcal{H}}{\partial \phi} = \dot{p}_\phi = a^3 \left(3H\pi_\phi + \dot{\pi}_\phi\right), \tag{3.30}$$

$$X_{\mathcal{H}}^{(p_a)} = -\tfrac{\partial \mathcal{H}}{\partial a} = \dot{p}_a = a^2 \left(2H\pi_a + \dot{\pi}_a\right). \tag{3.31}$$

Note that the terms $\dot{\pi}_i$ will, in general, contain second derivatives of the generalised coordinates. These can be eliminated by the equations of motion which can be shown to be independent of a. The easiest way to see this is by writing the Lagrangian as $\mathcal{L} = a^3\lambda$. Then the equation of motion for a, which gives $\dot{H}$, is given by the Euler-Lagrange equations and taking derivatives with respect to H instead of $\dot{a}$ gives:

$$a^2 \left(3\lambda - \left[2H\frac{\partial \lambda}{\partial H} + \frac{d}{dt}\frac{\partial \lambda}{\partial H}\right]\right) = 0. \tag{3.32}$$

That is, the a dependency has factored out of the equation of motion. A similar approach for the ϕ equation of motion yields:

$$a^3 \left(3\frac{\partial \lambda}{\partial \phi} - \left[3\frac{\partial \lambda}{\partial \dot{\phi}} + \frac{d}{dt}\frac{\partial \lambda}{\partial \dot{\phi}}\right]\right) = 0. \tag{3.33}$$

Now, all that remains is to manipulate the partial derivatives terms in equations (3.28) and (3.29). This is a simple inversion of the expressions:

$$\frac{\partial p_i}{\partial p_j} = \frac{\partial \dot{\phi}}{\partial p_j}\frac{\partial p_i}{\partial \dot{\phi}} + \frac{\partial H}{\partial p_j}\frac{\partial p_i}{\partial H}. \tag{3.34}$$

Re-writing this as a matrix equation,

$$\begin{pmatrix} \frac{\partial p_\phi}{\partial p_\phi} \\ \frac{\partial p_\phi}{\partial p_a} \\ \frac{\partial p_a}{\partial p_\phi} \\ \frac{\partial p_a}{\partial p_a} \end{pmatrix} = \begin{pmatrix} 1 \\ 0 \\ 0 \\ 1 \end{pmatrix} = \boldsymbol{D} \begin{pmatrix} \frac{\partial \dot{\phi}}{\partial p_\phi} \\ \frac{\partial H}{\partial p_\phi} \\ \frac{\partial \dot{\phi}}{\partial p_a} \\ \frac{\partial H}{\partial p_a} \end{pmatrix}, \tag{3.35}$$

where $\boldsymbol{D}$ is a 4×4 matrix of partial derivatives, allows the flow vector components to be written in a compact form. The matrix $\boldsymbol{D}$ takes the explicit form:

$$\boldsymbol{D} = \begin{pmatrix} \frac{\partial p_\phi}{\partial \dot{\phi}} & \frac{\partial p_\phi}{\partial H} & 0 & 0 \\ \frac{\partial p_a}{\partial \dot{\phi}} & \frac{\partial p_a}{\partial H} & 0 & 0 \\ 0 & 0 & \frac{\partial p_\phi}{\partial \dot{\phi}} & \frac{\partial p_\phi}{\partial H} \\ 0 & 0 & \frac{\partial p_a}{\partial \dot{\phi}} & \frac{\partial p_a}{\partial H} \end{pmatrix} = \begin{pmatrix} \boldsymbol{A} & \boldsymbol{0} \\ \boldsymbol{0} & \boldsymbol{A} \end{pmatrix}, \tag{3.36}$$

where $\boldsymbol{A}$ is now a 2×2 matrix. Since $\boldsymbol{D}$ takes a block form the system of equations can be written as:

$$\begin{pmatrix} 1 \\ 0 \end{pmatrix} = \boldsymbol{A} \begin{pmatrix} \frac{\partial \dot{\phi}}{\partial p_\phi} \\ \frac{\partial \dot{H}}{\partial p_\phi} \end{pmatrix}, \tag{3.37}$$

$$\begin{pmatrix} 0 \\ 1 \end{pmatrix} = \boldsymbol{A} \begin{pmatrix} \frac{\partial \dot{\phi}}{\partial p_a} \\ \frac{\partial \dot{H}}{\partial p_a} \end{pmatrix}. \tag{3.38}$$

Given this decomposition of the equations the flow vector components can be written as:

$$X_{\mathcal{H}}^{(\dot{\phi})} = \dot{p}_\phi {\boldsymbol{A}^{-1}}_{1,1} + \dot{p}_a {\boldsymbol{A}^{-1}}_{2,1}, \tag{3.39}$$

$$X_{\mathcal{H}}^{(H)} = \dot{p}_\phi {\boldsymbol{A}^{-1}}_{1,2} + \dot{p}_a {\boldsymbol{A}^{-1}}_{2,2}. \tag{3.40}$$

The matrix $\boldsymbol{A}^{-1}$ is given by:

$$\boldsymbol{A}^{-1} = \frac{1}{a^3\chi} \begin{pmatrix} \frac{\partial \pi_a}{\partial H} & -a\frac{\partial \pi_\phi}{\partial H} \\ -\frac{\partial \pi_a}{\partial \dot{\phi}} & a\frac{\partial \pi_\phi}{\partial \dot{\phi}} \end{pmatrix}, \tag{3.41}$$

where

$$\chi = \frac{\partial \pi_\phi}{\partial \dot{\phi}}\frac{\partial \pi_a}{\partial H} - \frac{\partial \pi_\phi}{\partial H}\frac{\partial \pi_a}{\partial \dot{\phi}}. \tag{3.42}$$

Despite the generality of the Horndeski action, this notation allows a clear form

for the expressions of the flow vector to be written down. These are:

$$X^{(\dot{\phi})}_{\mathcal{H}} = \frac{1}{\chi}\left[H\left(3\pi_\phi\frac{\partial\pi_a}{\partial H} - 2\pi_a\frac{\partial\pi_\phi}{\partial H}\right) + \dot{\pi}_\phi\frac{\partial\pi_a}{\partial H} - \dot{\pi}_a\frac{\partial\pi_\phi}{\partial H}\right], \tag{3.43}$$

$$X^{(H)}_{\mathcal{H}} = \frac{1}{\chi}\left[H\left(2\pi_a\frac{\partial\pi_\phi}{\partial\dot{\phi}} - 3\pi_\phi\frac{\partial\pi_a}{\partial\dot{\phi}}\right) + \dot{\pi}_a\frac{\partial\pi_\phi}{\partial\dot{\phi}} - \dot{\pi}_\phi\frac{\partial\pi_a}{\partial\dot{\phi}}\right]. \tag{3.44}$$

That is, there is no dependence on the scale factor in the $\dot{\phi}$ and H components of the flow vector. This, along with the ability to write the constraint surface in terms of only ϕ and $\dot{\phi}$ as shown in the previous section are exactly the criteria laid out in section 3.4 to consider the $\phi - \dot{\phi}$ space as an *effective phase space* following the definition by Remmen and Carroll in Ref. [88]. While the result is presented here for the Horndeski theory, it follows from the argument used here that the result holds for any theory where the Friedmann equation is independent of a and the momentum can be factorised as in equations (3.24) and (3.25).

3.6 Examples

In this section specific theories that are often discussed in cosmological contexts are used to highlight interesting points that arise when considering theories more general than a minimally coupled, canonical scalar field.

3.6.1 Conformally-Coupled Scalar Fields

Theories with an action of the form:

$$S = \int d^4x\sqrt{-g}\left[\frac{1}{2}\Omega(\phi)R + X + V(\phi)\right], \tag{3.45}$$

have been considered to be viable or important in the context of inflation for several reasons. These stem from the original Starobinksy model of inflation [99] through to the more recent superconformal ideas of Kallosh and Linde [55, 56, 58] and Higgs inflation [13]. Due to this interest it makes sense to pay particular attention to important issues that arise when dealing with this set of actions in this context. These theories are a subset of the Horndeski action given in equation (1.35) with $P(\phi, X) = X + V(\phi)$, $G_4(\phi, X) = \frac{1}{2}\left[1 + \Omega(\phi)\right]$ and $G_3(\phi, X) = G_5(\phi, X) = 0$.

Following the prescription outlined in section 3 the first key stage to arrive at is the Hamiltonian of a theory whose action is given by equation 3.45. In calculating this Hamiltonian the conjugate momenta are found to be:

$$p_\phi = \frac{\partial L}{\partial \dot{\phi}} = \frac{a^3\left(\dot{\phi} - 3H\partial_\phi\Omega(\phi)\right)}{N_{\text{lapse}}}, \tag{3.46}$$

$$p_a = \frac{\partial L}{\partial \dot{a}} = \frac{-3a^2\left(2H\Omega(\phi) + \dot{\phi}\partial_\phi\Omega(\phi)\right)}{N_{\text{lapse}}}. \tag{3.47}$$

The Hamiltonian of theories of this type is then given as:

$$\mathcal{H} = \frac{-a^3(t)\left(6\Omega(\phi)H^2 + 6\dot{\phi}\partial_\phi\Omega(\phi)H + 2V(\phi)N_{\text{lapse}}^2 - \dot{\phi}^2\right)}{2N_{\text{lapse}}}. \tag{3.48}$$

The Hamiltonian constraint gives the Friedmann equation, (3.49), defining a three-dimensional hypersurface in the full phase space or two-dimensional surface in the $\phi - \dot{\phi}$ space,

$$2V(\phi) + \dot{\phi}^2 = 6H^2\Omega(\phi) + 6H\dot{\phi}\partial_\phi\Omega(\phi). \tag{3.49}$$

The shape of a slice of the constraint surface for a particular coupling is shown in Figure 3.1. It should be noted that, due to the form of equation (3.49) there are two solutions for H. This was not important in the work of Remmen and Carroll as the solutions had an exact $H \to -H$ symmetry but, as can be seen in Figure 3.1, the symmetry does not necessarily exist in this model. Indeed, this is generally true for any model with $G_4 \neq 1/2$ which is another reason that this example is particularly instructive. This highlights the importance of the caveat introduced in section 3.4, namely that we are mapping from some region of the full phase space, in this case the H^+ or H^- regions.

The components of the Hamiltonian flow vector are then calculated to be:

$$X_{\mathcal{H}}^{(\dot{\phi})} = \frac{3\partial_\phi\Omega(\phi)\left[2V(\phi) - \dot{\phi}^2 + 4H\dot{\phi}\partial_\phi\Omega(\phi))\right]}{6[\partial_\phi\Omega(\phi)]^2 + 4\Omega(\phi)} - \frac{2\Omega(\phi)\left[2\partial_\phi V(\phi) + 3H^2\partial_\phi\Omega(\phi) + 2H\dot{\phi}\partial_\phi^2\Omega(\phi)\right]}{6[\partial_\phi\Omega(\phi)]^2 + 4\Omega(\phi)}, \tag{3.50}$$

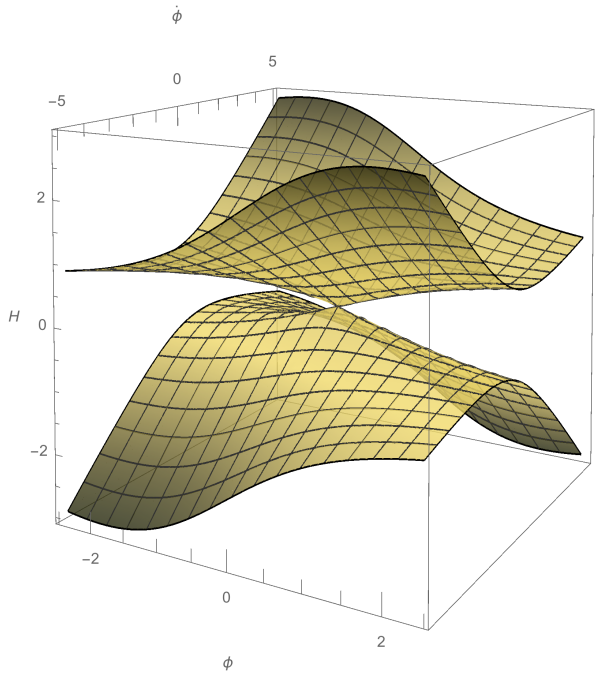

Figure 3.1 *A two dimensional slice, $C_{a_\star}$, of the Hamiltonian constraint surface for a model with a Lagrange density given by equation (3.45) with $\Omega(\phi) = \frac{1}{6}\phi^2$ and $V(\phi) = \frac{1}{2}\phi^2$.*

$$X^{(H)}_{\mathcal{H}} = \frac{6H^2[\partial_\phi\Omega(\phi)]^2 + 2H^2\Omega(\phi) + 2H\dot{\phi}\partial_\phi\Omega(\phi)\left[3\partial^2_\phi\Omega(\phi) + 2\right]}{6[\partial_\phi\Omega(\phi)]^2 + 4\Omega(\phi)} + \frac{2V(\phi)\dot{\phi}^2 + 2\partial_\phi V(\phi)\partial_\phi\Omega(\phi)}{6[\partial_\phi\Omega(\phi)]^2 + 4\Omega(\phi)}. \quad (3.51)$$

The importance of the asymmetric form of the constraint surface can now be seen. Depending on whether the positive or negative solution for H is chosen, two different vector fields are arrived at, Figure 3.2. In many cosmological contexts, for example inflation or quintessence scenarios, this is not a problem because we choose the expanding solution. However, if the scenario of interest was a cosmology where a bounce occurs then this asymmetry in the constraint surface would suggest that the space of $\phi - \dot{\phi}$ would not constitute an effective phase space as there is not a vector field invariant map from the full region that would have to be considered. There have been explorations of the use of $\dot{\phi} - H$ as an effective phase space in simple Horndeski bounce models as it is possible to move between the positive and negative solutions [30, 31].

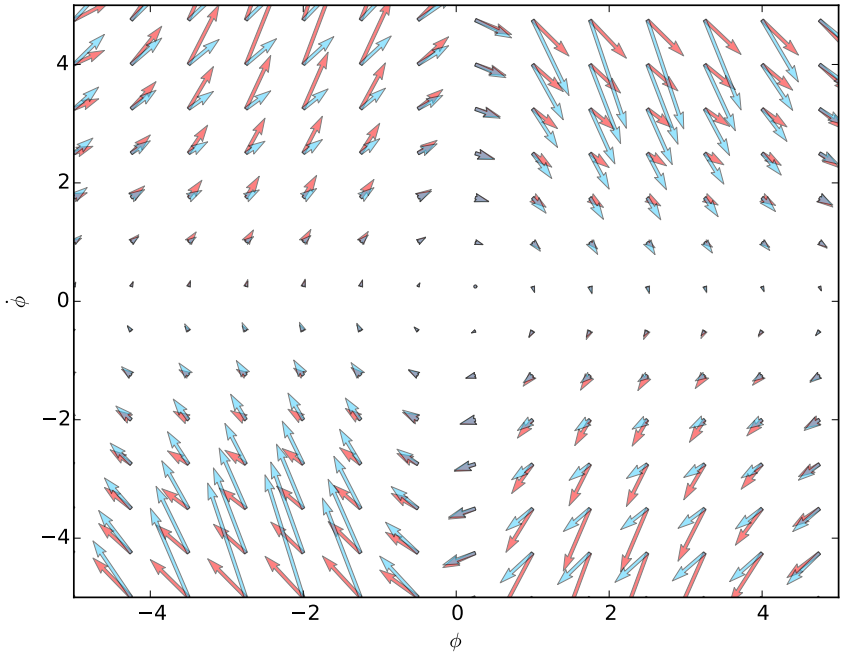

Figure 3.2 *The two different vector fields obtained on $\phi - \dot{\phi}$ when choosing either a positive (red arrows) or negative (blue arrows) H for a model with a Lagrange density given by equation (3.45) with $\Omega(\phi) = \frac{1}{6}\phi^2$ and $V(\phi) = \frac{1}{2}\phi^2$.*

3.6.2 k-flation

While the previous example shows one of the features that needs to be considered when dealing with more general actions, it is possible to make the calculation using the exact method of Remmen and Carroll. The simplest theory that shows the need for the method presented in this paper is that of k-flation [6]. The action, equation (3.52), in this case contains only $P(\phi, X)$ and the usual Einstein-Hilbert term, that is $G_4(\phi, x) = \frac{1}{2}$. All the other terms from equation (1.35) are zero,

$$S = \int d^4x\sqrt{-g}\left[\frac{1}{2}R + P(\phi, X)\right]. \tag{3.52}$$

Once again, using the procedure of Section 3.5, the canonical momenta can be calculated and are found to be:

$$p_\phi = \frac{a^3 P_X \dot{\phi}}{N_{\text{lapse}}}, \tag{3.53}$$

$$p_a = \frac{6a^2 H}{N_{\text{lapse}}}. \tag{3.54}$$

In these equations the complications that prevent the method of Remmen and Carroll being extended to more general cases than considered in Ref. [88] are evident. Without knowing precisely what form $P(\phi, X)$ takes there is no way of inverting equations (3.53) and (3.54) to form expressions for $\dot{\phi}$ and H. The Friedmann equation for k-flation is:

$$3H^2 + P = P_X \dot{\phi}^2. \tag{3.55}$$

In this case the $H \to -H$ symmetry in the constraint surface is not broken so the potential ambiguity seen in section 3.6.1 is not present in the k-flation case. Using the method described above, expressions for the flow vector components are found to be:

$$X_{\mathcal{H}}^{(\dot{\phi})} = -\frac{P_\phi}{P_X}, \tag{3.56}$$

$$X_{\mathcal{H}}^{(H)} = 2H^2 + \dot{H}. \tag{3.57}$$

Equation (3.57) highlights another subtlety with this method: the appearance of second-order derivatives, in the form of $\dot{H}$, in the flow vector components. While in this case it is the second derivative of a that appears, in other examples it may be $\ddot{\phi}$ that will feature. By using the equation of motion for a, the acceleration equation, $\dot{H}$ can be replaced. The equation of motion in this case is:

$$\dot{H} = \frac{1}{2}\left(P - 5H^2\right). \tag{3.58}$$

This gives the final expression for the H component of the flow vector as:

$$X_{\mathcal{H}}^{(H)} = \frac{1}{2}\left(P - H^2\right). \tag{3.59}$$

Once again the flow vector components, equations (3.56) and (3.59), are independent of a. This, coupled with the ability to parameterise the constraint surface in terms of just ϕ and $\dot{\phi}$ (captured in equation 3.55) is the requirement for $\phi - \dot{\phi}$ to be considered an effective space.

3.7 Conclusion

The purpose of this chapter is to show that the most general scalar-tensor theory with a single scalar field and second-order equations of motion, Horndeski Theory, permits a reduction to a two-dimensional effective phase space. This is an extension of a previous result of Remmen and Carroll [88], who showed the same for a canonical, minimally coupled scalar field. There are several features that make the general theory harder to deal with but these are elucidated through the use of specific example theories: conformally-coupled theories and k-flation.

There is still work to be done. In Ref. [88] conditions are laid out for defining an effective Liouville measure on $\phi - \dot{\phi}$. Since these conditions are not proven to hold for a general potential in the simple case considered in Ref. [88], no attempt has been made in this paper to show they always hold in the general case. This will need to be considered on a model by model basis. It should be noted that the measure on the effective phase space is distinct from the Liouville measure on the full phase space. If it proves possible to define a Liouville measure then more sophisticated weighting could be used in numerical calculations of inflationary observables. Instead of uniform weighting in $\phi - \dot{\phi}$, uniform weighting in the Liouville measure could be used as in Ref. [89]. If it can be shown to exist then this measure is the correct classical measure on the effective phase space as it defined by the flow trajectories and is conserved along this flow. A flat measure on $\phi - \dot{\phi}$ is not conserved by the flow along trajectories and as such is not a valid choice.

Chapter 4

Universal Attractors

4.1 Introduction

The strong upper limit set on the tensor-to-scalar ratio r by the *Planck* satellite mission [86] prompted considerable interest in inflationary models predicting low values of r. Amongst those are models where r is of order $(1-n_{\rm s})^2$, where $n_{\rm s}$ is the scalar spectral index. This class includes the original R^2, or Starobinsky, model of inflation [99], the non-minimally coupled Higgs inflation model [13], and a set of models motivated by superconformal symmetry often referred to as 'Universal Attractor' models [58]. These models turn out to be closely related to each other [59]. The quadratic dependence of r on $1-n_{\rm s}$ allows for a tilted spectrum with a small value of the tensor-to-scalar ratio. In Section 4.2.1 the phenomenological idea of these models is briefly reviewed before the remainder of the first half of the chapter outlines a new, detailed investigation of the attractor structure of these models through both analytic and numerical calculation.

The observational situation sharpened considerably in the immediate aftermath of the detection of B-mode polarisation by the BICEP2 experiment [4], which had competing interpretations as a consequence of polarised emission from dust [4, 39, 79] or as due to primordial tensor perturbations. While the former interpretation eventually won out [14] and, as such, the situation is unchanged from *Planck* [79], the latter brought the models considered in this chapter to the fore as such a detection would, for the first time, impose a meaningful constraint on the magnitude of the non-minimal coupling. The second part of this chapter explores

the constraints that could be imposed by results inspired by the BICEP2 data, considering also models where the non-minimal coupling is of quadratic form.

This work was undertaken in the spring and summer of 2014 and is heavily tilted towards the observational picture at that time. The initial release of the BICEP2 result [4] was in March 2014. The combined *Planck* and BICEP2 analysis [14] was released in February 2015.

4.2 The Universal Attractor models

4.2.1 The models

The Universal Attractors are a sub-class of scalar-tensor theories of gravity that feature a particular non-minimal coupling between the inflaton field, ϕ, and the scalar curvature, R. The starting point for the Universal Attractor models is a Lagrangian of the form

$$\mathcal{L}_{\mathrm{J}} = \sqrt{-g}\left[\frac{1}{2}\Omega(\phi)R - \frac{1}{2}(\partial\phi)^2 - V_{\mathrm{J}}(\phi)\right], \tag{4.1}$$

with

$$\Omega(\phi) = 1 + \xi f(\phi) \quad ; \quad V_{\mathrm{J}}(\phi) = \lambda^2 f^2(\phi)\,. \tag{4.2}$$

The non-minimal coupling allows the models to be viable candidates for inflation regardless of the form of $V_{\mathrm{J}}(\phi)$ [58]. This is both in the sense that there are regions of the potential that allow enough inflation and that the predictions from the inflationary epoch are consistent with observation. In this section ξ is always taken to be positive (in this sign convention), which is necessary to get Universal Attractor behaviour. The motivation for such models is rooted in superconformal theories and, while there are 'naturalness' problems in the connection between the coupling term and Jordan frame potential [59], under a certain set of conditions they all imply the same scalar spectral index and tensor-to-scalar ratio, regardless of the function $f(\phi)$. Moreover, the combined values of those are well placed within the *Planck* contours in the n_{s}–r plane [86].

The Jordan frame Lagrangian, equation (4.1), can be transformed to the Einstein frame by use of the conformal transformation:

$$g_{\mu\nu} \to \Omega^{-1}(\phi) g_{\mu\nu}\,, \tag{4.3}$$

which gives the Einstein frame Lagrangian

$$\mathcal{L}_{\rm E} = \sqrt{-g}\left[\frac{1}{2}R - \frac{1}{2\Omega^2(\phi)}\left(\Omega(\phi) + \frac{3}{2}\left[\frac{d\Omega(\phi)}{d\phi}\right]^2\right)(\partial\phi)^2 - \frac{V_{\rm J}(\phi)}{\Omega^2(\phi)}\right]. \tag{4.4}$$

It is then desirable to make a field transformation to obtain a Lagrangian with a canonical kinetic term in the Einstein frame, so that all the inflationary dynamics are contained in the potential as in the standard single scalar field case. This required transformation is

$$\left[\frac{\partial\varphi}{\partial\phi}\right]^2 = \frac{1}{\Omega^2(\phi)}\left(\Omega(\phi) + \frac{3}{2}\left[\frac{d\Omega(\phi)}{d\phi}\right]^2\right). \tag{4.5}$$

This allows the potential slow-roll parameters, equations (2.60) and (2.61), to be calculated as

$$\epsilon \equiv \frac{\Omega^4(\phi)}{V_{\rm J}^2(\phi)}\left(\frac{d}{d\phi}\left[\frac{V_{\rm J}(\phi)}{\Omega^2(\phi)}\right]\right)^2\left(\frac{\partial\phi}{\partial\varphi}\right)^2 \quad ; \quad \eta \equiv \frac{\Omega^2(\phi)}{V_{\rm J}(\phi)}\frac{\partial\phi}{\partial\varphi}\frac{d}{d\phi}\left(\frac{\partial\phi}{\partial\varphi}\frac{d}{d\phi}\left[\frac{V_{\rm J}(\phi)}{\Omega^2(\phi)}\right]\right). \tag{4.6}$$

By utilizing these expressions in the usual expression for the number of e-foldings, it is possible to show [58] attractor behaviour at strong coupling, where $\xi f(\phi) \gg 1$. The first slow-roll parameter is given in terms of the function $f(\phi)$ by

$$\epsilon = \left[\frac{2f'(\phi)}{f(\phi)}\right]^2 \frac{1}{(2 + 2\xi f(\phi) + 3[\xi f'(\phi)]^2)}. \tag{4.7}$$

Then the number of e-foldings is

$$N = \int \frac{1}{\sqrt{2\epsilon}}d\varphi = \frac{1}{4}\int \frac{f(\phi)}{f'(\phi)}\frac{2 + 2\xi f(\phi) + 3[\xi f'(\phi)]^2}{1 + \xi f(\phi)}d\phi\,. \tag{4.8}$$

In the strong-coupling limit N is given by

$$N = \int_{\phi_{\rm end}}^{\phi_N}\left(\frac{3}{4}\xi f'(\phi) + \frac{f(\phi)}{2f'(\phi)} - \frac{3f'(\phi)}{4f(\phi)}\right)d\phi\,, \tag{4.9}$$

which can then be simplified further. The explicit conditions for the simplification are most easily seen when equation (4.9) is re-written as

$$N = \frac{3\xi}{4}\int_{\phi_{\rm end}}^{\phi_N} f'(\phi)\left(1 + \frac{2f(\phi)}{3\xi[f'(\phi)]^2} - \frac{1}{\xi f(\phi)}\right)d\phi\,. \tag{4.10}$$

The third term in the integrand is small compared to the first by the earlier

condition $\xi f(\phi) \gg 1$, and it is assumed that the part of the potential being considered is not in the vicinity of any extrema, which also prevents the second term being large [58]. This second condition is equivalent to

$$3\left[\xi f'(\phi)\right]^2 > 2\xi f(\phi)\,. \tag{4.11}$$

This expression is useful in determining the ξ at which the attractor solution is approached and this idea is discussed in section 2.3. Following these steps N is given by

$$N \simeq \frac{3}{4}\xi\left[f(\phi_N) - f(\phi_{\rm end})\right]\,, \tag{4.12}$$

and ϵ by

$$\epsilon \simeq \frac{4}{3\xi^2 f^2(\phi)}\,. \tag{4.13}$$

This expression for ϵ fixes $\xi f(\phi_{\rm end}) \sim 1 \ll N$ (incidentally showing that the strong-coupling assumption $\xi f(\phi) \gg 1$ will marginally fail towards the end of inflation) and so the field value at the end of inflation will contribute negligibly to the number of e-foldings giving the final expression for N as

$$N \simeq \frac{3}{4}\xi f(\phi_N)\,. \tag{4.14}$$

This means that $f(\phi_N)$ is fixed in a potential independent manner and can be used in the expression for ϵ at large ξ. A similar approach yields a potential-independent expression for η. This is most easily arrived at using

$$\eta = 2\epsilon + \frac{\partial\epsilon}{\partial\varphi}\frac{1}{\sqrt{2\epsilon}}\,. \tag{4.15}$$

In the strong-coupling limit the second term is

$$\frac{\partial\epsilon}{\partial\varphi}\frac{1}{\sqrt{2\epsilon}} \simeq -\frac{4}{3\xi f(\phi)}\,. \tag{4.16}$$

Taking the leading order of $1/N$ gives the Universal Attractor solution as [58]:

$$r = \frac{12}{N^2} \quad ; \quad n_{\rm s} = 1 - \frac{2}{N}\,. \tag{4.17}$$

This is exactly the same point in the $n_{\rm s}$–r plane as is given by the Starobinsky model (hereafter referred to as the 'Starobinsky Point') and indicates a deep-seated connection between the two models which is fully explored in Ref. [59].

4.2.2 The nature of the attractor solution

In previous work on the Universal Attractor models the attractor point itself has been discussed in such a way as to either imply it coincides exactly with the Starobinsky point [58] or state that it does [59]. However this is not true (e.g. in Figure 1 in Ref. [58] it can be seen that the numerically-generated trajectories converge to a point displaced from the Starobinsky point), and the Starobinsky point is actually only a first-order approximation to the true attractor point. The discrepancy stems from the simplification of the expression for the number of e-foldings.

The third term in the integrand of equation (4.10) is actually non-negligible. This can be seen by considering equation (4.14), which fixes this term to be of order $1/N$ regardless of how large ξ becomes. This means that, in the strong coupling regime, it is never completely negligible and when it is included the expression for N becomes

$$N = \frac{3}{4}\xi f(\phi_N) - \frac{3}{4}\log\frac{f(\phi_N)}{f(\phi_{\rm end})}\,. \tag{4.18}$$

This extra term can be thought of as altering the precise number of e-foldings that are considered in the analysis, so that instead of N the equations for the attractor point now contain $N + \delta N$. Following this modification through it is found that

$$\delta r = -\frac{24\delta N}{N^3} = -\frac{12}{N}\delta n_{\rm s}\,. \tag{4.19}$$

So it is seen that the correction to $n_{\rm s}$ is of order $1/N^2$ and so ϵ must be included in the expression for $n_{\rm s}$ when considering the exact location of the Starobinsky point (to first order in slow-roll parameters). From equation (4.19) it may be expected that the solutions would fall along this line with some dependence on the particular potential used. However δN is in fact independent of $f(\phi)$. This can be seen by using an iterative approach. Taking $f(\phi_N)_1$ to be given by equation (4.14), then

$$f(\phi_N)_{i+1} = \frac{4}{3\xi}\left(N + \frac{3}{4}\log\left[\frac{f(\phi_N)_i}{f(\phi_{\rm end})}\right]\right)\,. \tag{4.20}$$

This now does not depend on the particular form chosen for $f(\phi)$ since $f(\phi_{\rm end})$ is independent of the functional form of the potential.

This shift of the attractor point can be seen in Figure 4.1. The trajectories are full numerical solutions to equation (4.8) and the green circle shows the point given by the potential-independent iterative method outlined above. The location of

this circle becomes fixed very close to the attractor point even after a only a few iterations. This point is shifted away from the Starobinsky point, but given the accuracy of current data the shift is not significant. It could prove to be important if the uncertainty on both $n_{\rm s}$ and N is reduced by a factor of approximately 10. The if the forecasted combined constraints of the upcoming LiteBIRD [75] and CORE [38] experiments are realised then $n_{\rm s}$ would be restrict to be 0.9625 ± 0.0014. This would be approximately a five-fold increase in precision. If this regime became reality then the next order of slow-roll parameters may have to be considered in the calculation of $n_{\rm s}$ using [100]

$$\frac{n_{\rm s}-1}{2} = -3\epsilon + \eta - \frac{5+36C}{3}\epsilon^2 + (8C-1)\epsilon\eta + \frac{1}{3}\eta^2 - \frac{3C-1}{3}\xi^2_{\rm SR}, \tag{4.21}$$

where $C \simeq -0.73$ and $\xi_{\rm SR}$ is the third slow-roll parameter defined as

$$\xi^2_{\rm SR} \equiv \frac{V'(\phi)V'''(\phi)}{V^2(\phi)}. \tag{4.22}$$

From this the only $1/N^2$ contributions would come from the $\eta^2/3$ and the $\xi^2_{\rm SR}$ terms and these contributions are included in Figure 4.1. The effect of including these two terms is to shift the predicted $n_{\rm s} - r$ point for both the Starobinsky and Universal Attractor models, but they do not contribute to the relative difference. There would also be next-order corrections to expression (4.8), due to the relation between the Hubble and potential slow-roll parameters. However we did not include these here as there is already a large uncertainty in the value which N should take and these extra corrections are well within this range. If the accuracy to which N is known was increased to the level suggested above, then the corrections become important and can be implemented using the expressions provided in Ref. [64].

4.2.3 Approaching the attractor solution

Planck's non-detection of primordial tensor modes reignited interest in the Starobinsky model and those closely related to it, since these models suppress tensor modes and, as such, are placed at the 'sweet spot' of the *Planck* data [86]. The Universal Attractors become equivalent to the Starobinsky model in the large-coupling regime [59], and so were generally considered where they were approaching the attractor behaviour.

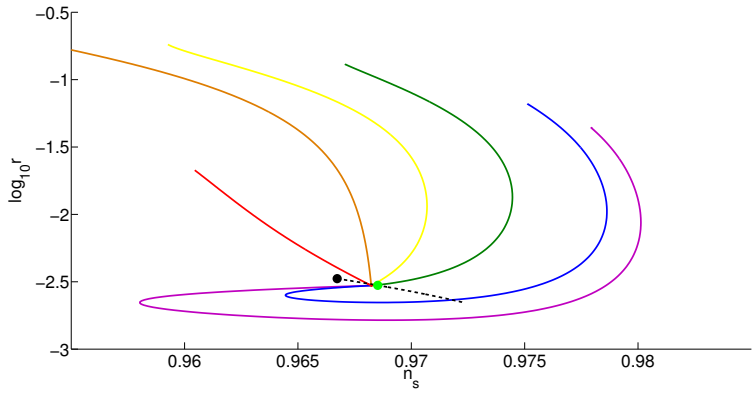

Figure 4.1 *An illustration of the attractor behaviour for monomial potentials* $V(\phi) = \phi^n$ *for* $n = 6, 4, 3, 2, 1, 2/3$ *with* n *decreasing towards the blue end of the spectrum. The upper ends of the lines correspond to* $\xi = 10^{-3}$*. The black dot gives the point predicted by the Starobinsky model, the dashed line is given by equation (4.19), and the green circle is the particular value on this line given by the potential-independent iterative approach.*

The parameter values where this happens are encapsulated in equation (4.11), which is required for the simplification of the expression for ϵ to equation (4.13) and is also the condition to neglect the second term in equation (4.10). Thus, once a potential is specified the minimum ξ required to be close to the attractor point is analytically calculable. In the case of the monomial potentials where $f(\phi) = \phi^{n/2}$, the minimum ξ is given in terms of n. Denoting this minimum as $\Xi(n)$, the expression for $\Xi(n)$ is

$$\Xi(n) \equiv \left(\frac{8}{3n^2}\right)^{n/4} \left(\frac{4N}{3}\right)^{1-n/4} . \tag{4.23}$$

This function is plotted in Figure 4.2 and can be seen to vary dramatically with n.

A similar analysis can be carried out with Natural Inflation [3], the other specific case considered in Ref. [58]. If the coupling function is taken to be $f(\phi) = \sqrt{1 + \cos(\phi/\mu)}$ then the minimum ξ is now a function of μ, $\Xi(\mu)$, given by

$$\Xi(\mu) \equiv \frac{4}{3}\sqrt{\frac{N^2}{2} + N\mu^2} . \tag{4.24}$$

This function is also plotted in Figure 4.2 and a comparison with the monomial case shows that the ξ value required to approach the attractor is very different for different forms of the potential.

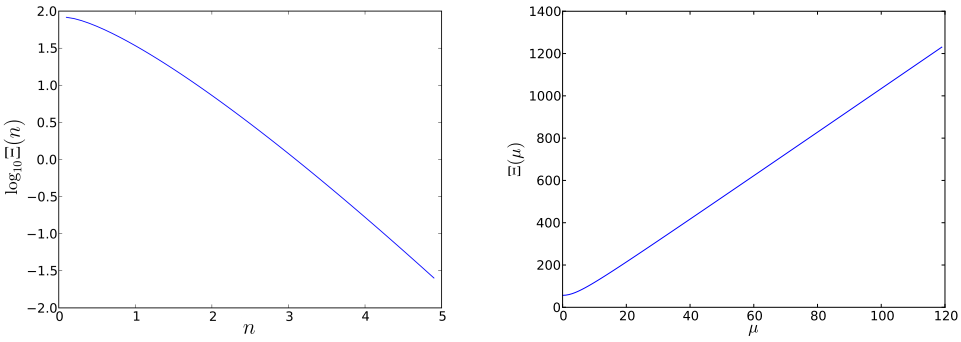

Figure 4.2 *The minimum coupling required to enter the attractor regime, encapsulated in the function $\Xi(n)$ (for the monomial potential, left panel) and $\Xi(\mu)$ (for the natural inflation potential, right panel).*

The general behaviour of $\Xi(n)$ and $\Xi(\mu)$ is similar in that both show that for a steeper potential (higher n and lower μ respectively) the attractor is approached more rapidly, agreeing with the general statement of Ref. [58].

In equation (4.23) the expression for the number of e-foldings is taken to be the simple expression, equation (4.14). Though this is only a first-order result, it suffices here to place an approximate lower bound on ξ.

4.3 Observational constraints from Non-Zero Measurements of the Tensor-Scalar Ratio

Now the implications that a constraint on the scalar-tensor ratio, r, from below, inspired by the claimed BICEP2 result [4], would have for these models is considered. Since the measured BICEP2 B-mode power spectrum has been shown to be dominated by polarised dust [4, 14, 39, 68, 79] , it is prudent to consider a scenario where the signal is noticeably lower than the BICEP2 result. This section considers the possibility that a smaller but still significantly non-zero fraction of the observed B-mode signal has primordial tensor origin. In that case, the Universal Attractor would become highly disfavoured.

From the analysis at the end of the previous section it is clear that the Universal Attractor is attained typically only in the limit of high ξ, and in the past there has been no meaningful upper limit on this parameter. If r is shown to be suitably non-zero, say $r > 0.01$, then an upper limit on ξ in different scenarios can be found. The evaluation of this upper limit on ξ is the main objective of

this section. The Universal Attractor models follow continuous trajectories in the n_s–r plane from the non-coupled case to the attractor point, meaning that they can cover a significant fraction of the new area of interest.

In this section the set of models under investigation is broadened. For the Universal Attractor model of equation (4.1), for completeness we now consider negative ξ as well as positive ξ, in anticipation that $\xi = 0$ will not be excluded and hence ξ can be bounded on either side. When ξ is negative, the trajectories in the n_s–r plane move upwards from the minimally-coupled case, and hence are strongly constrained by *Planck*. Additionally, the case where the non-minimal coupling is always of quadratic form, $\Omega(\phi) = 1 + \xi\phi^2/2$, rather than being related to the potential, is considered; such models have been widely discussed since the early days of inflation (for example Refs. [36, 52, 93]). In the case where the potential is quartic, the quadratic coupling and Universal Attractor models coincide. For the quadratic-coupling model, a particular case of interest is the conformally-coupled case which is $\xi = -1/6$ in our conventions. In each case we focus on monomial chaotic inflation models, $V(\phi) = \phi^n$.

As a starting point the BICEP2 data [4] is used to importance sample the Markov Chain Monte Carlo (MCMC) chains provided by the *Planck* Collaboration [86] so that an area in the n_s–r plane corresponding to a 95% confidence region is obtained, shown in blue in Figure 4.3. Since the results of BICEP2 have been shown to be dust dominated, alterations to likelihood are also looked at. Specifically, Ref. [4] shows various foreground models which, to a good approximation, have the effect of rescaling the likelihood in r. Using this idea, importance sampling of the *Planck* Collaboration's MCMC chains for a modified likelihood, the left panel of Figure 4.3, corresponding to the strongest foreground model in Ref. [4], gives another area in the n_s–r plane to consider, shown in red in the right panel of Figure 4.3. This area is actually not so different from the one obtained using the original BICEP2 likelihood, because the rescaled BICEP2 likelihood has less tension with the *Planck* one and so is less prone to be dragged down in the r direction by it.

The constraints placed on the Universal Attractors by the unaltered BICEP2 result are shown in Figure 4.4. This gives an upper bound of $\xi < 0.07$ regardless of n and a lower bound, for well-motivated n, of $\xi > -0.5$. For specific n values the bounds are even tighter, typically in a range of 0.1 or less. These are the first bounded constraints that have been possible for the Universal Attractor models.

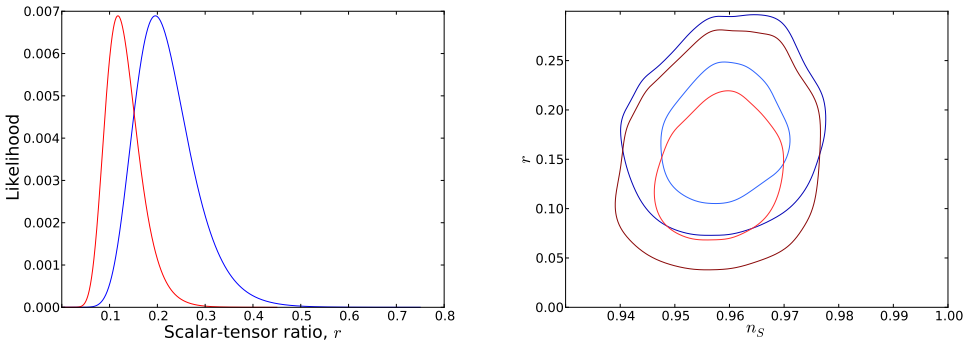

Figure 4.3 *Left panel: the BICEP2 likelihood for r (blue) and the modified likelihood where $r \to 0.6r$ (red). Right panel: the 68% and 95% confidence contours of the importance-sampled Planck MCMC chains using the unmodified BICEP2 likelihood (blue) and the modified likelihood (red).*

Models with a quadratic coupling also follow trajectories in the n_s–r plane, Figure 4.5[1], and so allow a similar analysis whose outcome is shown in Figure 4.6. The bounds for $\xi < 0$ at $n < 4$ are significantly tighter than in the Universal Attractor case, notably excluding the the conformal coupling case, $\xi = -1/6$, and are then broadly similar for $n > 4$ so that the overall constraint on $\xi < 0$ is greatly improved. Just as in the case of the Universal Attractor it is not yet possible to completely constrain ξ for arbitrary n. Whereas for the Universal Attractor the tail that caused the problems was at very small n and so not problematic for well-motivated models, when considering the quadratic coupling the tail exists at $n \to 4^+$ and so cannot be ignored. This tail to infinity occurs because the trajectories begin to curl upwards at a certain value of ξ, seen in Figure 4.5, and this value increases asymptotically as $n \to 4^+$. For larger values of n this flick-back occurs before the observational contours are ever reached, explaining why no models with $n \gtrsim 5.5$ are allowed. Then decreasing n the flick-back now occurs inside the contours giving the wide range of allowed ξ values at $n \simeq 4.5$. As n is decreased still further the flick-back occurs after the trajectory has passed through the observational contours meaning that the peak in Figure 4.6 will fold back at higher ξ values, going to infinity as $n \to 4^+$. In the case where $n = 4$, the Universal Attractor model and the quadratic coupling model are exactly the same and these 'flick-back' trajectories cease to exist and the constraints from both models are seen to be identical. Tighter observational constraints on n_s and r may be able to resolve the issue of the tail to infinity if they rule out the

[1]While these trajectories may look odd, the analysis was done in Matlab originally and then repeated, from the start, in python with both analyses giving the same result.

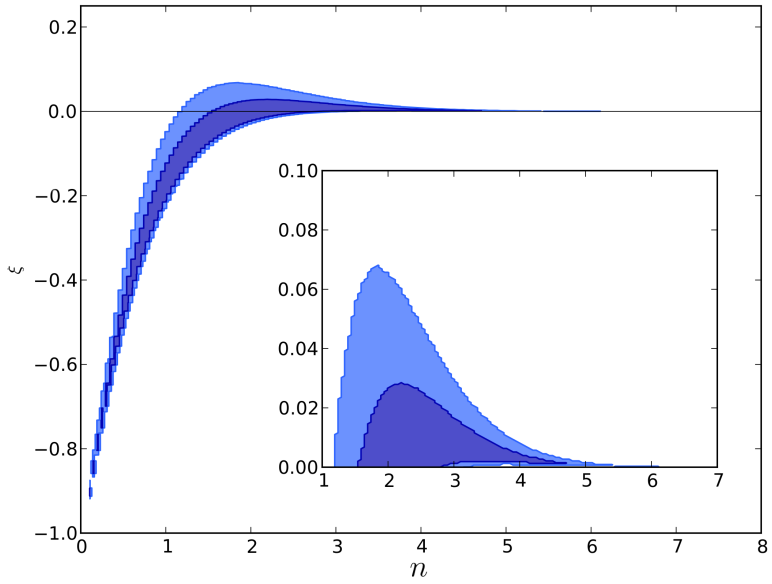

Figure 4.4 *Constraints on the possible values of n and ξ for a Universal Attractor model with a monomial potential using the raw BICEP2 likelihood with the dark blue indicating parameter combinations that give n_s and r values inside the blue 68% confidence region of Figure 4.3, and light blue those inside the 95% confidence region.*

flick-back part of the trajectories.

Even in the case of a significantly-reduced tensor contribution, as depicted in Figure 4.3, the constraint on ξ for the case of the Universal Attractors with a monomial potential is robust; Figure 4.7 shows an upper bound of $\xi < 0.22$ and a lower bound of $\xi > -0.5$. For the models with quadratic coupling the overall picture does not change substantially, with a slightly broader range of allowed ξ for a given n, as in Figure 4.8. The parameters are now constrained from above even in the limit $n \to 4^+$ since as $n = 4$ is approached the 'flick-back' part of the tail begins to miss the shifted contours. This can be seen in Figure 4.8 as there is now a truncated spike instead of the asymptotic behaviour seen from the unmodified BICEP2 analysis.

4.4 Conclusions

The attractor point of the Universal attractor model is discussed at length in the literature. In this chapter an effort has been made to develop the knowledge

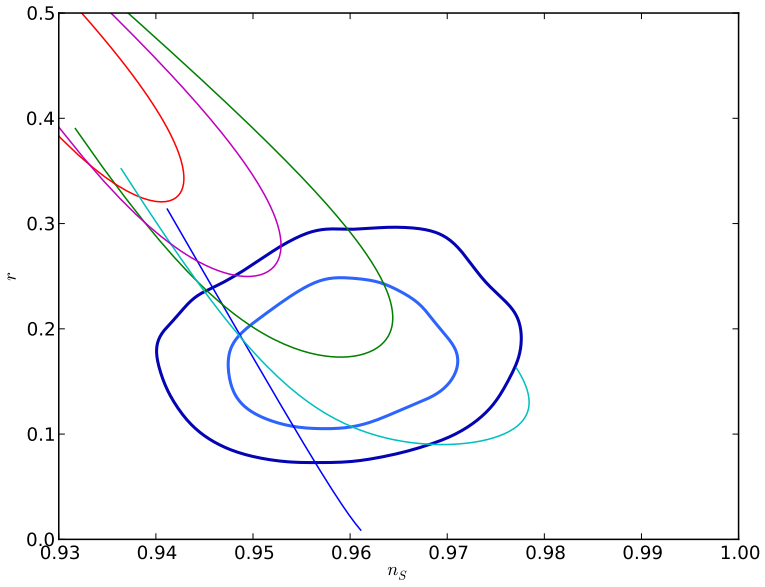

Figure 4.5 *The trajectories followed in the n_s–r plane by the quadratically-coupled models, showing ξ increasing from 0 to 0.15 for $n = 4, 4.5, 5, 5.5, 6$ (represented by blue, cyan, green, purple and red respectively). There is a tail which loops round as ξ is increased and can re-enter the allowed contours. The $\xi = 0$ points are those given by the minimally coupled models and so are those at the end of the trajectories above and to the left of the observational contours.*

surrounding the models to give a more detailed summary of their current status. An in-depth analysis of the high-coupling limit of models shows a shift away from the Starobinsky point which had not been previously acknowledged. The exact positioning of the attractor point is currently a theoretical curiosity, but could be of interest if future CMB measurements improve sufficiently to constrain both n_s and r by a further factor of ten.

The BICEP2 results highlighted an unexplored area of investigation for the Universal Attractors. A non-zero measurement of r would allow strong constraints to be placed on the Universal Attractors for the first time. For monomial potentials the magnitude of the coupling is restricted to $|\xi| < 1$ for well-motivated potentials by the BICEP2 result. This situation is not markedly changed when allowing for a less severe constraint on r.

Finally, the same analysis can be performed on models with a quadratic non-minimal coupling of the inflaton field. Again considering the Jordan frame potential to be a monomial, the coupling is once again restricted to $|\xi| < 1$ for

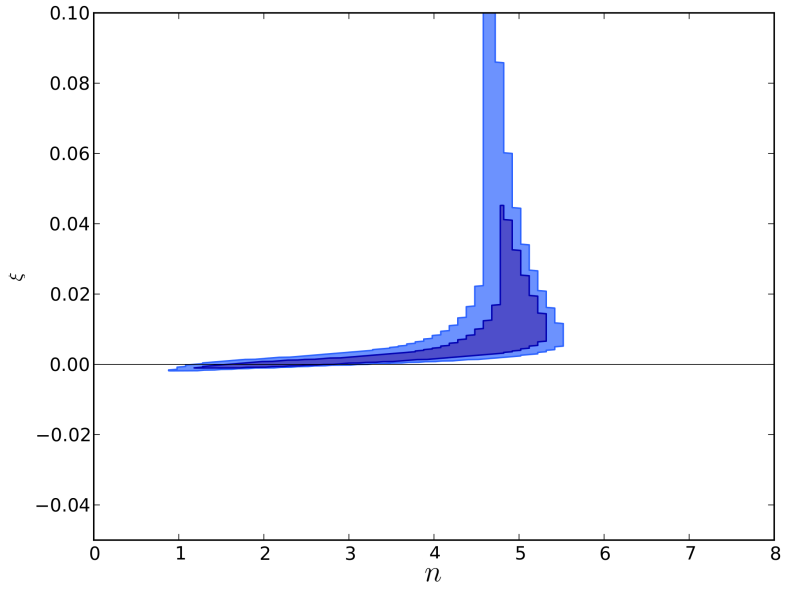

Figure 4.6 *Constraints on the possible values of n and ξ for an inflation model with quadratic non-minimal coupling and a monomial potential using the raw BICEP2 likelihood. The dark blue indicates parameter combinations that give n_s and r values inside the blue 68% confidence region of Figure 4.3, and light blue those inside the 95% confidence region.*

the majority of the possible powers. There is a tail to infinity as $n \to 4^+$, which prevents a comprehensive bound being placed. However slight improvements in the observational constraints to n_s and r could remove this entirely. Once again, allowing for an altered constraint on r does not change the result, other than removing the tail to infinity due to a shift in the contours.

Given the developments on the interpretation of the BICEP2 measurement [14] the work in this chapter would require some small alterations to bring it up-to-date. The joint analysis of the BICEP2 and *Planck* gives the best current constraints on the tensor-to-scalar ratio limiting it to $r < 0.07$. Notably, the joint analysis does not rule out $r = 0$. In this regime the best that the analysis presented in this chapter can achieve is to put a lower bound on ξ.

Future CMB experiments are expected to put stringent bounds on the tensor-to-scalar ratio and as such the analysis in this chapter could put even tighter bounds on ξ than shown here. The CORE [38] and PIXIE [17] experiments are expected to be sensitive to $r \sim 10^{-3}$. If the tensor-to-scalar were pushed this low then the attractor point would be ruled out. This means that the observational viability

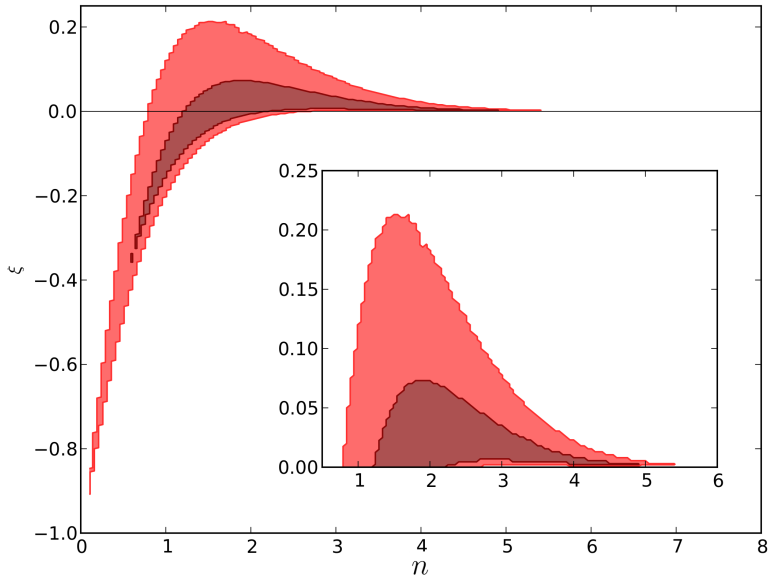

Figure 4.7 *Constraints on the possible values of n and ξ for a Universal Attractor with a monomial potential. Dark red indicates parameter combinations that give n_s and r values inside the red 68% confidence region of Figure 4.3 and light red indicates those that are inside the 95% confidence region.*

of the Universal Attractors would become potential dependent as trajectories in the $n_s - r$ plane would have to be found the loop far below the attractor point, such as some of those shown in Figure 4.1. Any constraints in the $n_s - r$ plane that did not exclude the attractor point would only allow lower bounds to placed on ξ and other means would have to be devised to measure the upper bound.

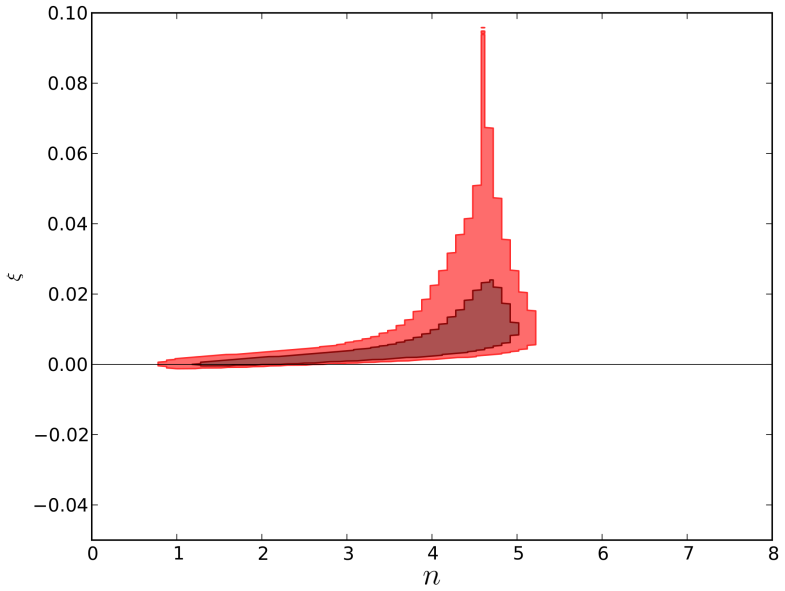

Figure 4.8 *Constraints on the possible values of n and ξ for an inflation model with quadratic non-minimal coupling and a monomial potential. Dark red indicates parameter combinations that give n_s and r values inside the red 68% confidence region of Figure 4.3 and light red indicates those that are inside the 95% confidence region.*

Chapter 5

Stability of the α-Attractors

5.1 Introduction

It has been proposed that inflationary models with a non-trivial field space metric can suffer from a geometric destabilisation that hugely modifies their dynamics [90]. This chapter outlines a numerical exploration of the evolution of a multi-field inflation model that corresponds to some of the most popular models on the market, namely the α-attractors and T-model attractors [54, 56]. These models are of particular interest because they claim to predict generic results for observable quantities, regardless of initial conditions and the particular form of potential considered. This generic result lies well within the combined constraints of *Planck* and *BICEP2* so any deviation from this could prove useful in ruling out such models.

To begin with the mechanism for this destabilisation is introduced in general terms. This is followed by an introduction to the models which leads to the introduction of an effective Lagrangian. The next section presents the results of our numerical investigations which are summarised in the final section.

5.2 Multi-field inflation

In general, there is no requirement for inflation to be restricted to the single-field case that has been considered in this thesis so far. It is entirely possible to have

an arbitrary number, N, fields all of which could contribute to inflation. This chapter is only concerned with two-field models and so the discussion is restricted, where appropriate, to that number to avoid unnecessary confusion.

There is a complication that arises when considering a multi-field model. In the case of a single scalar field it is always possible to take a kinetic term of the form $f(\phi)(\partial\phi)^2$ and construct a field redefinition to obtain a canonical kinetic term. This is not true in the case of a two-field (or N-field) model. In general the kinetic terms for a N-field model appear in the Lagrangian as:

$$\mathcal{L}_{KE} = G_{ij}\partial^\mu\varphi^i\partial_\mu\varphi^j, \tag{5.1}$$

where the term G_{ij} defines the mixing between the partial derivatives of the various fields and the sum of i, j should be understood to be over the fields. G_{ij} is known as the field-space metric and so the methods of Riemannian geometry as outlined in chapter 1 can be applied. The condition for being able to write the kinetic terms canonically normalised is exactly the same condition that says whether or not the metric of a space can be written as the Euclidian metric. This means that for canonical kinetic terms the field-space must be flat in the sense that ${R^{(\text{field})}}^i_{jkl} = 0$. Since this chapter is concerned with models where the field-space is not flat, it is sufficient to present a condition that, if satisfied, shows that the field-space is not flat. In particular, if ${R^{(\text{field})}}^i_{jkl} = 0$, then

$$R^{(\text{field})} = G^{jl}{R^{(\text{field})}}^k_{jkl} = 0, \tag{5.2}$$

and since $R^{(\text{field})}$ is a scalar quantity it is conserved under coordinate transformations (i.e. field redefinitions) and so if $R^{(\text{field})} \neq 0$ for one set of field choices then it is not possible to make field redefinitions to make the kinetic term canonically normalised.

In the case of two or more scalar fields the background equation of motion for each field is given by [94]:

$$\mathcal{D}_t\dot{\varphi^n} + 3H\dot{\phi}^n + G^{ab}V_{,b} = 0, \tag{5.3}$$

where $\mathcal{D}_t X^a = \frac{dX^a}{dt} + \Gamma^n_{ab}X^b\frac{d\phi^c}{dt}$. The linearised equations for the evolution of the perturbations are:

$$\mathcal{D}_t\mathcal{D}_t\delta\varphi^I + 3H\mathcal{D}_t\delta\varphi^I + \nabla^2\delta\varphi^I + M^I_J\delta\varphi^J = 0, \tag{5.4}$$

where M^I_J is the mass matrix. The individual entries are given by:

$$M^I_J = V_{;J}^{\ I} - R_f s^I_{KLJ}\dot{\phi}^K\dot{\phi}^L - \frac{1}{a^3}\mathcal{D}_t\left(\frac{a^3}{H}\dot{\phi}^I\dot{\phi}_J\right). \tag{5.5}$$

In the two-field scenario it is useful to define an 'adiabatic' and 'entropic' direction for the field evolution. Firstly, in the case with fields ϕ and χ the adiabatic field is given as:

$$\dot{\sigma} = (\cos\theta)\dot{\phi} + (\sin\theta)\dot{\chi}, \tag{5.6}$$

where

$$\cos\theta = \frac{\dot{\phi}}{\sqrt{\dot{\phi}^2 + \dot{\chi}^2}}, \quad \sin\theta = \frac{\dot{\chi}}{\sqrt{\dot{\phi}^2 + \dot{\chi}^2}}. \tag{5.7}$$

With this definition of $\dot{\sigma}$ each small increment $\delta\sigma$ follows the background field evolution. The background field density is a unique function of the total density, ρ, in the same way as a single inflationary field would be. This means that it follows the adiabatic condition [70]. In a similar way, the entropic direction is defined as:

$$\delta s = (\cos\theta)\delta\chi - (\sin\theta)\delta\phi. \tag{5.8}$$

Given this definition $\delta s = 0$ along the background trajectory. However, there is no guarantee that the change in the density of the field s caused by a perturbation δs would give a density which is unique as a function of ρ. This means that the s direction does not follow the adiabatic condition and hence sources entropic (or isocurvature perturbations.) The two directions are shown schematically in Figure 5.1.

5.3 The Geometric Destabilisation

As described in section 5.2 when considering two-field inflationary models it is useful to consider a decomposition of the evolution into adiabatic and entropic directions [44]. In potentials with "valleys", i.e. one heavy and one light field, the evolution is usually assumed to develop along the bottom of the valley once it has reached it, Figure 5.2, so that the direction of the valley describes the entropic direction. However, in Ref. [90] a mechanism is highlighted that suggests when the field-space of a theory is negatively curved it is possible for the entropic direction to have negative effective mass squared rendering it unstable to perturbations.

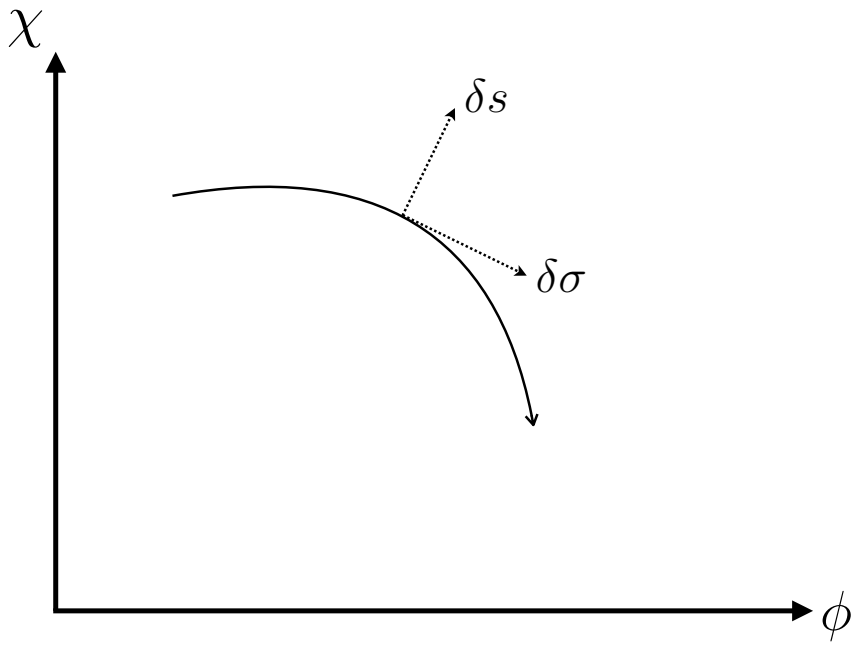

Figure 5.1 *The breakdown of the background two-field inflation trajectory into an adiabatic direction, σ, and an entropic direction ,s. Note that the entropic direction is perpendicular to the overall direction of background evolution.*

Beginning from the general expression for the evolution of field perturbations in a curved field-space, equation (5.4), and projecting it on to the entropic direction using the unit vector

$$e_s = \left(\frac{\dot{\phi}}{\sqrt{\dot{\phi}^2 + \dot{\chi}^2}}, -\frac{\dot{\chi}}{\sqrt{\dot{\phi}^2 + \dot{\chi}^2}} \right) \tag{5.9}$$

gives an expression for the evolution of entropic perturbations. From this the effective mass squared of the entropic direction, m_s is

$$\frac{m_s^2}{H^2} = \frac{V_{;ss}}{H^2} + 3\eta_\perp^2 + \epsilon_H R^{\text{field}} \quad . \tag{5.10}$$

The first term in this equation is just the Hessian contribution, $V_{;ss} = e_s^I e_s^J \left(V_{,IJ} - \Gamma_{IJ}^K V_{,K} \right)$. The second term measures the deviation from geodesics; this commonly occurs in the contexts of turns in the trajectory of the evolution. Finally, the last term is the geometric term that can cause the tachyonic instability. When the field space curvature is negative and with a large enough magnitude then m_s^2 can go negative. This, in general, will occur towards the end of

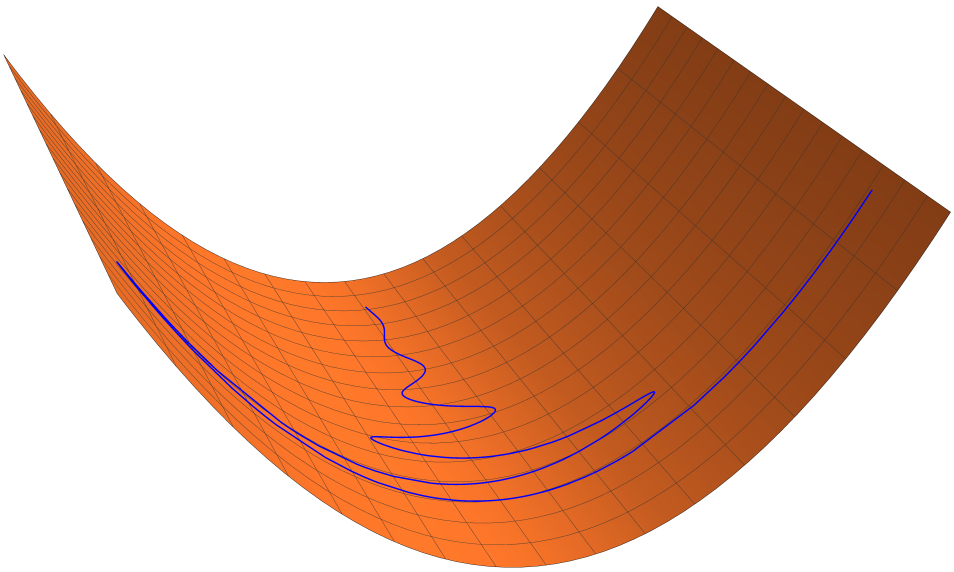

Figure 5.2 *A schematic of the standard multi-field inflation scenario. The blue line represents the evolution of the inflaton from the slopes of the "heavy" potential down into the valley so that it becomes effectively a one dimensional evolution.*

inflation when the slow-roll parameter, ϵ_H, becomes of order one. The particular question this chapter seeks to answer is whether or not this destabilisation occurs in the $\alpha-$attractor and related models, an example specifically highlighted in Ref. [90], as being susceptible to geometric destabilisation.

To get a rough picture of the effect that the mechanism can have, one can consider the neighbourhood of field-space close to the bottom of the valley which the inflationary trajectory "sees" as it evolves. More concretely, suppose that the effective mass squared as given by equation (5.10) were actually due to only the second derivative of the potential - what would such a potential look like? Figure 5.3 gives a rough indication of the answer.

5.4 Methodology

This chapter will ask whether the instability occurs during the inflationary evolution of a model for a given set of model parameters. While the models considered are motivated in different ways and have slight differences in their presentation, they all share some common features. Firstly, they all exhibit

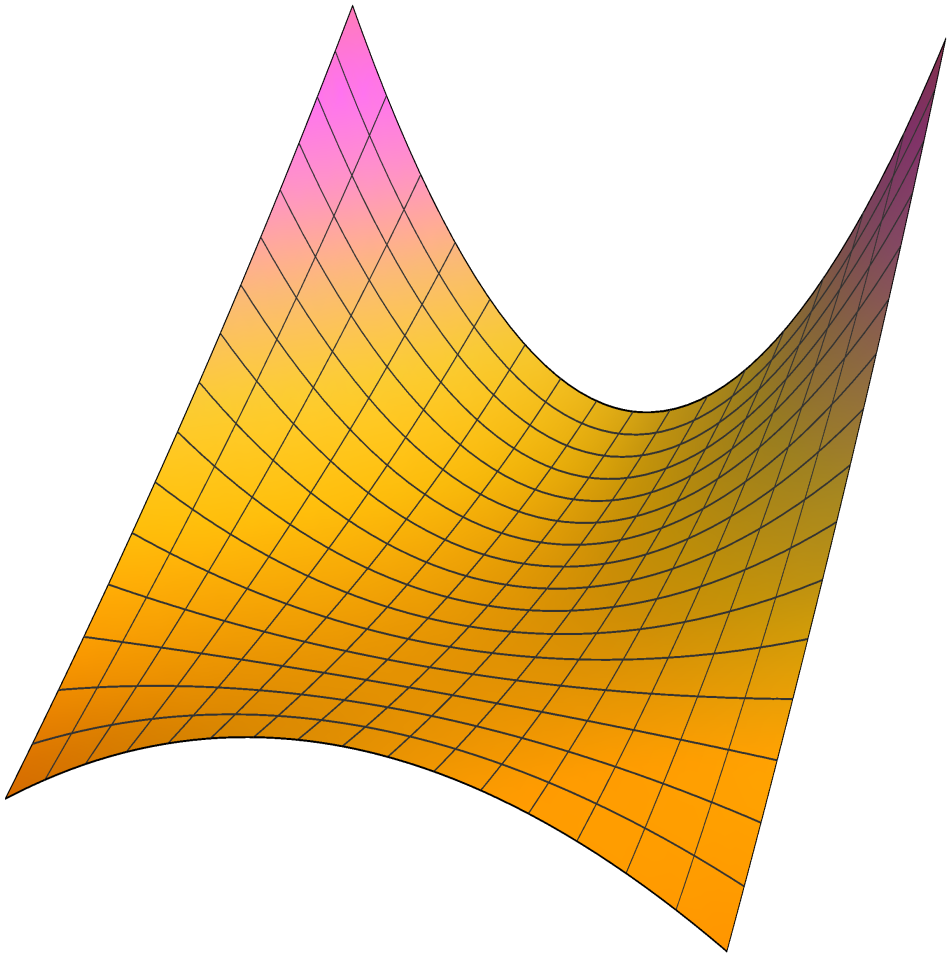

Figure 5.3 *A schematic of the destabilisation scenario. As the inflationary trajectory evolves from back of the plot towards the front it can be seen that $V_{;ss}$ goes from being positive to negative. Thus, instead of the trajectory being well stabilised it actually lives on the top of a ridge and will immediately diverge from the apparent valley that would be expected from looking at the bare potential in the action.*

pseudo-one-field evolution with no complications such as non-canonical kinetic terms or non-minimal coupling to gravity. If sustained this greatly simplifies the Lagrangian and, hence, the equations of motion. This pseudo-one-field inflation is sustained, in the previous analysis of these models, by a valley of precisely the type that may be rendered unstable by the second common feature that these models share: a non-zero field-space curvature that can become large and negative at certain field values.

There is a major benefit of the realisation that the evolution follows a kinetically-canonical, minimally coupled single field. The equations of motion are incredibly straight-forward to numerically solve and there is no need to to employ the

slow-roll approximation to generate results. This is particularly important here since the destabilisation effect will only occur for either large values of R^{field} or large values of ϵ_H. These large values of ϵ_H occur precisely as the slow-roll approximation is beginning to breakdown at the end of inflation. In single-field, minimally coupled inflation $\epsilon_H \leq \epsilon_V$, if $\eta_H < \epsilon_H$ as is usually the case [70]. This can be seen by expressing the first PSR parameter in terms of the HSR parameters. This can be done algebraically [64] giving the expression:

$$\epsilon_V = \epsilon_H \left(\frac{3 - \eta_H}{3 - \epsilon_H} \right)^2 . \tag{5.11}$$

If $\eta_H < \epsilon_H$ then the fraction on the RHS is greater than 1 so that $\epsilon_H \leq \epsilon_V$. Therefore, it seems possible that effects may be incorrectly inferred to exist by assuming the slow-roll approximation.

The best possible case for these models is that they are safely at the bottom of their valley early in the inflationary epoch. The work in this chapter can be considered a stress-test of these models and so this best case scenario is the adopted starting point. Given that they are at the bottom of the valley then it is appropriate to use only the simple pseudo-single-field evolution and simply test the effective squared-mass, equation (5.10), as the trajectory evolves to see if it becomes negative. Despite using only the pseudo-single-field evolution the full multi-field Lagrangian is required to calculate the field-space curvature. The methodology can be summarised as:

1. Begin with full multi-field Lagrangian.
2. Make a field redefinition to ensure that the field of the classical trajectory has a canonical kinetic term. This generally may change the form of the kinetic terms of all the fields.
3. Use this rescaled Lagrangian to calculate an expression for the field-space curvature, R^{field}.
4. Fix the multi-field evolution to the classical trajectory starting at the base of the valley. In the models considered here, this corresponds to considering just one of the fields to undergo evolution.
5. Calculate the field evolution (the full single-field evolution, not simply a slow-roll approximation) and use this to calculate the effective squared mass throughout the evolution.

5.5 The Models

This section will introduce the models that will be examined for geometric instability. All of these models will follow an effective two-field Lagrangian. This effective Lagrangian will have the general form:

$$\mathcal{L}_{\text{eff}} = \sqrt{-g}\left[\frac{1}{2}R + \frac{1}{2}G^{IJ}\partial^{\mu}\phi_I\partial_{\mu}\phi_J - V(\phi_i)\right], \tag{5.12}$$

where $G^{IJ} \equiv G^{IJ}(\phi_i)$ and $V(\phi_i)$ are determined by the specific model. Note that all of these models can be written in a frame where they are minimally coupled to gravity and there are no higher-order kinetic terms such as $\Box\phi_i$.

5.5.1 No-Scale Starobinsky Model

For the No-Scale Starobinsky model [35], the starting point is (5.12)[1], with two real scalar fields, ϕ and ψ, and the field-space metric taken to be:

$$G^{IJ} = \sec^2\left(\sqrt{\frac{2}{3}}\psi\right)\begin{bmatrix} 1 & 0 \\ 0 & 1 \end{bmatrix}, \tag{5.13}$$

and the potential:

$$V(\phi,\psi) = \frac{\mu^2 e^{-\sqrt{2/3}\phi}}{2}\sec^2\left(\sqrt{\frac{2}{3}}\psi\right)\left(\cosh\left[\sqrt{\frac{2}{3}}\phi\right] - \cos\left[\sqrt{\frac{2}{3}}\psi\right]\right), \tag{5.14}$$

and the shape of this potential can be seen in Figure 5.4. The potential would appear to be stable in the ψ-direction at first glance as $\partial^2 V/\partial\psi^2 > 0$. However, the field-space metric is non-trivial and leads to a field-space curvature scalar of $R_{fs} = -4/3$ and so this model falls into the broad category of models under threat from the destabilising mechanism and is even highlighted as a specific example in Ref. [90] as becoming unstable.

At this point it is worth highlighting a slight difference between the effective Lagrangian set out in equation (5.13) and the example used in Ref. [90]. The effective Lagrangian used here is the full expression whereas the Lagrangian in

[1]This starting point already assumes that a complex scalar field, given the interpretation of a modulus field or supersymmetric partner depending on the model has already been stabilised. The remaining complex "matter" field is then separated into its real and imaginary parts with the real part being considered the inflaton.

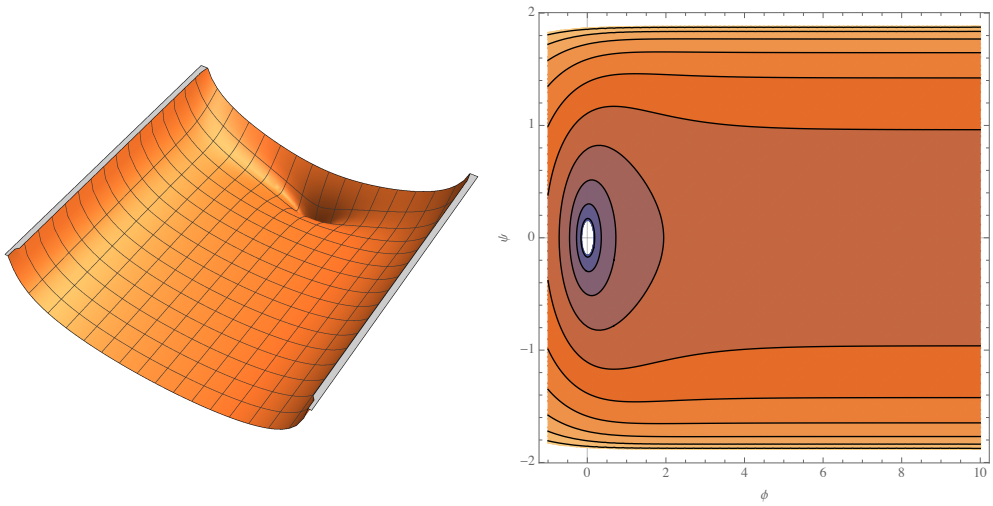

Figure 5.4 *Representations of the two-field potential, equation (5.14), for the No-Scale Starobinsky Model. In the figures the z-direction is* $\log_{10} V$*; this has been chosen to highlight the structure in the potential which is very suppressed.*

Ref. [90] corresponds to an expansion to second order in ψ. The basic argument for destabilisation is as follows. If there has been sufficient time for the field configuration to reach the valley then the field ϕ will be slowly rolling with the ψ field restricted to being at the bottom of its potential valley.

The investigation in this chapter asks whether the simplification to the slow-roll regime is valid when testing for the instability. Given that the scalar curvature is not large compared to 1 and that $m_\psi^2 > H^2$ (to ensure that it is a heavy field not taking part in inflation to begin with), then the value of ϵ required to create the instability is of at least $\mathcal{O}(1)$. This means that the end of inflation is the period under consideration and, as this is the region where the slow-roll approximation breaks down, this alone is enough to warrant further investigations into the claim. As outlined above this model has an effective one-field description when ψ is at the bottom of its potential valley. The Lagrangian simplifies considerably allowing a full numerical solution to calculate calculate H^2 and ϵ_H. The one-field effective Lagrangian of the background evolution is:

$$\mathcal{L}_{\text{eff},\phi} = \sqrt{-g}\left[\frac{1}{2}R - \frac{1}{2}\partial^\nu\phi\partial_\nu\phi - \frac{\mu^2}{2}e^{-\sqrt{2/3}x}\left(\cosh\sqrt{\frac{2}{3}}\phi - 1\right)\right]. \tag{5.15}$$

As a further simplification the particular model under investigation allows equation (5.10) to simplify greatly. The non-zero field-space Christoffel symbols

are given by:

$$\Gamma^{\phi}_{\phi\psi} = \Gamma^{\psi}_{\psi\psi} = -\Gamma^{\psi}_{\phi\phi} = \sqrt{\frac{2}{3}} \tan \sqrt{\frac{2}{3}}\psi, \tag{5.16}$$

but this is 0 when $\psi = 0$ so the Hessian term in equation (5.10) is simply $V_{,\psi\psi}$. Thus, the effective mass squared of the entropic direction is given by:

$$\frac{m_s^2}{H^2} = \frac{V_{,\psi\psi}}{H^2} - \frac{4}{3}\epsilon_H. \tag{5.17}$$

5.5.2 α-Attractors

In this section two separate versions of the α-attractors [53, 54, 56, 57] will be tested for the geometric instability are introduced. The idea is to test two separate regimes to see which, if any, suffers from the instability first. The difference between the two versions is the number of complex scalar-fields that are present in the model. First, the case with just one complex scalar-field is examined to see if the truncation to just the real part of the field is stable. Secondly, a model with two complex scalar-fields that are assumed to truncate stably to real fields is considered to test whether the second field will destabilise irrespective of the imaginary parts. This will allow two separate constraints to be placed on the parameter α.

The α-attractors are a family of models constructed using superconformal symmetry as the starting point. Generically, such theories are based on a Lagrangian described using two functions. The first of these is the Kähler manifold, $\mathcal{N}$, and the second is the superpotential, $\mathcal{W}$. The scalar-gravity part of the Lagrangian is given as:

$$\mathcal{L} = -\frac{1}{6}\mathcal{N}(X, \bar{X})R - G_{I\bar{J}}\mathcal{D}^{\mu}X^{I}\mathcal{D}_{\mu}\bar{X}^{\bar{J}} - G^{I\bar{J}}\mathcal{W}_{I}\bar{\mathcal{W}}_{\bar{J}}, \tag{5.18}$$

where

$$G_{I\bar{J}} = \partial_I \partial_{\bar{J}} \mathcal{N}, \tag{5.19}$$

and the covariant derivatives $\mathcal{D}_{\mu}$ are covariant with respect to the local $U(1)\,\mathcal{R}$ symmetry. The fields that appear in the Lagrangian are chiral multiplets which will get fixed as complex fields once the symmetries of the theory are broken. In the models that are being considered here, the set of chiral multiplets contains a conformal compensator which will always be denoted X^0. This field is used to break the conformal and $U(1)\,\mathcal{R}$ symmetries and in this role is fixed to a constant

value, $X^0 = \sqrt{3}$. The form of the super potential is not fixed and in this work it is chosen to give a simple form of the potential in the limit where there is only a single real field that is responsible for inflation.

For both models the set-up of the potential is the same. The assumption taken as the starting point is that the inflaton is rolling along a valley that is directed along one direction and is at the minimum of the valley in the second direction. The potential has the general form:

$$V_E(\rho, \theta) = V_r(\rho) + V_a(\theta), \tag{5.20}$$

where ρ denotes the field which is responsible for inflation and θ is the field which should remain stabilised.

Firstly, consider the part of the potential which is responsible for inflation, $V_r(\rho)$. Since in these models the canonically normalised radial field is related to the Jordan frame radial field by $\rho_J = \sqrt{6}\tanh\frac{\rho}{\sqrt{6\alpha}}$, the large ρ regime concerns a highly flat potential, regardless of the exact functional form. We then consider a variety of different monomial potentials to explore the effect of varying steepness towards the end of inflation on the instability. In particular, the potentials of the form $V_r(\rho) = V_{r0}\tanh^n\frac{\rho}{\sqrt{6\alpha}}$ with $n = 2/3, 2, 4$ are used. It is assumed that taking the minimum of the potentials to be at $\rho = 0$ is acceptable for the investigation.

Secondly, consider the stabilising part of the potential, $V_a(\theta)$. Given that this chapter is investigating the behaviour of the inflaton as it rolls along a valley, only the neighbourhood of this potential near the minimum is of importance. Thus, the form of potential used is simply taken as $V_a(\theta) = V_{a0}\theta^2$.

Finally, consider the relative heights of the two parts of the potential. This requires fixing the ratio V_{r0}/V_{a0}. Once again looking at the primary motivation for this work, considering potentials which are "random", the value of this ratio which is selected here is $V_{0r}/V_{0a} = 10^{-1}$. This is chosen as there should *a priori* be no difference between the heights of the two field potentials in cartesian directions so the relative heights should be fairly equal. However, in the field redefinitions the radial direction gets stretched relative to the angular one. This suggests that, when focusing on one valley, the radial direction is less high than the angular.

The α-attractors are of particular interest as they have a particularly simple observational expressions (in the case that they are stabilised). For both varieties,

the scalar spectral index, n_s, and the tensor-to-scalar ratio, r, are given by:

$$n_s = 1 - \frac{2}{N}, \qquad r = \frac{12\alpha}{N^2}. \tag{5.21}$$

Single-field α-attractors

The single-field α-attractors, despite their name, can be considered to be a two-field model. This is because the single inflaton field in the model is a complex scalar field which, in the usual presentation of the theory gets stabilised so that only the real part is non-zero.

To begin with, the model is defined using equation (5.18) with:

$$\mathcal{N} = -|X^0|^2 \left(1 - \frac{|X^1|^2 + |S|^2}{|X^0|^2}\right)^{\alpha}, \tag{5.22}$$

where S is a sgoldstino and throughout the analysis in this chapter it is assumed to be fixed at $S = 0$. From here the conformon is fixed at $X^0 = \sqrt{3}$ and the inflaton is a complex scalar field, $X^1 = \Phi$. Then this field is split into real and imaginary parts as $\Phi = \phi + i\psi$. The final stage is to ensure that the real part of the field is canonically normalised when the imaginary part is stabilised. This requires a field redefinition:

$$\rho = \sqrt{3}\tanh(\phi/\sqrt{6\alpha}). \tag{5.23}$$

This redefinition stretches the potential in the real direction justifying the use of the very flat potentials outlined above in the analysis. The final two-field Lagrangian is:

$$\begin{aligned}\mathcal{L} = \frac{1}{2}R + V(\rho,\psi) - \frac{1}{2\left[\psi^2 + 3\tanh^2\frac{\rho}{\sqrt{6\alpha}} - 3\right]^2}\Bigg[&3(\alpha\psi^2 - 3)\mathrm{sech}^4\frac{\rho}{\sqrt{6\alpha}}\dot{\rho}^2 \\ &+18\alpha\left(\alpha\tanh^2\frac{\rho}{\sqrt{6\alpha}} - 1\right)\dot{\psi}^2 + (6\alpha)^{3/2}\tanh\frac{\rho}{\sqrt{6\alpha}}\mathrm{sech}^2\frac{\rho}{\sqrt{6\alpha}}\dot{\rho}\dot{\psi}\Bigg].\end{aligned} \tag{5.24}$$

From this Lagrangian the field-space curvature can be calculated as:

$$R_{fs} = 2\frac{(2-9\alpha)\alpha + 4\alpha^2 \text{sech}^2\frac{\rho}{\sqrt{6\alpha}} - (\alpha-1)^2\cosh\sqrt{\frac{8\rho}{3\alpha}}}{3\alpha\left[\alpha+1-(\alpha-1)\cosh\sqrt{\frac{2\rho}{3\alpha}}\right]^2} + \frac{4(3\alpha+2)(\alpha-1)\cosh\sqrt{\frac{2\rho}{3\alpha}} - 6}{3\alpha\left[\alpha+1-(\alpha-1)\cosh\sqrt{\frac{2\rho}{3\alpha}}\right]^2}. \quad (5.25)$$

This form for R_{fs} means that this case is not only physically distinct from the previous examples but also qualitatively as R_{fs} changes sign during the evolution of the field. This reduces the possible range of ρ at which the instability may occur.

Taking the case where the imaginary field is stabilised so $\psi = 0$ as being the classical trajectory then allows the Lagrangian to be reduced to the effective one-field form:

$$\mathcal{L} = \frac{1}{2}R + \frac{1}{2}\dot{\rho}^2 + V(\rho). \quad (5.26)$$

Multi-field α-Attractors

The focus is shifted to the multi-field generalisation of the α-attractor model and a slightly different tack is taken compared to the preceding analysis. Here the stability of the imaginary field is assumed and then the question is: does the curved field-space of the fields that are taking part in inflation break the apparent stability of the model in terms of those fields?

The starting point for this model is the Lagrangian in equation (5.18) with:

$$\mathcal{N} = -|X^0|^2\left(1 - \frac{|X^1|^2 + |X^2|^2}{|X^0|^2}\right)^\alpha. \quad (5.27)$$

This section is interested in testing the potential instability solely due to the inclusion of the second field X^2 even if both X^1 and X^2 can be reduced to real scalar-fields[2] . With this in mind, equation (5.27) can be re-written as:

$$\mathcal{N} = -\chi^{2(1-\alpha)}\left[\chi^2 - (\phi_1^2 + \phi_2^2)\right]^\alpha, \quad (5.28)$$

where χ, ϕ_1, ϕ_2 are real scalar-fields. Following through the required calculations

[2]As before, in writing equation (5.27) it has been assumed that S is at the minimum of its potential

leads to the generalisation of the multi-field T-model [54]. In fact, this model essentially extends the multi-field T-model in the same way as is done for the single-field T-model, see e.g. Ref. [57]. The final effective Lagrangian that is arrived at has the form:

$$\mathcal{L} = \frac{1}{2}R - \frac{1}{2}(\partial\rho)^2 - \frac{1}{2}6\sinh^2\left(\frac{\rho}{\sqrt{6\alpha}}\right)(\partial\theta)^2 - V_E(\rho,\theta), \tag{5.29}$$

where θ is an angular coordinate and ρ is a canonically normalised radial coordinate. This scheme of field redefinitions follows that laid out in Ref. [54]. The scalar curvature of field-space for this model is:

$$R_{fs} = -\frac{\cosh\left[\sqrt{\frac{2}{3\alpha}}\rho\right] - 3}{24\alpha\sinh^2\left[\frac{\rho}{\sqrt{6\alpha}}\right]}. \tag{5.30}$$

Once again, as is the case for the single-field α-attractors the field-space curvature does not have a constant sign over the entire space. It specifically changes sign at $\rho_{R=0} = \sqrt{\frac{3\alpha}{2}}\cosh^{-1}3$.

All the pieces for an evaluation of whether the destabilisation occurs for these models are now in place. Now, by taking $\theta = 0$ during the classical evolution an effective single-field Lagrangian is arrived at:

$$\mathcal{L}_{\text{eff},\rho} = \frac{1}{2}R - \frac{1}{2}(\partial\rho)^2 - V_r(\rho). \tag{5.31}$$

5.6 Results

In this section, the instability results are presented with a particular attention paid to the difference between the approximate slow-roll results and the results using the full numerical solutions. Throughout the results which use the slow-roll approximation are presented in red and those where it is not used are presented in blue.

There is a result common to all the models considered in this chapter. The range of field values where the instability looks to be trigger under the slow-roll approximation coincides with the break down of the slow-roll approximation. Therefore, the PSR and HSR parameters are diverging and the slow-roll approximation is not good enough to say whether or not there is geometric destabilisation.

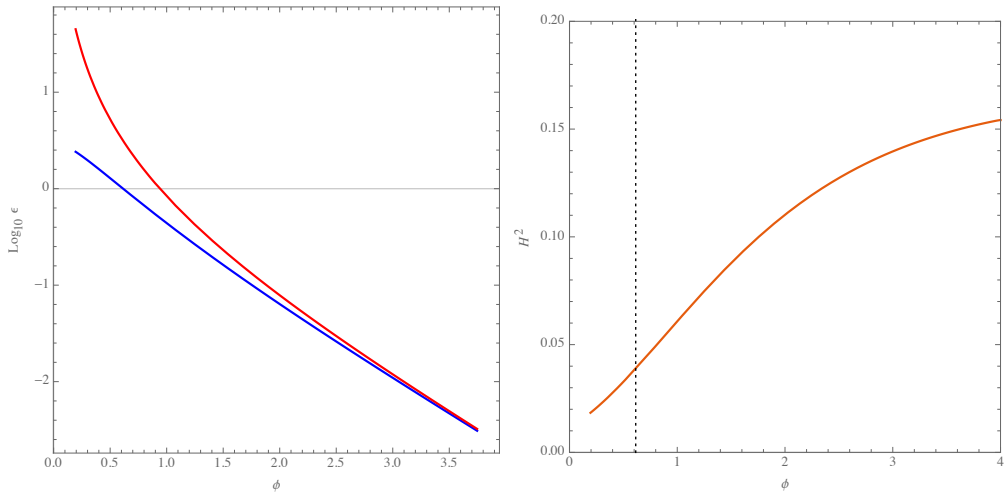

Figure 5.5 *Left panel: The first PSR parameter, ϵ_V, in red and the first HSR parameter, ϵ_H in blue. It can be seen that in the region where ϵ_V is becoming $\mathcal{O}(1)$ there is a noticeable difference between the two parameters. Right panel: The square of the Hubble parameter tracked over the same range of ϕ as the slow-roll parameters in the left panel with the vertical dotted line marking the end of inflation ($\epsilon_H = 1$).*

5.6.1 No-Scale Starobinsky

The No-Scale Starobinsky model gives the first indication that the slow-roll approximation is not sufficient for probing geometric instability. It can be seen, Figure 5.5, that the range of ϕ values where ϵ_V is large enough to suggest the instability will be triggered is in the range where the slow-roll approximation is beginning to break down and the PSR and HSR parameters are diverging.

The effect that this difference in the slow-roll parameters has on the final outcome is large, Figure 5.6. Using the correct HSR parameter rather than the approximate PSR parameter shows that the entropic direction actually remains stable throughout the inflationary epoch. This can be understood by considering the product ϵH^2. Towards the end of inflation the value of H^2 drops rapidly, Figure 5.5 right panel, much quicker than the value of ϵ_H rises. This means that the destabilising term never gets large enough, relative to the Hessian contribution to the mass, to destabilise ψ. However, the PSR parameter, ϵ_V, grows much more rapidly, Figure 5.5 left panel, and this would appear to eclipse the decrease in H^2 if the fact that ϕ is no longer slow-rolling is ignored.

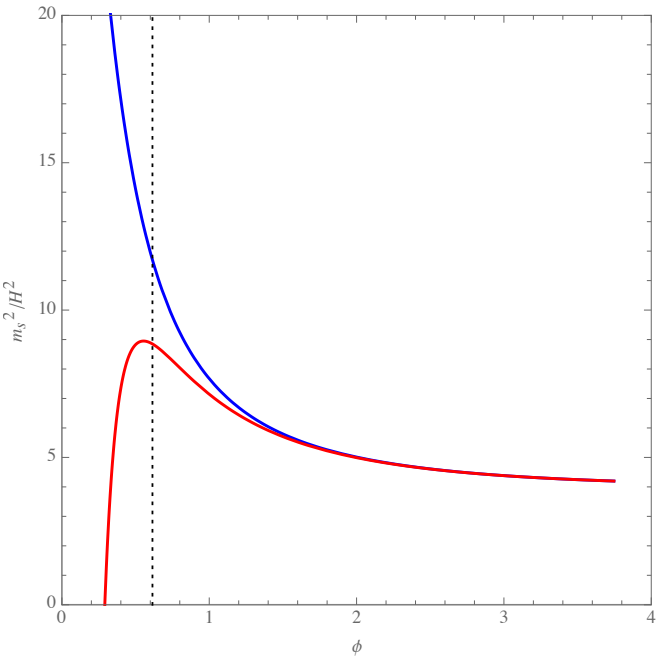

Figure 5.6 *The effective mass squared of the entropic direction calculated from equation (5.17) when the expression for the accurate HSR parameter, ϵ_H, is used, the blue line, and when the approximate PSR, ϵ_V, is used, the red line. The vertical dotted line marks the end of inflation ($\epsilon_H = 1$).*

n	α_{min}
2/3	$10^{-21/25}$
2	$10^{-24/25}$
4	$10^{-24/25}$

Table 5.1: Table presenting the value of α where the geometric instability occurs for the single-field α-attractors.

5.6.2 Single-field α-attractors

For the single-field α-attractors the instability does not occur for all values of α, Figure 5.7, but does appear when α becomes suitably small. This means that there is some minimum stable α, α_{min}, below which the instability occurs. The value of α_{min} has some slight dependence on n, which is presented in Table 5.1.

As highlighted in Ref. [90] it is theoretically uncertain as to how the calculations of observables should proceed once the instability occurs. The different possibilities are not within the scope of this chapter so instead it is assumed that the instability occurring at all is enough to push the model's predictions out of the observational constraints. This is assumed even when this occurs after the end of inflation along

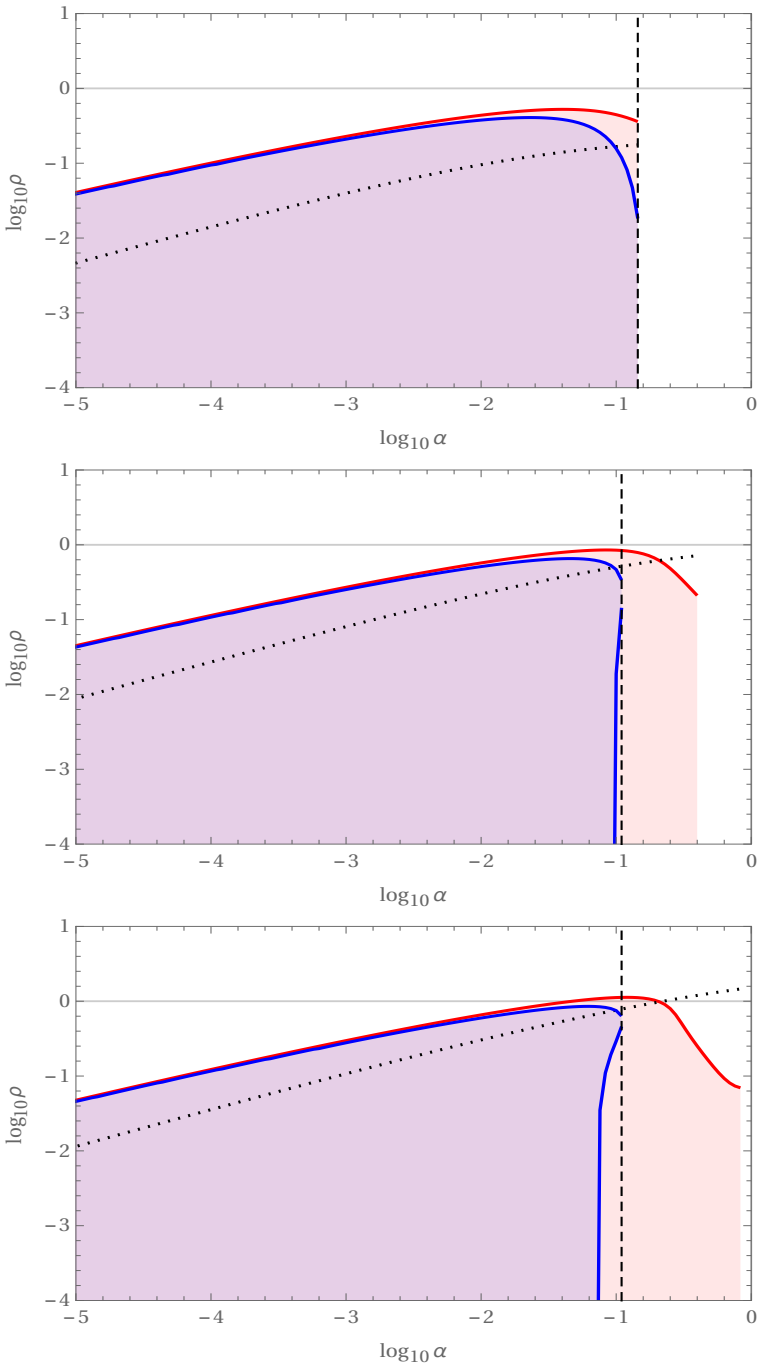

Figure 5.7 *The three destabilisation plots for the single-field α-attractors with $n = 2/3, 2, 4$. The shaded region in each case shows the range of ρ values where the effective mass squared of the θ direction is negative. The red regions are if slow-roll is assumed and the blue if it is not. The value of $\alpha_{\min}$ is shown by the dashed vertical line and is calculated as the largest α at which the destabilisation occurs when slow-roll is not assumed. The dotted line shows the end of inflation.*

the classical trajectory. Note that this latter assumption does not actually affect the conclusions substantially. In the case $n = 2/3$ (where the effect would be largest) the value of α_{min} changes from $\sim 10^{-0.8}$ to $\sim 10^{-1}$ if the extra requirement of the instability occurring before the end of inflation is imposed. Since there is a direct relation between α and the tensor-scalar ratio, equation (5.21), means that it is possible to place a lower bound on the multi-field α-attractors prediction for r. Using equation (5.21) along with $\alpha > 0.1$ and $N = 50$ gives $r > 0.0005$.

5.6.3 Multi-field α-attractors

For the multi-field α-attractors, the results for α_{min} are laid out in Table 5.2. This value of α_{min} does exhibit a small shift upwards as the value of n is increased, see Figure 5.8, but this is less than an order of magnitude.

n	α_{min}
2/3	$10^{-70/25}$
2	$10^{-119/50}$
4	$10^{-54/25}$

Table 5.2: Table presenting the value of α which the geometric instability occurs for the multi-field α-attractors.

Once again, it is possible to put a constraint on r. Since $\alpha_{\text{min}} > 10^{-3}$ for all of values of n then this corresponds to $r > 4.8 \times 10^{-6}$, for $N = 50$.

Even if the angular field was stabilised in the multi-field α-attractors there would still be an imaginary field associated with the radial direction (which was assumed to be stabilised when testing if the angular field became unstable). This means that the multi-field attractors would be more strongly constrained by the instability of that imaginary field, as the α_{min} values calculated in the single-field case are substantially larger than for the multi-field case.

5.7 Conclusion

The purpose of this chapter was to investigate the geometric instability from a different angle than in previous analysis of the effect [90]. In particular, three distinct models are analysed and time is taken to assess the impact of the slow-roll approximation on deciding whether the instability is present.

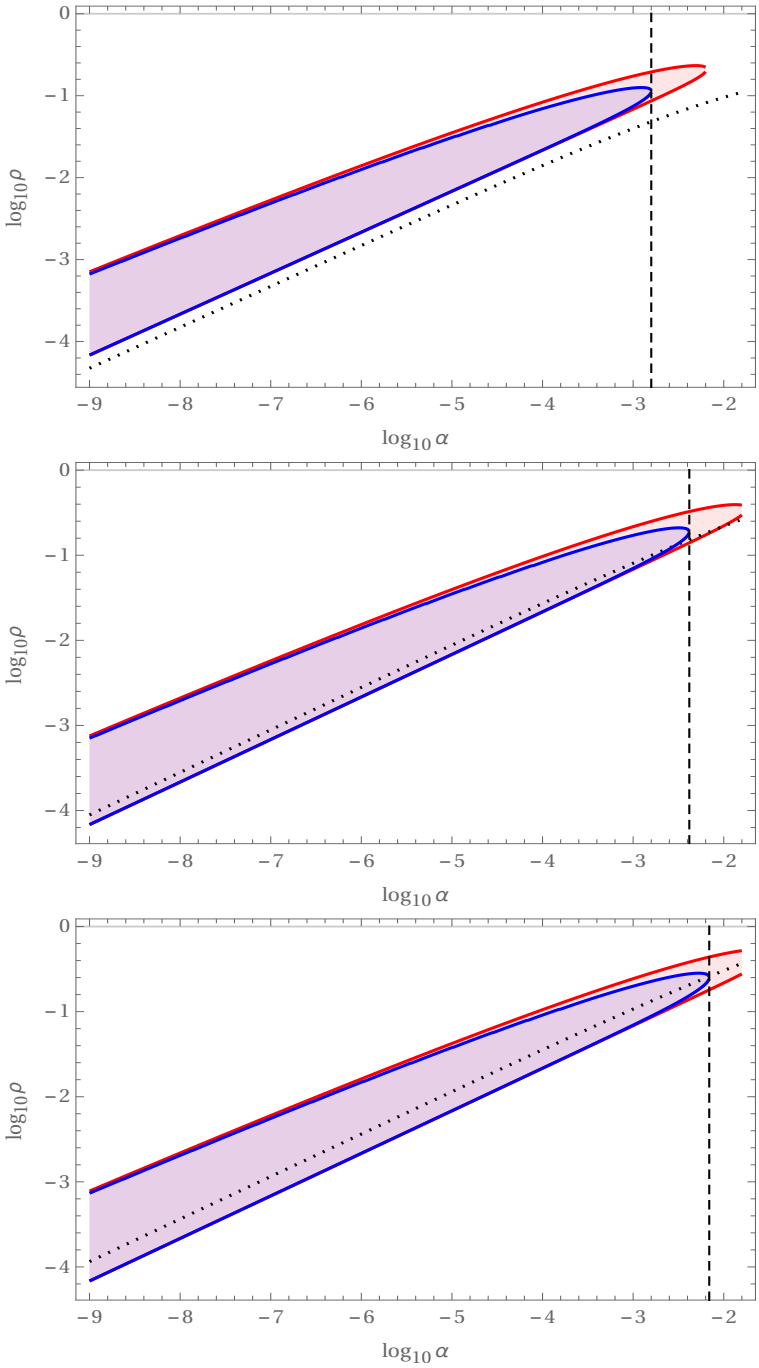

Figure 5.8 *The three destabilisation plots for the multi-field α-attractors with $n = 2/3, 2, 4$. The shaded region in each case shows the range of ρ values where the effective mass squared of the θ direction is negative. The red regions are if slow-roll is assumed and the blue if it is not. The value of $\alpha_{\min}$ is shown by the dashed vertical line and is calculated as the largest α at which the destabilisation occurs when slow-roll is not assumed. The dotted line shows the end of inflation.*

In all cases it is found that there is a marked difference in prediction between the slow-roll approximation and a non-approximated evolution. In the case of the the No-scale Starobinsky model the instability is found not to exist when the full, numerical calculation is made even though it is seen to when the slow-roll approximation is assumed. For the α-attractors, varying the α parameter leads to the onset of the instability but once again, the use of the slow-roll approximation would greatly change the value of α at which the instability occurs. This is true for both the single-field and multi-field models. Given the assumption that any emergence of the instability is fatal to the model it becomes possible to place a constraint on the tensor-scalar ratio, r. For the single-field model the constraint is $r > 0.0005$ and for the multi-field model $r > 4.8 \times 10^{-6}$.

In terms of the direction of future work, there are several ideas that seem to warrant further investigation. First of all, it would seem sensible to explore the stability of the extra fields that have been assumed to stabilised in all the models. Given the results that have been found here suggesting that the instability is generically found in the α-attractors the stability of the sgoldstino field is also in question. A second area that requires further exploration is the question of what happens if the instability does exist. Both of these directions would require substantial work, requiring calculating the Lagrangian including S. Further to that, the exploration of the evolution of the stability would require solving the full, coupled equations of motion for the scalar fields on a curved field-space which is highly non-trivial, though the code presented in Ref. [26] could be repurposed for such an investigation.

Chapter 6

Conclusion

Inflation was first proposed to solve two classical problems of the Big Bang scenario [45]. A phase of pseudo-de-Sitter expansion in the very early Universe was immediately understood to provide a mechanism to explain the homogeneity of the Universe and drive it to flatness. Shortly after the inception of inflation, the calculation of the curvature perturbation [7, 47, 80] was understood to be an important mechanism to rule out potential models. The main focus of early model building was on specific models derived from Grand Unified Theories and required an initial condition of thermal equilibrium [70, 73, 74]. However, the suggestion of a new paradigm, chaotic inflation [65], seemed to solve a wide range of the problems that inflation was suffering from.

The main thrust of the chaotic paradigm is that inflation is a potentially generic state of the early Universe and that slow-roll inflation can happen for a wide-variety of potentials. This idea is has recently come under threat from a variety of sources, e.g. [42, 50, 51], and the current status of inflation is that it is a far from universally accepted theory and its standing as a scientific theory at all is under attack in Ref. [51]. There are two competing viewpoints in this discussion. The first is given in Ref. [50] and alleges that the "classical" theory of inflation is both observationally unlikely and conceptually unsound whereas a more recent "post-modern" theory is flawed in a more serious sense.

An early attack on "classical" inflation can be found in Ref. [42] where the authors argue that the initial conditions for inflation are exponentially unlikely. Their argument stems from a reversal of the well known inflationary attractor behaviour, see Section 2.5.2, run in reverse. If trajectories through the space

$\phi - \dot{\phi}$ approach each other exponentially quickly then they must also diverge from each other exponentially quickly if they are evolved backwards through time. According to Ref. [42] this would mean that there are almost 0 trajectories which will approach the inflationary attractor solution as they are all kinetically dominated.

This argument seems flawed since, at its root, it requires the selection of a particular surface of constant H over which your initial conditions are specified. There seems to be no reason to take this surface to be at the end of inflation rather than at any other point in the history of the Universe, indeed the authors of Ref. [42] admit as much. Changing where this point is decided to be can radically change how likely inflationary trajectories are, see Figure 6.1. In fact, the result that inflation is exponentially unlikely is in direct contrast to the result of Ref. [89] that says precisely the opposite despite having used broadly the same type of approach of considering the classical measure which is conserved throughout the inflationary evolution. It seems that understanding the differences between the two arguments and why the end results are so contradictory is an important next step.

A slightly different argument as to the problem of drawing conclusions from the approach taken in Ref. [42] is highlighted in Ref. [66]. The measure used in Ref. [42] is the classical measure on the full phase-space of a universe containing only a (classical) scalar field. The beginning of inflation is expected to be very shortly after the emergence of 4-dimensional spacetime [66]. This means that the initial conditions of inflation are likely to be defined by a quantum theory of gravity and as such the most information that the evolution of the classical trajectories can provide is how initial conditions from some quantum theory will evolve. Put another way, since there is only one Universe to observe we have no information about the distribution of the initial conditions over the classical measure and so cannot draw a direct conclusion from it.[1]

Interestingly, the problem of kinetically dominated initial conditions is also raised in a separate context in Ref. [50] (whose authors will henceforth be referred to as ISL). The starting-point for the argument is that plateau-like potentials seem to be those favoured by Planck. This causes problems as potentials of this form are

[1]This would seem to be essentially the view espoused by the authors of Ref. [42] : "What the canonical measure does is allow one to discuss in a quantitative way how different proposals for the big bang, or the beginning of the universe, cut down the space of classical trajectories and hence make predictions about the state of the universe today". Their viewpoint is best summarised as it seems unlikely that inflation is likely.

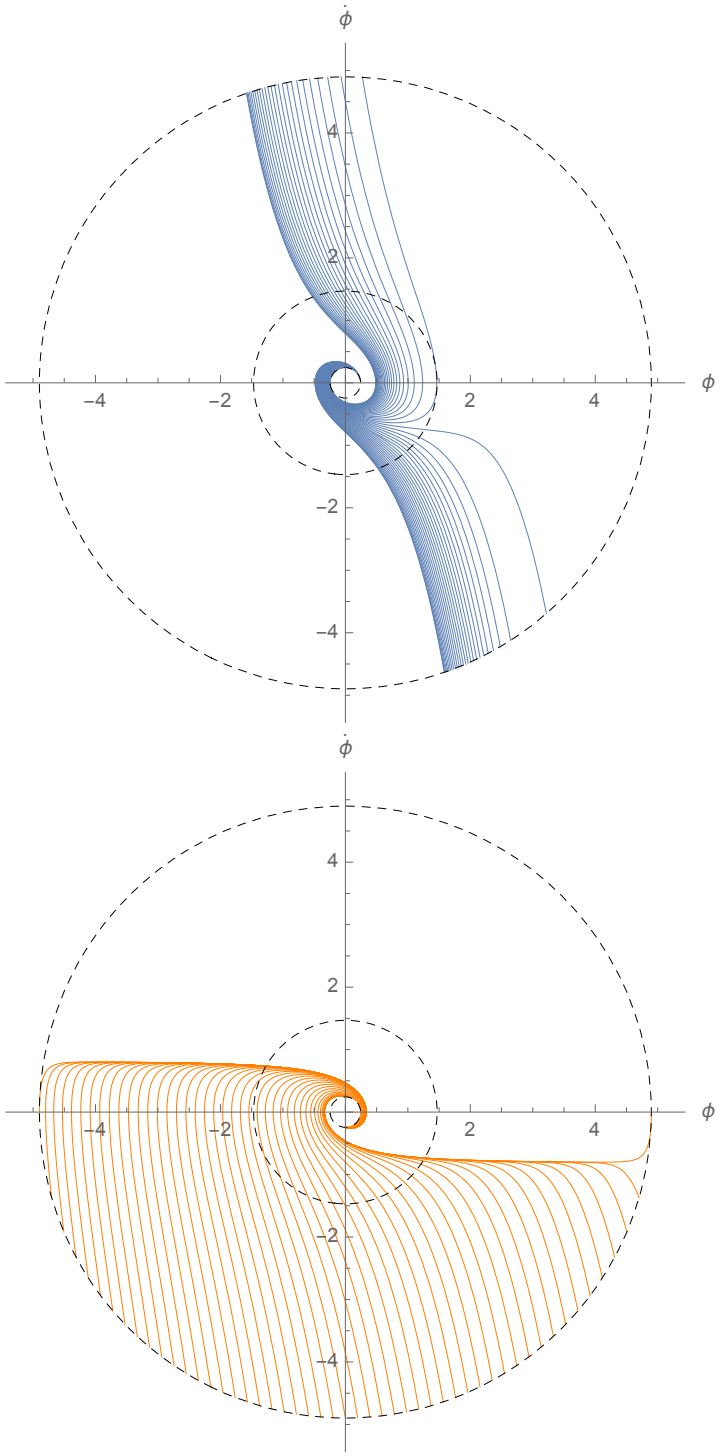

Figure 6.1 *A schematic example of the effect of choosing two separate surfaces of constant H to define initial conditions on. In the upper panel a small value of H is chosen (the inner dashed circle, roughly corresponding with the end of inflation) and the equations are evolved backwards in time. It can be seen that the curves diverge rapidly from the attractor (in black). These trajectories would allow for a very small amount of inflation. In contrast, in the lower panel the initial conditions are set on the outer Hubble surface and evolved forward in time. Here, the usual rapid approach to the attractor behaviour is seen and the standard inflationary picture is reached.*

necessarily bound from above (i.e. have a maximum value) then the constraints on the amplitude of primordial spectrum place an upper limit on the maximum value the potential can take, which is of order $10^{-12}M_P^4$. This conclusion is in direct contrast with the chaotic paradigm which is predicated on a roughly even spread of initial energies in the early Universe, $V(\phi) \sim \dot{\phi}^2$.

A second problem highlighted in Ref. [50] is that inflation on a plateau is unlikely in a second sense. The argument is essentially that inflation on areas of a potential which are plateau-like is less likely than on those which are power-law-like for two reasons. Firstly, there is a much reduced range of field values that would accommodate enough inflation (i.e. around 50+ e-foldings) on the plateau. Secondly, the areas where power-law inflation is allowed would generally give a much larger number of e-foldings of inflation, and so take up a larger volume of the Universe thus corresponding with being a "more likely" observation.

A final problem discussed in Ref. [50] is that the classic inflationary paradigm does not provide predictability. This is because there are no 'generic' predictions of the paradigm. Instead, models can be constructed and initial conditions found that predict a huge variety of different outcomes. The problem with this is that it becomes impossible to discount inflation with observational data as a new model can be created or an existing one tweaked to give the desired results. This problem seems substantially different in nature to the others presented by ISL, as it is an issue with the way in which models should be used and whether the goal of observations is to discount models entirely or restrict the available parameter space. If the purpose is the latter then it seems as though without any notion of which values of the model parameters are likely then little progress can be made in saying whether a model of the Early Universe fits well with observations.

The solution to these problems that is presented in Ref. [46] is one which leads to the introduction of what was later described [51] as the "post-modern" paradigm. The idea here is that the original models of inflation, a single-field model with a ϕ^n potential should be considered nothing more than toy models which provide guidance but not truth. Instead, potentials of multiple, interacting scalar-fields are more "realistic" (in that they are generically predicted from high-energy theories) and so it is perfectly plausible for multiple periods of evolution of a scalar-field into a local minima, eventual decay through quantum tunnelling and then subsequent evolution in a separate field direction. Only the last of these need be the standard slow-roll inflation that matches with observations.

This approach would seem to solve many of the issues that are raised against inflation [46]. It cannot be understated however that this marks a substantial shift in thinking in what may be learned from inflation. The original purpose of inflation was to allow a number of circumstances in the early Universe as generic, they would appear given almost any combination of initial conditions. The "post-modern" approach however suggests that there is no need to for this type of thinking; instead the measure of initial conditions is to be constructed so that scenarios that give universes similar to the one we observe are more common. For ISL this is a catastrophic downfall which should spell the end of the inflationary paradigm completely. They argue that this should remove the status of scientific theory from "post-modern" inflation since there is no predictability.

The place of this thesis lies somewhere between the two contrasting views of Refs. [50, 51] and those of Refs. [46, 67]. The ability to predict a near scale-invariant power spectrum of perturbations from a relatively simple matter content is not one which should be lightly abandoned. The potential problems that exist with the "classical" approach to inflation are often inextricably linked to physics which is not well understood or based upon assumptions about what may happen in that regime. This seems to render such speculation effectively useless couched in caveats of the form "if X then Y". Likewise, it is also impossible to completely defend inflation from the criticisms raised against it apart from by highlighting the caveats and plausible scenarios for escaping any problems. Both sides of the argument have their place and are required but firm conclusions should not yet be drawn.

The position of this author is that a period of inflation should itself be treated as a method through which some high-energy physics theories achieve a universe which matches observation rather than a theoretical necessity that should be constructed at all costs. That is, it is sufficient to describe the observations but not necessary. In some ways this accepts the post-modern view of a complicated potential that leads to the conclusion that the predictions of the theory may rest almost exclusively on its initial conditions. However, the idea that predictions from initial conditions flexible enough to allow any observational prediction should be considered a proof of the theory seems to be something that should be rejected. Instead, theories that make predictions concerning the early Universe (and cannot be constrained solely by observations thereof) should not be considered in a vacuum but combined with other probes. If, after comparisons with a range of observations have been made, the theories which predict inflation

are still standing then it can be considered a success. In this context it is of utmost importance that the predictions made by inflation be fully understood. Work on inflation should then challenge assumptions and search out unexpected consequences of the theories that have been constructed. This last sentence is the driving sentiment behind the work presented in the preceding pages.

In justifying the claim that slow-roll behaviour is generic in inflation, the well known attractor is appealed to. Until recently [88], there was an unresolved discrepancy between this behaviour and Louville's theorem which should not allow attractors to exist. The resolution to this mystery is to show that $\phi - \dot{\phi}$ is an effective phase-space in the sense that it contains all the information about the dynamics of the system. From there, it is possible to define a measure on $\phi - \dot{\phi}$ which is conserved under Hamiltonian flow.

In chapter 3 it is shown that the space of $\phi - \dot{\phi}$ can always be considered to be an effective phase-space if the theory that is under consideration is a subset of Horndeski's theory. This result can be considered the first stage in extending the full result of Ref. [88] to the full Horndeski theory. The intermediary stage itself highlights some interesting features that are worth considering. Non-minimally coupled theories appear to generically introduce some asymmetry in the Hamiltonian constraint surface that can restrict the projection to $\phi - \dot{\phi}$ if a universe goes through a bounce. This result could have an impact if a measure constructed on $\phi - \dot{\phi}$ was ever used to try and weight the likelihood of of different outcomes of a bouncing model.

The Universal attractor models were introduced in Ref. [58]. The main selling point of the model is that a huge variety of potentials seem to provide an identical observational prediction in the strong-coupling limit. Furthermore, at first sight they seem to provide a possible solution to the initial condition problem as they approach an asymptotically flat potential in a strongly coupled limit, approaching the plateau potential regime discussed in Ref. [50]. While whether they do provide such a solution or not is debated, as highlighted above, there are still interesting questions to be asked even if you do accept the premise of the model.

Firstly, since the attractor behaviour is first shown through the use of approximations it is worth checking that these approximations are valid and that there are not any effects that may have a small, but noticeable influence. This is the investigation undertaken in the first part of chapter 4. There it was found that the overall conclusion of Ref. [58] can be considered to hold even when non-leading

order terms are included in the calculation. However, originally it was claimed that the model's attractor location in the $n_s - r$ plane coincided exactly with that of Starobinsky inflation. In chapter 4 it is shown that this is not the case because towards the end of inflation a term with fixed size becomes important relative to the terms which dominate during the early part of inflation. Remarkably, despite this extra term appearing to depend on the particular form of potential and coupling chosen, it is shown to be independent of them and so the offset from the Starobinksy observables is fixed regardless of potential. This fact is the basis of saying that overall spirit of the original conclusion of the model is preserved despite a slight difference in observational predictions.

The idea is to think of the Universal Attractor models as a low-energy effective limit of some high-energy theory. With this in mind it seems to be possible (or rather desirable) that in the future the strength of the non-minimal coupling between the scalar and gravitational sector may be theoretically predicted or at least constrained (either from theory or complimentary experiments). With the slightly optimistic frame-of-mind that one day it is plausible that a confirmation of a non-zero tensor spectrum may be made, the second section of chapter 4 sets about trying to ascertain what kind of limits cosmology might be able to place on the coupling constant. These limits could then, in the future, be compared with those from other sources. It is found that surprisingly strong limits look to be able to be placed on the coupling with a constraint on r somewhat less robust than was originally reported by BICEP2. While the particular constraints from chapter 4 may be, in the future, superseded the question that it asks is likely to gain in relevance.

The final new investigation presented in this thesis is the analysis of the geometric instability initially discussed in Ref. [90]. This instability has the potential to markedly change the observational predictions of the various models including the α-attractors.

In chapter 5 this instability is probed along the classical trajectory of inflation. This allows for a detailed examination of the difference between the slow-roll approximation and full numerical calculation with regards to the instability manifesting itself. It is found that the slow-roll approximation is not good enough for the probing the instability in the No-Scale Starobinsky model and the α-attractors as it occurs at the point where the slow-roll approximation is breaking down. This would seem to be the case for all models where the scalar curvature of field-space is not much larger than 1, as this would require ϵ_H to be of at least

order 1.

The onset of the instability allows a theoretical limit to be set on the α parameter. This assumes that any occurrence of the instability is fatal for the observational worthiness of the model. However, it is also in contrast to the existing literature on the α-attractors which discusses the limit $\alpha \to 0$. This limit cannot be achieved given the assumptions laid out in chapter 5. Moreover, given the direct relationship between α and the tensor-scalar ratio, r, the existence of a minimum α allows a lower bound to placed on r for these models. The value of r that this corresponds to is significantly below the current observational limit.

Overall the work in this thesis seeks to challenge assumptions held in the wider literature. In two cases these challenges did not find interesting new results but provided a solid platform upon which future work can be built. The assumption that the space $\phi - \dot{\phi}$ could be used as an effective phase-space was found to hold for all models that can be written as using the Horndeski action. The Universal Attractor models were found to be both universal and attractors, albeit with a slight deviation from the first-order result. However, the last avenue of investigation did discover that some of the assumptions going into a popular set of models were not valid. The α-attractors were not found to stand-up to the problem of geometric instability, potentially dramatically altering the observational predictions for some range of α.

Bibliography

[1] Abbott, T. et al. (2005). The dark energy survey.

[2] Abbott, T. M. C. et al. (2017). Dark Energy Survey Year 1 Results: Cosmological Constraints from Galaxy Clustering and Weak Lensing.

[3] Adams, F. C., J. R. Bond, K. Freese, J. A. Frieman, and A. V. Olinto (1993). Natural inflation: Particle physics models, power law spectra for large scale structure, and constraints from COBE. *Phys.Rev. D47*, 426–455.

[4] Ade, P. A. R., W. Aikin, R. D. Barkats, J. Benton, S. A. Bischoff, C. J. Bock, J. A. Brevik, J. I. Buder, E. Bullock, D. Dowell, C. L. Duband, P. Filippini, J. S. Fliescher, R. Golwala, S. M. Halpern, M. Hasselfield, R. Hildebrandt, S. C. Hilton, G. V. Hristov, V. D. Irwin, K. S. Karkare, K. P. Kaufman, J. G. Keating, B. A. Kernasovskiy, S. M. Kovac, J. L. Kuo, C. M. Leitch, E. M. Lueker, P. Mason, B. Netterfield, C. T. Nguyen, H. R. O'Brient, W. Ogburn, R. A. Orlando, C. Pryke, D. Reintsema, C. S. Richter, R. Schwarz, D. Sheehy, C. K. Staniszewski, Z. V. Sudiwala, R. P. Teply, G. E. Tolan, J. D. Turner, A. G. Vieregg, A. L. Wong, C. and W. Yoon, K. (2014). Detection of B-Mode Polarization at Degree Angular Scales by BICEP2. *Phys. Rev. Lett. 112*, 241101.

[5] Ade, P. A. R. et al. (2016). Planck 2015 results. XIII. Cosmological parameters. *Astron. Astrophys. 594*, A13.

[6] Armendáriz-Picón, C., T. Damour, and V. Mukhanov (1999). k-Inflation. *Physics Letters B 458*, 209–218.

[7] Bardeen, J. M., P. J. Steinhardt, and M. S. Turner (1983). Spontaneous creation of almost scale-free density perturbations in an inflationary universe. *Phys. Rev. D 28*, 679–693.

[8] Baumann, D. Cosmology, Part III Mathematical Tripos.

[9] Baumann, D. (2011). Inflation. In *Physics of the large and the small, TASI 09, proceedings of the Theoretical Advanced Study Institute in Elementary Particle Physics, Boulder, Colorado, USA, 1-26 June 2009*, pp. 523–686.

[10] Berera, A. (1995). Warm Inflation. *Physical Review Letters 75*, 3218–3221.

[11] Berera, A., I. G. Moss, and R. O. Ramos (2009). Warm inflation and its microphysical basis. *Reports on Progress in Physics 72*(2), 026901.

[12] Bergé, J., P. Touboul, and M. Rodrigues (2015). Status of MICROSCOPE, a mission to test the Equivalence Principle in space. *J. Phys. Conf. Ser. 610*(1), 012009.

[13] Bezrukov, F. and M. Shaposhnikov (2008). The Standard Model Higgs boson as the inflaton. *Physics Letters B 659*, 703–706.

[14] BICEP2/Keck and Planck Collaborations, P. A. R. Ade, N. Aghanim, Z. Ahmed, R. W. Aikin, K. D. Alexander, M. Arnaud, J. Aumont, C. Baccigalupi, A. J. Banday, and et al. (2015). Joint Analysis of BICEP2/Keck Array and Planck Data. *Physical Review Letters 114*(10), 101301.

[15] Biswas, T., E. Gerwick, T. Koivisto, and A. Mazumdar (2012). Towards singularity and ghost free theories of gravity. *Phys. Rev. Lett. 108*, 031101.

[16] Brawer, R. (1996). *Inflationary cosmology and horizon and flatness problems: the mutual constitution of explanation and questions*. Ph. D. thesis, Massachusetts Institute of Technology.

[17] Calabrese, E., D. Alonso, and J. Dunkley (2017). Complementing the ground-based CMB-S4 experiment on large scales with the PIXIE satellite. *Phys. Rev. D95*(6), 063504.

[18] Carroll, S. (2004). *Spacetime and Geometry: An Introduction to General Relativity*. Addison Wesley.

[19] Carroll, S. M. (1997). Lecture notes on general relativity.

[20] Carroll, S. M. (2014). In What Sense Is the Early Universe Fine-Tuned?

[21] Chan, T. K., D. Kereĺ, J. Oñorbe, P. F. Hopkins, A. L. Muratov, C. A. Faucher-Giguère, and E. Quataert (2015). The impact of baryonic physics on the structure of dark matter haloes: the view from the FIRE cosmological simulations. *Mon. Not. Roy. Astron. Soc. 454*(3), 2981–3001.

[22] Clowe, D., M. Bradac, A. H. Gonzalez, M. Markevitch, S. W. Randall, C. Jones, and D. Zaritsky (2006). A direct empirical proof of the existence of dark matter. *Astrophys. J. 648*, L109–L113.

[23] Comstock, D. F. (2014). The principle of relativity. *Science 31*.

[24] Dafermos, M. (2012). Part III differential geometry lecture notes.

[25] Deffayet, C., X. Gao, D. A. Steer, and G. Zahariade (2011). From k-essence to generalized Galileons. *Phys. Rev. D 84*(6), 064039.

[26] Dias, M., J. Frazer, and D. Seery (2015). Computing observables in curved multifield models of inflation - A guide (with code) to the transport method. *JCAP 1512*(12), 030.

[27] Dicke, R. H. and P. J. E. Peebles (1979). The big bang cosmology - enigmas and nostrums. In S. W. Hawking and W. Israel (Eds.), *General Relativity: An Einstein centenary survey*, pp. 504–517.

[28] Duffy, A. R., J. Schaye, S. T. Kay, C. Dalla Vecchia, R. A. Battye, and C. M. Booth (2010). Impact of baryon physics on dark matter structures: a detailed simulation study of halo density profiles. *Mon. Not. R. Aston Soc. 405*, 2161–2178.

[29] Dyer, E. and K. Hinterbichler (2009). Boundary terms, variational principles, and higher derivative modified gravity. *Phys. Rev. D 79*(2), 024028.

[30] Easson, D. A., I. Sawicki, and A. Vikman (2011). G-Bounce. *JCAP 1111*, 021.

[31] Easson, D. A., I. Sawicki, and A. Vikman (2013). When Matter Matters. *JCAP 1307*, 014.

[32] Edwards, D. C. (2016). The effective two-dimensional phase space of cosmological scalar fields. *JCAP 1608*(08), 063.

[33] Edwards, D. C. and A. R. Liddle (2014). The observational position of simple non-minimally coupled inflationary scenarios. *JCAP 9*, 52.

[34] Efstathiou, G. and K. J. Mack (2005). The Lyth bound revisited. *JCAP 0505*, 008.

[35] Ellis, J., D. V. Nanopoulos, and K. A. Olive (2013). No-scale Supergravity Realization of the Starobinsky Model of Inflation. *Physical Review Letters 111*(11), 111301.

[36] Faraoni, V. (1996). Nonminimal coupling of the scalar field and inflation. *Phys.Rev. D53*, 6813–6821.

[37] Feynman, R., F. Morinigo, B. Hatfield, and W. Wagner (1999). *Feynman Lectures on Gravitation*. Penguin Press Science Series. Penguin.

[38] Finelli, F. et al. (2016). Exploring Cosmic Origins with CORE: Inflation.

[39] Flauger, R., J. C. Hill, and D. N. Spergel (2014). Toward an Understanding of Foreground Emission in the BICEP2 Region.

[40] Fulton, T., F. Rohrlich, and L. Witten (1962). Conformal Invariance in Physics. *Reviews of Modern Physics 34*, 442–457.

[41] Gibbons, G. W. and S. W. Hawking (1977). Action integrals and partition functions in quantum gravity. *Phys. Rev. D 15*, 2752–2756.

[42] Gibbons, G. W. and N. Turok (2008). The Measure Problem in Cosmology. *Phys. Rev. D77*, 063516.

[43] Gleyzes, J., D. Langlois, F. Piazza, and F. Vernizzi (2015). Healthy theories beyond Horndeski. *Phys. Rev. Lett. 114*(21), 211101.

[44] Gordon, C., D. Wands, B. A. Bassett, and R. Maartens (2001). Adiabatic and entropy perturbations from inflation. *Phys. Rev. D 63*(2), 023506.

[45] Guth, A. H. (1981). Inflationary universe: A possible solution to the horizon and flatness problems. *Phys. Rev. D 23*, 347–356.

[46] Guth, A. H., D. I. Kaiser, and Y. Nomura (2014). Inflationary paradigm after Planck 2013. *Phys. Lett. B733*, 112–119.

[47] Guth, A. H. and S.-Y. Pi (1982). Fluctuations in the new inflationary universe. *Phys. Rev. Lett. 49*, 1110–1113.

[48] Horndeski, G. W. (1974). Second-order scalar-tensor field equations in a four-dimensional space. *International Journal of Theoretical Physics 10*(6), 363–384.

[49] Hubble, E. (1929). A Relation between Distance and Radial Velocity among Extra-Galactic Nebulae. *Proceedings of the National Academy of Science 15*, 168–173.

[50] Ijjas, A., P. J. Steinhardt, and A. Loeb (2013). Inflationary paradigm in trouble after Planck2013. *Phys. Lett. B723*, 261–266.

[51] Ijjas, A., P. J. Steinhardt, and A. Loeb (2014). Inflationary schism. *Phys. Lett. B736*, 142–146.

[52] Kaiser, D. I. (1995). Primordial spectral indices from generalized Einstein theories. *Phys.Rev. D52*, 4295–4306.

[53] Kallosh, R. (2015). Planck 2013 and Superconformal Symmetry. In *Proceedings, 100th Les Houches Summer School: Post-Planck Cosmology: Les Houches, France, July 8 - August 2, 2013*, pp. 525–545.

[54] Kallosh, R. and A. Linde (2013a). Multi-field conformal cosmological attractors. *JCAP 12*, 006.

[55] Kallosh, R. and A. Linde (2013b). Universality class in conformal inflation. *JCAP 7*, 2.

[56] Kallosh, R., A. Linde, and D. Roest (2013). Superconformal inflationary α-attractors. *Journal of High Energy Physics 11*, 198.

[57] Kallosh, R., A. Linde, and D. Roest (2014a). Large field inflation and double α-attractors. *Journal of High Energy Physics 8*, 52.

[58] Kallosh, R., A. Linde, and D. Roest (2014b). Universal Attractor for Inflation at Strong Coupling. *Physical Review Letters 112*(1), 011303.

[59] Kehagias, A., A. Moradinezhad Dizgah, and A. Riotto (2014). Remarks on the Starobinsky model of inflation and its descendants. *Phys. Rev. D 89*(4), 043527.

[60] Kiefer, C. (2004). *Quantum Gravity*. International series of monographs on physics. Clarendon Press.

[61] Kolmogorov, A., S. Fomin, and R. Silverman (2012). *Introductory Real Analysis*. Dover Books on Mathematics. Dover Publications.

[62] Liddle, A. (2013). *An Introduction to Modern Cosmology*. Wiley.

[63] Liddle, A. R. and S. M. Leach (2003). How long before the end of inflation were observable perturbations produced? *Phys. Rev. D68*, 103503.

[64] Liddle, A. R., P. Parsons, and J. D. Barrow (1994). Formalizing the slow-roll approximation in inflation. *Phys. Rev. D 50*, 7222–7232.

[65] Linde, A. (1983). Chaotic inflation. *Physics Letters B 129*(3), 177 – 181.

[66] Linde, A. (2008). Inflationary Cosmology. *Lect. Notes Phys. 738*, 1–54.

[67] Linde, A. (2015). Inflationary Cosmology after Planck 2013. In *Proceedings, 100th Les Houches Summer School: Post-Planck Cosmology: Les Houches, France, July 8 - August 2, 2013*, pp. 231–316.

[68] Liu, H., P. Mertsch, and S. Sarkar (2014). Fingerprints of Galactic Loop I on the Cosmic Microwave Background.

[69] Lord, E. (1976). *Tensors, relativity and cosmology*. Tata McGraw-Hill.

[70] Lyth, D. and A. Liddle (2009). *The Primordial Density Perturbation: Cosmology, Inflation and the Origin of Structure*. Cambridge University Press.

[71] Lyth, D. H. (1984). A bound on inflationary energy density from the isotropy of the microwave background. *Physics Letters B 147*, 403–404.

[72] Lyth, D. H. (1997). What would we learn by detecting a gravitational wave signal in the cosmic microwave background anisotropy? *Phys. Rev. Lett. 78*, 1861–1863.

[73] Lyth, D. H. (2008). Particle physics models of inflation. *Lect. Notes Phys. 738*, 81–118.

[74] Lyth, D. H. and A. Riotto (1999). Particle physics models of inflation and the cosmological density perturbation. *Phys. Rept. 314*, 1–146.

[75] Matsumura, T. et al. (2014). Mission design of LiteBIRD.

[76] McAllister, L., E. Silverstein, and A. Westphal (2010). Gravity Waves and Linear Inflation from Axion Monodromy. *Phys. Rev. D82*, 046003.

[77] Misner, C., K. Thorne, and J. Wheeler (1973). *Gravitation*. Number pt. 3 in Gravitation. W. H. Freeman.

[78] Misner, C. W. (1969). Mixmaster universe. *Phys. Rev. Lett. 22*, 1071–1074.

[79] Mortonson, M. J. and U. Seljak (2014). A joint analysis of Planck and BICEP2 B modes including dust polarization uncertainty.

[80] Mukhanov, V. F. and G. V. Chibisov (1981). Quantum fluctuations and a nonsingular universe. *ZhETF Pisma Redaktsiiu 33*, 549–553.

[81] Ostrogradski, M. (1850). *Mem. Acad. St. Petersbourg VI*.

[82] Overduin, J., F. Everitt, P. Worden, and J. Mester (2012). Step and fundamental physics. *Classical and Quantum Gravity 29*(18), 184012.

[83] Padilla, A. and V. Sivanesan (2012). Boundary terms and junction conditions for generalized scalar-tensor theories. *Journal of High Energy Physics 8*, 122.

[84] Peacock, J. (1999). *Cosmological Physics*. Cambridge Astrophysics. Cambridge University Press.

[85] Peacock, J. A. (2008). A diatribe on expanding space.

[86] Planck Collaboration, P. A. R. Ade, N. Aghanim, C. Armitage-Caplan, M. Arnaud, M. Ashdown, F. Atrio-Barandela, J. Aumont, C. Baccigalupi, A. J. Banday, and et al. (2013). Planck 2013 results. XXII. Constraints on inflation.

[87] Pound, R. V. and G. A. Rebka (1959). Gravitational Red-Shift in Nuclear Resonance. *Physical Review Letters 3*, 439–441.

[88] Remmen, G. N. and S. M. Carroll (2013). Attractor solutions in scalar-field cosmology. *Phys. Rev. D 88*(8), 083518.

[89] Remmen, G. N. and S. M. Carroll (2014). How many e-folds should we expect from high-scale inflation? *Phys. Rev. D 90*(6), 063517.

[90] Renaux-Petel, S. and K. Turzyński (2016). Geometrical Destabilization of Inflation. *Physical Review Letters 117*(14), 141301.

[91] Roos, M. (1997). *Introduction to Cosmology*. Wiley.

[92] Rumsey, C., Y. C. Perrott, M. Olamaie, R. D. E. Saunders, M. P. Hobson, A. Stroe, M. P. Schammel, and K. J. B. Grainge (2017). AMI SZ observation of galaxy-cluster merger CIZA J2242+5301: perpendicular flows of gas and dark matter.

[93] Salopek, D. S., J. R. Bond, and J. M. Bardeen (1989). Designing density fluctuation spectra in inflation. *Phys. Rev. D 40*, 1753–1788.

[94] Sasaki, M. and E. D. Stewart (1996). A General analytic formula for the spectral index of the density perturbations produced during inflation. *Prog. Theor. Phys. 95*, 71–78.

[95] Schmidt-May, A. and M. von Strauss (2016). Recent developments in bimetric theory. *J. Phys. A49*(18), 183001.

[96] Schutz, B. (1980). *Geometrical Methods of Mathematical Physics*. Cambridge University Press.

[97] Schutz, B. (1985). *A First Course in General Relativity*. Series in physics. Cambridge University Press.

[98] Silverstein, E. and A. Westphal (2008). Monodromy in the CMB: Gravity Waves and String Inflation. *Phys. Rev. D78*, 106003.

[99] Starobinsky, A. A. (1980). A new type of isotropic cosmological models without singularity. *Physics Letters B 91*, 99–102.

[100] Stewart, E. D. and D. H. Lyth (1993). A more accurate analytic calculation of the spectrum of cosmological perturbations produced during inflation. *Physics Letters B 302*, 171–175.

[101] Touboul, P., M. Rodrigues, G. Métris, and B. Tatry (2001). Microscope, testing the equivalence principle in space. *Comptes Rendus de l'Académie des Sciences - Series IV - Physics 2*(9), 1271 – 1286.

[102] Tsujikawa, S. (2003). Introductory review of cosmic inflation. In *2nd Tah Poe School on Cosmology: Modern Cosmology Phitsanulok, Thailand, April 17-25, 2003*.

[103] Tsujikawa, S. (2014). Distinguishing between inflationary models from cosmic microwave background. *PTEP 2014*(6), 06B104.

[104] Weinberg, S. (2008). *Cosmology*. Cosmology. OUP Oxford.

[105] Whitt, B. (1984). Fourth-order gravity as general relativity plus matter. *Physics Letters B 145*(3), 176 – 178.

[106] Woodhouse, N. (2007). *General Relativity*. Springer Undergraduate Mathematics Series. Springer London.

[107] York, J. W. (1972). Role of conformal three-geometry in the dynamics of gravitation. *Phys. Rev. Lett. 28*, 1082–1085.